




ESA Climate Change Initiative – Fire_cci

D1.1 User Requirements Document (URD)

Project Name	ECV Fire Disturbance: Fire_cci
Contract N°	4000126706/19/I-NB
Issue Date	28/04/2021
Version	7.2
Author	Angelika Heil, M. Lucrecia Pettinari
Document Ref.	Fire_cci_D1.1_URD_v7.2
Document type	Public

*To be cited as: Heil A.; Pettinari M.L. (2021) ESA CCI ECV Fire Disturbance: D1.1
User requirements document, version 7.2. Available from:
<https://climate.esa.int/en/projects/fire/key-documents/>*

	Fire_cci User Requirements Document	Ref.	Fire_cci_D1.1_URD_v7.2		
		Issue	7.2	Date	28/04/2021
		Page			2

Project Partners

Prime Contractor/ Scientific Lead & Project Management	UAH – University of Alcalá (Spain)
Earth Observation Team	UAH – University of Alcalá (Spain) UPM – Universidad Politécnica de Madrid (Spain) CNR-IREA - National Research Council of Italy – Institute for Electromagnetic Sensing of the Environment (Italy)
System Engineering	BC – Brockmann Consult (Germany)
Climate Modelling Group	MPIM – Max Planck Institute for Meteorology (Germany) CNRS - National Centre for Scientific Research - Laboratory for Sciences of Climate and Environment (France)



National Research Council of Italy




Max-Planck-Institut
für Meteorologie



Distribution

Affiliation	Name	Address	Copies
ESA	Clément Albergel (ESA)	clement.albergel@esa.int	electronic copy
Project Team	Emilio Chuvieco (UAH) M. Lucrecia Pettinari (UAH) Joshua Lizundia (UAH) Gonzalo Otón (UAH) Mihai Tanase (UAH) Consuelo Gonzalo (UPM) Dionisio Rodríguez Esparragón (UPM) Daniela Stroppiana (IREA) Mirco Boschetti (IREA) Thomas Storm (BC) Angelika Heil (MPIM) Idir Bouarar (MPIM) Florent Mouillot (CNRS) Philippe Ciais (CNRS)	emilio.chuvieco@uah.es mlucrecia.pettinari@uah.es joshua.lizundia@uah.es gonzalo.oton@uah.es mihai.tanase@uah.es consuelo.gonzalo@upm.es dionisio.rodriguez@ulpgc.es stroppiana.d@irea.cnr.it boschetti.m@irea.cnr.it thomas.storm@brockmann-consult.de angelika.heil@mpimet.mpg.de idir.bouarar@mpimet.mpg.de florent.mouillot@cefe.cnrs.fr philippe.ciais@lsce.ipsl.fr	electronic copy

	Fire_cci User Requirements Document	Ref.	Fire_cci_D1.1_URD_v7.2	
		Issue	7.2	Date 28/04/2021
		Page		3

Summary

This document is the version 7.2 of the User Requirements Document for the Fire_cci project. It refers to Task 1, Work Package 1100. It describes burned area requirements according to the user needs, providing background information to the data provider.

	Affiliation/Function	Name	Date
Prepared	MPIM	Angelika Heil M. Lucrecia Pettinari	28/04/2021
Reviewed	UAH – Project Manager UAH - Science Leader	M. Lucrecia Pettinari Emilio Chuvieco	28/04/2021
Authorized	UAH - Science Leader	Emilio Chuvieco	28/04/2021
Accepted	ESA - Technical Officer	Clément Albergel	

This document is not signed. It is provided as an electronic copy.

Document Status Sheet

Issue	Date	Details
1.0	01/12/2010	First Document Issue
2.0	09/02/2011	Restructured and updated Document
3.0	08/07/2011	Full (re)writing of sections 3, 4 and 5
3.1	10/07/2011	Editorial reworking
3.3	26/07/2011	Layout and formal review
3.4	31/08/2011	Layout and formal review
3.5	14/09/2011	Review addressing ESA comments
4.0	26/11/2015	First document for Phase 2 of Fire_cci. Full (re)writing of the document
4.1	15/01/2016	Review addressing ESA comments
5.0	22/09/2016	Revised version of the document
5.1	30/12/2016	Addressing comments of CCI-FIRE-EOPS-MM-16-0128
5.2	20/12/2017	Revised version of the document
6.0	01/08/2019	Full rewriting of the document synthesising all user requirement surveys with recent scientific publications and product developments
7.0	27/11/2019	Major reorganization of the text according to the comments on ESA-CCI-EOPS-FIRE-MEM-19-0322
7.1	26/03/2021	Update of the document
7.2	28/04/2021	Addressing comments of Fire_cci D1.1 URD v7.1 RID

Document Change Record

Issue	Date	Request	Location	Details
2.0	04/02/2011	ESA, Fire_cci partners	Whole document	Major editing taking into account review comments by S. Plummer (ESA) and other information and feedback
3.0	08/07/2011	ESA, Fire_cci partners	Sections 3, 4 and 5	Full (re)writing of indicated sections
3.1	10/07/2011	Fire_cci partners	Whole document	Editorial
3.3	26/07/2011	Fire_cci partners	Whole document	Literature review on user requirements and products, layout and formal review
3.4	31/08/2011	GAF	Whole document	Typo and grammar correction, updating references

Issue	Date	Request	Location	Details
3.5	14/09/2011	IRD, LSCE, JÜLICH	Whole document Section 3.1	Revision following review comments from Stephen Plummer (ESA), updating references, Data Inter-comparison – separated paragraph introduced
4.0	26/11/2015	MPIC, Fire_cci partners	Whole document	New naming convention for the document New format and layout Full (re)writing of the document
4.1	15/01/2016	ESA	Sections 1, 2.1, 3, 3.1.4, 3.2, 4.1.1, 4.1.3, 4.1.5, 4.1.6, 4.2, 5.1, 5.2.4, 5.4, 5.4.1, 5.4.2, 5.4.4, 5.4.6, 6.5. Table 1 Section 4.1 Section 5.1 Section 7 Annex 1	Minor changes in the text Minor changes in the line corresponding to Fire_cci The sub-sections of this section were re-ordered New paragraphs added New references added Inclusion of new acronyms
5.0	22/09/2016	MPIC, Fire_cci partners	Section 3 Section 4 Section 4.1.2 Section 4.1.4 Section 4.2 Section 5 Section 6 Annex 2	Updated and expanded; characteristics of burned area products with on-going development are discusses separately from “obsolete” products Updated and expanded. Added description of BB5CMIP6 Added description of FireMIP benchmark system New web of science database query on publications using burned area information Restructured, updated and synthesized Restructured and updated Added annex with commonly used definitions
5.1	30/12/2016	ESA	Section 3.1.5 Section 3.2 Sections 3.3, 5.1, 5.2.6 Section 5.2.8 Sections 6.1, 6.2	Changed the reference of C-GLOPS to GIO-GL1. Sentence added to better interpret the error results, and Figure 1 replaced. Small changes in the text. Last sentence deleted. Information added.
5.2	20/12/2017	MPIC	Sections 1, 3.2, 5.2.12, 5.2.13 Sections 2.1, 4.1.1, 5.2.6, 5.2.14, 6, 6.2 Section 2.4 Section 3.1 Section 4.1.4 Section 4.1.5 Section 5.1 Section 5.2.1 Section 5.2.7 Section 5.2.8 Section 5.3	Text expanded. Small changes in the text. Deleted section of structure of the document. Updated tables, added new sub-sections with new products. Added summary on FireMIP workshop October 2017. Added study by Lehsten et al. (2010). Added GCOS-200 (2016) and update FireMIP requirements, added IBBI 2017 workshop. Update results from user requirement surveys, including Fire_cci product user statistics and the 2017 Fire_cci user workshop survey. Expanded on explanations of what uncertainty characterisation mean. Expanded on quality assurance indicator requirements. Expanded on on-going user requirement surveys, including GCOS survey.

Issue	Date	Request	Location	Details
			Section 6.1 Section 6.3 Section 6.4 Annex 2 Annex 3 Annex 4	Specified temporal resolution requirements. Added uncertainty characterisation. Specified ancillary data layer requirements. Updated description of measurement uncertainty. Added Fire_cci user survey form. Added 2017 Fire_cci user workshop report
6.0	01/08/2019	MPIM	All sections	Rewriting of the entire document towards a user requirement document synthesis, while, at the same time, updating it for recent burned area product developments, applications and recently released scientific publications.
7.0	27/11/2019	ESA - MPIM	Sections 1, 2.1, 2.2, 7 Sections 3, 4 Section 5 Sections 6.2, 6.3, 6.7	Sections updated Information rearranged, with new sections and subsections created New section added Text expanded
7.1	26/03/2021	MPIM UAH	Sections 1, 2.1, 4.2.1, 4.2.2, 5 Section 3 and sub-sections Section 6 and sub-sections Section 7	Minor text updates Added information on burned area products released since the URD v7.0; moved table with outdated burned area products into the Annex Text updated. Added new sub-section describing burned area product requirements for fire danger and early warning systems Text updated. Added table summarising key requirements
7.2	28/04/2021	UAH	Table 1 Table 6 Section 8	Some items updated Identified the references with the participation of Fire_cci consortium members. Additional references were added. More references added.

Table of Contents

1. Executive Summary.....	8
2. Introduction	10
2.1. Background	10
2.2. Purpose of the document.....	10
3. Global satellite-derived burned area products	11
3.1. Product evolution and key characteristics.....	11
3.1.1. Product release evolution.....	11
3.1.2. Specification of contemporary product releases	12
3.1.3. Product validation and spatial accuracy.....	15
3.2. Characteristics of contemporary global burned area products	16
3.2.1. OLCI C3S v1.0 (C3SBA10)	16
3.2.2. MODIS Fire_cci v5.1 (FireCCI51).....	17
3.2.3. AVHRR LTDR Fire_cci v1.1 (FireCCILT11).	17
3.2.4. MODIS MCD64A1 Collection 6 ("MCD64C6") and MCD64CMQ	18
3.2.5. GABAM.....	19

3.2.6. Global Fire Emission Database v4 (GFED4) and v4s (GFED4s)	19
3.2.7. Global Fire Atlas (GFA)	20
3.2.8. FRY global database of fire patch functional traits	20
3.2.9. GlobFire database	21
4. Regional satellite-derived burned area products.....	21
4.1. Product evolution and key characteristics	21
4.2. Characteristics of contemporary regional burned area products	24
4.2.1. FireCCISFD11 (Sub-Saharan Africa).....	24
4.2.2. FireCCIS1SA10 (Amazon basin)	24
4.2.3. BAECV (Conterminous United States)	25
5. Product access and product format	25
6. Burned area applications and requirements.....	25
6.1. Terrestrial models using prescribed burned area.....	25
6.2. Fire-enabled Dynamic Global Vegetation Models (DGVMs)	26
6.3. Atmospheric chemistry modelling	27
6.4. Greenhouse gas (GHG) inventories in support of the UNFCC.....	29
6.5. Statistical analysis to quantify fire controls and fire feedbacks	31
6.6. Fire danger and early warning systems	32
6.7. Usage statistics of burned area information	33
6.8. Usage statistics of Fire_cci products	35
6.9. User requirement surveys.....	40
7. Recommendations.....	42
8. References.....	46
Annex 1: Acronyms and abbreviations	62
Annex 2: Supplementary information	65

List of Tables

Table 1: Characteristics of contemporary global burned area products from space-borne remote sensing, sorted by the date they were first released (see Annex 1 for abbreviations).	13
Table 2: Characteristics of contemporary global fire patch products from space-borne remote sensing, sorted by the date they were first released (see Annex 1 for abbreviations).	14
Table 3: Accuracy metrics [in %] estimated from global validation of burned area products (Oe: omission error; Ce: commission error; relB: relative bias).	16
Table 4: Characteristics of regional burned area products (selection) (see Annex 1 for abbreviations).	23
Table 5: Validation results of regional burned area products (Oe and Ce quantify the omission and commission error ratio).	24
Table 6: Peer-reviewed publications using of Fire_cci products.	37
Table 7: Key recommendations for future fire ECV developments.	43

Table 8: Characteristics of global burned area products that are superseded or with abandoned product development (see Annex 1 for abbreviations and Table 1 caption notes).	65
--	----

List of figures

Figure 1: Web of Science (WoS) literature database query results on the temporal evolution of peer-reviewed papers dealing with burned area across 1980 to 2020: annual number of publications and sum of times cited (without self-citations).....	33
Figure 2: Web of Science (WoS) literature database query results on the temporal evolution of peer-reviewed papers dealing with burned area across 1980 to 2020: a) annual number of publications per selected sensors, b) annual number of publications per selected widely used burned area products, c) annual number of publications per climatic regions, and d) number of publications per year mentioning some selected topic keywords.	34
Figure 3: Tree-map showing, in terms of author affiliation, the top 25 countries in all publications dealing with burned area during 1980 to 2020 (Web of Science database query).....	35

1. Executive Summary

Vegetation fires and climate change are closely related. Fires emit large amounts of greenhouse gases and aerosols that exert global climate effects. Fires modify land cover, they alter terrestrial carbon pools and energy and water fluxes, and these processes have direct and indirect implications on climate. Reversely, climate changes induce changes in fire regimes. Fire–climate feedbacks are complex and there is active research to enhance its understanding in support of climate change mitigation and adaption. Apart from climate effects, fires cause substantial damages to society and environment. They are an imminent direct threat to people's lives and infrastructure, a source of air pollution, and an agent of deforestation and wildlife habitat changes. Governments are actively working at implementing fire management and surveillance systems to mitigate the damages. Fire research and fire management systems have strongly benefited and are still benefiting from the emergence of regional to global scale fire observations from satellites.

Fire activity can be monitored from space either from thermal sensors, by detecting the fire's heat signature (active fire counts or fire radiative power), or from optical sensors by delineating the burned surfaces from the induced changes in surface reflectance. Since the emergence of the first global satellite-derived fire products more than two decades ago, they are more and more widely used, including in various climate-related applications, and the number of related scientific publications has grown exponentially. Remote sensing has several advantages over field-surveyed fire information. One aspect is that it is a relatively cheap, transparent and rapid method of acquiring up-to-date information over a large geographical area, including remote and inaccessible regions.

This document is the User Requirements Document (URD) of the Fire_cci project within Phase 1 of the Climate Change Initiative (CCI) extension (2018–2021) following the terms of reference stated in ESA (2018). The Fire_cci project aims at generating long time series of burned area observations that are adapted to the needs of climate research. This URD describes the characteristics of available burned area products, their applications and user communities. It pinpoints the requirements of key climate users of burned area products in terms of product characteristics, product quality and means of data delivery. This URD is a synthesis update of the URDs of Fire_cci Phases 1 and 2 (Heil et al., 2017; Schultz et al., 2011).

Global satellite-derived burned area products are essential to climate modelling, and especially to dynamic global vegetation and carbon cycle modelling. The models target the understanding of long-term interactions between fire, vegetation, carbon, emissions, and ultimately climate. Burned area observations are used to parameterise and benchmark fire processes in these models. These applications require long-term, temporally consistent global time series, which are spatially and temporally aggregated to Climate Modelling Grids (CMG) products of 0.25° spatial and monthly to daily temporal resolution. In atmospheric chemistry modelling, burned area information is used to create regional or global fire emission estimates. Key product requirement here is a high accuracy combined with daily to hourly temporal and 0.1° spatial resolution, while the length of the time series is of secondary importance. The one to two years of latency in delivery of contemporary products is no drawback for most climate-related applications.

Satellite burned area products can substantially support national reporting of GHG emissions to the United Nations Framework Convention on Climate Change (UNFCCC). Target requirements for this application are high spatial resolution of the burned area information, quantified uncertainties, and time series reaching backwards up to 1990, and

forward product continuity. Additional information on the land cover type burned and on fuel consumption is beneficial.

The aspect of size distribution of individual fires, their morphology and dynamics has gained increasing attention over the last decade in climate research and fire patch products are nowadays widely requested. Whether pixel, patch or grid products are most beneficial to users largely depends on the type of application. NetCDF, HDF5/4, and GeoTIFF are the data formats in which most burned area products are provided and to which most users are accustomed. Internet access to the products shall be open and by means that allow for fast and automatized download.

Users of burned area products also request ancillary satellite-derived information on the vegetation type burned, fuel consumption, the rate of spread and indicators for the impact of fire on vegetation (e.g. fire frontline intensity, fire-induced tree mortality).

Product-provided uncertainty estimates are still immature and generally not yet considered in science applications. Instead, estimates of uncertainties are derived from the spread in burned area reported by multiple products, but this approach underestimates the true uncertainties. Significant progress needs to be made in order to provide users with burned area products that contain the uncertainty information they need and understand.

There is a general consensus that product developments shall achieve higher accuracies than delivered in existing burned area products. There is a clear demand for rigorous state-of-the-art product validation prior to the product's release, and it is essential that the quality assessment extends over the entire time series. A clear description of product error characteristics, detailing what fire types are commonly missed or where and when commission is frequent is a common requirement among users. There is a particular increasing interest in burned area products from high-resolution sensors that can resolve small fires hitherto missed by most satellite sensors.

To promote that burned area products are widely applied and used in an adequate manner, the products shall include mature metadata and be accompanied with a product user guide that provides instructions on how to correctly understand and apply individual product variables.

2. Introduction

2.1. Background

Fire disturbance has been identified as Essential Climate Variable (ECV) by the Global Climate Observing System (GCOS) programme (World Meteorological Organization, 2006, 2010, 2016). An ECV is a physical, chemical or biological variable that critically contributes to the characterisation of Earth's climate and that can, from a feasibility perspective, be globally observed or derived with current observing systems (Bojinski et al., 2014). Long term, high-quality and traceable ECV data records are essential to advance evidence-based climate research, monitoring and services. To address this need, the European Space Agency (ESA) launched the Climate Change Initiative (CCI) in 2009. The aim is to provide satellite-based climate data records (CDRs) for around 25 individual ECVs of which "Fire Disturbance" is one.

The Fire_cci project launched within this initiative aims to develop long-term time series of burned area (BA) products from satellite observations that are adapted to the needs of climate modellers (Chuvieco et al., 2016). Key achievements of the first two project phases (2010-2014, 2015-2018) are the development, production, validation and release of several new global burned area products based on MERIS, MODIS and AVHRR observations: FireCCI31/41 (Alonso-Canas and Chuvieco, 2015; Chuvieco et al., 2016), FireCCI50/51 (Chuvieco et al., 2018; Lizundia-Loiola et al., 2020a), and the FireCCILT10 BETA product (Otón et al., 2019). In addition, several regional burned area products have been generated from higher spatial resolution sensor data (Sentinel-2 and Sentinel-1) and FireCCIS1SA10 (that allow a better detection of small fires: FireCCISFD11 for Africa (Roteta et al., 2019) and FireCCIS1SA10 for the Amazon basin (Belenguer-Plomer et al. 2019). Finally, the uncertainty characterization of the Fire_cci burned area products was improved and products were extensively validated.

During the Climate Change Initiative extension (CCI+) phase of the Fire_cci project (2019-2022), the long-term burned area dataset FireCCILT11 (Otón, 2020) was released, which replaces FireCCILT10 BETA. Due to an improved algorithm, FireCCILT11 aims at providing more consistent burned area time series. With a temporal coverage over 36 years (1982-2018, data gap in 1994), it represents the longest global burned area dataset ever publicly released. In addition, a global, operational burned area product based on Sentinel-3 OLCI imagery, called C3SBA10, was developed and released as part of the Copernicus Climate Change Service (C3S).

To ensure that the products generated in the Fire_cci project approach the actual user requirements, the project's User Requirements Document (URD) is regularly revisited and adapted to incorporate evolved user requirements and priorities. This document is the second update of the Fire_cci URD in the project's CCI+ extension. For earlier URD versions produced within Fire_cci, please refer to Heil et al. (2017, 2019), Pettinari et al. (2017) and Schultz et al. (2011), and the peer-reviewed paper of Mouillot et al. (2014).

2.2. Purpose of the document

This Fire_cci User Requirements Document (URD) summarises the user's needs with respect to burned area and related fire disturbance products as requested in the statement of work of ESA CCI (ESA, 2018). It is a major input for establishing the Fire_cci Algorithm Development Plan (ADP), which describes product improvements expected for the on-going Fire_cci project phase.

3. Global satellite-derived burned area products

3.1. Product evolution and key characteristics

3.1.1. Product release evolution

Over the past two decades, more than twenty global satellite-derived burned area products have been developed and publicly released. The products exploit information from various satellite sensors and apply different burned area detection algorithms (cf. Chuvieco et al., 2019). An overview of contemporary and of outdated product releases is given in Table 1 and Table 8, respectively.

ATSR2 and VGT surface reflectance imagery of the year 2000 provided the basis for the first global burned area products that were released in 2002. In the subsequent years, global burned area products based on AATSR, AVHRR, MODIS, MERIS or PROBA-V reflectance data were being developed and released. Since recently, developments based on Landsat, VIIRS and OLCI have been launched. Over the course of the years, several of the released global burned area products, in particular those relying on MODIS information, have been superseded by improved versions of the same product line. Concurrently, the further development of products that exploited VGT, ATSR2, AATSR or MERIS surface reflectance imagery has been abandoned because of irreconcilable quality limitations (Table 8; Humber et al., 2019; Moreno Ruiz et al., 2019).

Most contemporary global burned area products rely on surface reflectance information from the MODIS sensor (Table 1). Most products, moreover, exploit so-called hotspot counts (HS) from the MODIS's thermals bands to guide burned area mapping. For this reason, burned area time series typically start with the emergence of MODIS information, i.e. at November 2000 or later, and therefore maximally span over a period of around 20 years. The time series of the MODIS-based GFED burned area products have been extended backwards up to 1995. This extension, however, builds upon scaled active fires detected by VIIRS and ATSR2, and not on surface reflectance observations.

Burned area products generated from MODIS surface reflectances use 500 m resolution images. The exception is the FireCCI50 product, and its successor, FireCC51, which exploit the MODIS 250 m reflectance bands. The global burned area product C3SBA10 uses surface reflectance information from 300 m Sentinel-3 OLCI imagery, but relies on MODIS HS seeding. FireCCILT11 is a 36-year long global burned area time series, which identifies burned pixels from 5 km AVHRR images and MODIS FireCCI51 to scale burned pixels to burned area.

Two global burned area products do not rely on information from the MODIS sensor: GIO-GL 300 m and GABAM are solely based on surface reflectance information from PROBA-V and Landsat, respectively. GIO-GL 300 m time series start in 2014. GABAM provides annual, 30 m maps for the years 2000, 2005, 2010, 2015 and 2018. Finally, the official release of the VNP61A1 global burned area product, which relies on 375 m surface reflectance and HS information from VIIRS, is expected in due term.

Over the past two decades, the developed global burned area products progressively exploit sensors that provide spectral information at higher spatial resolution. Table 8 in the Annex 2 provides an overview of the historic evolution of the early versions of global satellite burned area products. The resolution of satellite observations that form the basis of the products released until the year 2008 is 1 km (Table 8). Subsequent product releases increasingly use satellite imagery with 500 m, 300 m, 250 m, and 30 m resolution. This development aims at better resolving smaller fires and thereby decreasing the product's

omission errors. Zhu et al. (2017), for example, demonstrated for boreal Asia that the burned area detection rate of the 500-m MODIS based MCD64C5 product strongly decreases with decreasing fire sizes, and is falling below 10% for fires smaller than 100 ha. GFED4s, released in 2015, attempts to address the limitations of MODIS 500 m spatial resolution imagery in resolving burned area of small fires. The attempt involves a complementary indirect small fire estimate based on HS observations.

Most global burned area products are delivered as pixel version (at the sensor's native spatial resolution) and as corresponding coarser resolution grid – so-called "Climate Modelling Grid" (CMG) products. The CMG products contain burned area summary statistics onto a regular, geo-references grid so that climate users can easily use and further process them according to their needs. The spatial resolution in which most CMG burned area products are provided has progressively increased from 1° x 1° to 0.25° x 0.25°. CMG products have monthly to 10-day temporal resolution, except for GFED4 that has monthly and daily resolution. Most of the pixel products provide information of the day of burn.

Andela et al. (2019), Laurent et al. (2018) and Artés et al. (2019) independently developed and publicly released global fire patch products: GFA (Global Fire Atlas), FRY and GlobFire, respectively (Table 2). These databases provide burned area information at the level of individual fire events – or so-called "patches". Each of them identifies burn patches from burned area pixel products (MCD64C5, MCD64C6 and/or FireCCI41), but with different algorithms. The end product is a database that provides information on the location, size, morphology and/or dynamic for each fire patch. In addition, CMG products with aggregated patch statistics are produced.

3.1.2. Specification of contemporary product releases

Burned area product specifications show a clear development towards more product layers, and hence towards providing more supplementary information to each burned area observation:

- State-of-the art pixel products nowadays not only contain a binary burned-unburned classification, but also information on the date of burn, quality flags, and eventually the land cover burned
- Grid products provide aggregated statistical summaries of the burned area and are commonly supplemented by information on the land cover type burned. In addition, information on the fraction of observed area is becoming standard in CMG burned area products.
- The GFED products provide gridded burned area together with fuel consumption and emission flux estimates, complemented by scalars to distribute the monthly emission fluxes to daily and 3-hourly temporal resolution.
- Only Fire_cci products (starting with the FireCCI50 product) provide a per pixel uncertainty characterisation, i.e. a probability that a pixel is burned based on sources of error within the input data and algorithm, and a grid-level uncertainty estimate that aggregates the pixel level uncertainties. Then again, per-pixel estimations of the uncertainty in the date of burn are only available in the MCD64A1 products.
- Pixel products are most commonly provided as monthly GeoTIFF or HDF files. Geographical sub-setting into 10° tiles or regional windows is common to limit the file sizes. Grid products are mostly provided as global NetCDF or HDF tiles. All global burned area products are produced with several months or years of latency. The exception is GIO-GL 300m, which is produced in almost near real-time (latency of ~2 days).

Table 1: Characteristics of contemporary global burned area products from space-borne remote sensing, sorted by the date they were first released (see Annex 1 for abbreviations).

Product	Period MM/YYYY	Release	Sensor/Method	Resolution		File format ^{*1}	Data layers	Reference	Data access
				spatial	temporal				
FireCCILT11	01/1982 12/2018	01/2021	AVHRR2-3; BA scaled with FireCCI51	p: 0.05° g: 0.25°	p: d g: m	p: GeoTIFF g: NetCDF	p: DOB, CL, BA, OB g: BA, UNC, FBURN, FOA	Otón (2020)	https://catalogue.ceda.ac.uk/uuid/b1bd715112ca43ab948226d11d72b85e & https://catalogue.ceda.ac.uk/uuid/62866635ab074e07b93f17fbf87a2c1a
C3SBA10 ^{*2}	01/2017 04/2020	04/2020- cont	OLCI SRC & MODIS C6 HS	p: 300m g: 0.25°	p: d g: m	p: NetCDF g: NetCDF	p: DOB, CL, LC g: BA, UNC, FBURN, FOA, LC	Lizundia- Loiola et al., (2021)	https://doi.org/10.24381/cds.f333cf85
VNP64C1 ^{*3}	01/2014 12/2018	10/2019 as sample	VIIRS C1 SRC & VIIRS C1 HS	p: 500m	p: d	p: HDF4	p: DOB, DOBUNC, QA, DOB (F&L)		https://e4ftl01.cr.usgs.gov/VIIRS/VN/P64A1.001/
FireCCI51	01/2001 12/2019	11/2018 - cont	MODIS C6 SRC & MODIS C6 HS	p: 250m g: 0.25°	p: d g: m	p: GeoTIFF & NetCDF4; 6 continental tiles g: NetCDF	p: DOB, CL, LC g: BA, UNC, FBURN, FOA, NOP, LC	Lizundia- Loiola et al., (2020a)	https://catalogue.ceda.ac.uk/uuid/3628cb2fdb443588155e15dee8e5352 & https://catalogue.ceda.ac.uk/uuid/58f00d8814064b79a0c49662ad3af537
MCD64CMQ	11/2000 10/2018	05/2018 - cont	<i>see MCD64C6</i>	g: 0.25°	g:m	HDF4	BA, FOA, QA, LC	Giglio et al., (2018a)	sftp://fire:burnt@fuoco.geog.umd.edu/data/MODIS/C6/MCD64CMQ
GABAM	2000, 2005, 2010, 2015, 2018	05/2018 - cont	Landsat8 SRC	p: 30m	p: y	GeoTIFF - 10°tiles	BA	Long et al., (2019)	https://vapd.gitlab.io/post/gabam/
MCD64C6	11/2000 now (lag ~4m)	01/2017 - cont	MODIS C6 SRC & MODIS C6 HS	p: 500m	p: d	HDF4-10°tiles GeoTIFF &SHP- 24 tiles	DOB, DOBUNC, QA, DOB (F&L)	Giglio et al., (2018a)	ftp://user:burnt_data@bal.geog.umd.edu/Collection6/
GIO-GL v1 300m	04/2014 now (lag ~3d)	04/2016 - cont	PROBA-V SRC	p: 300m	p: d	NetCDF & GeoTIFF	DOB, NOO, SEAS	Tansey et al., (2008)	https://land.copernicus.eu/global/products/ba (registration required)
GFED4s	01/1997 12/2016	07/2015 - cont ^{*4}	<i>see GFED4</i> ; MODIS C5 HS as small fire proxy	g: 0.25°	g: m, d, h ^{*5}	HDF5	BA, BAS, EMIS, FCR	van der Werf et al., (2017)	https://www.geo.vu.nl/~gwerf/GFED/GFED4/

Note: Product names are given as abbreviation; the full product name is provided along with the description of the individual products in section 3.2. Period denotes the product's temporal coverage. Release denotes the date of the product's first release; '-cont' indicates that the product is temporally extended as time progresses.

^{*1} Data provided in single global file, if not specified otherwise. ^{*2} The C3SBA10 uses the FireCCI51 algorithm, adapted to Sentinel-3 OLCI reflectances. ^{*3} Data product has been released on a provisional on limited basis only due to falsely identified burned areas. ^{*4} The GFED4s emission production continues beyond 2017, but does not contain a burned area layer. ^{*5} From 2003 onwards, supplementary scalars (based on Mu et al., 2011) are provided to redistribute monthly emission fluxes to daily and 3-hourly emission estimations.



fire
cci

Fire_cci
User Requirements Document

Ref.	Fire_cci_D1.1_URD_v7.2		
Issue	7.2	Date	28/04/2021
Page			14

Table 2: Characteristics of contemporary global fire patch products from space-borne remote sensing, sorted by the date they were first released (see Annex 1 for abbreviations).

Product	Period	Release	Sensor/Method	Resolution		File format ^{*1}	Data layers	Reference	Data access
	MM/YYYY			spatial	temporal				
GlobFire	10/2000 06/2018	11/2018	data mining on MCD64C6 pixel	pa:>21 ha	pa: cut 5d	pa: SQL, SHP	pa: MORPH, DOB	Artés et al. (2019)	https://doi.pangaea.de/10.1594/PANGAEA.895835
FRY	(a)11/2000 12/2016 (b) 01/2005 12/2011	09/2018	flood-fill on (a) MCD64C6 pixel (b) FireCCI41 pixel	pa:>5pixels g: 1°	pa: cut 3, 5, 9 & 14d g: time- average	pa: CSV g: NetCDF	pa/g: 25 layers, e.g. SIZ, NPIX, PER, MORPH , FRP	Laurent et al., (2018, 2019)	https://doi.org/10.15148/0e999ffc-e220-41ac-ac85-76e92ecd0320
GFA	01/2003 12/2016	08/2018	ignition point plus growth dynamics on MCD64C6 pixel	pa:>21ha p: 500m g: 0.25°	pa+p: d g: m	pa: SHP p: GeoTIFF g: GeoTIFF	pa+p: IGNS, PER, DOB, MORPH, DYN g: see pa+p, but no DOB	Andela et al., (2019)	https://doi.org/10.3334/ORNLDAAAC/1642 & DAAC

3.1.3. Product validation and spatial accuracy

Many global burned area products underwent only limited validation when first publicly released (i.e. CEOS stage 1 following Boschetti et al., (2009)). Examples are Globcarbon, L3JRC, Geoland2, MCD45, GIO-GL 300 m and 1000 m, MCD64A1 C5/C5.1. This means that product accuracies were assessed by comparison with a relatively small set of reference data, which, most commonly, are derived from 30 m resolution Landsat data. When first released, GABAM, FireCCI31/41, the MCD64A1 C6 product were validated to around stage 2. This stage implies validation with a set of spatially and temporally distributed reference data and with results published in peer-reviewed journals. The only global burned area products that were released with stage 3 validation are the Fire_cci FireCCI50 and FireCCI51 products. This stage comprises validation against a large set of randomly sampled reference that cover a multi-year time period (Padilla et al., 2018). Several products have been retrospectively validated at stage 2 or 3 by the multiproduct validation exercises of Padilla et al. (2015, 2018). Lastly, Boschetti et al., (2019) present stage 3 validation results of the MCD64C6 product.

The validation approach is critical for the outcome of the estimates product accuracies. Table 3 shows that omission or commission error rates for individual products may drastically differ dependent on the chosen validation approach. Boschetti et al., (2019) stress that stage 2 validation results do not reliably reflect the global product accuracy since the underlying sampling approach of the reference data does not ensure unbiased estimations. Finally, product validation is not always performed by independent third-parties; closeness between the validators of burned area products and those developing and generating the products may entail conflicts of interest and an enhanced risk for biases (Ban et al., 2018).

The results of recent stage 3 validation efforts of global burned area products indicate omission (Oe) and commission error (Ce) ratios of 62 – 81% and 35 – 64%, respectively (Table 3). The beta-release FireCCILT10 has comparable Oe, but substantially higher Ce (92%). The first Landsat-based global product, GABAM, exhibits the lowest omission and commission error estimates (13 and 30%, respectively); however, these results may not be representative due to the underlying stage 2 validation approach.

Moreover, Campagnolo et al. (2021) stress that fire size is a fundamental driver of accuracy, and therefore validation of burned area products should be linked to the description of fire size distribution to facilitate the interpretation of the validation metrics.

Altogether, the validation results indicate that, at present, no global burned area product meets the GCOS-200 accuracy requirements of 15% (Ce and Oe), compared to 30 m reference observations (World Meteorological Organization, 2016).

Giglio and Roy (2020) emphasize that product validation may not unveil critical temporal and spatial product inconsistencies, because it relies on a limited sample of independent reference data. In addition to product validation, it is therefore imperative to perform a qualitative product assessment which explores the consistency and plausibility of patterns, optimally by integrating independent observations of related variables (e.g. plausibility of soil moisture observations with fire patterns). Franquesa et al. (2020) have released the first public compilation of standardized burned area validation reference data – complying the request repeatedly expressed by the burned area product user communities (e.g. Heil 2017; Humber et al., 2019). While the database facilitates product validation by product users, this does not substitute the product validation and quality assessment for which the product producers – ideally supported by a third-party validation

experts – are responsible for prior to the release (Ducanson et al. 2019; CMUG CCI+, 2021). Climate modellers, as they handle a multitude of observational data for model parameterisation and benchmarking, expect fit-for-purpose observational products, and do have the expertise and capacities to perform product quality assessments.

Table 3: Accuracy metrics [in %] estimated from global validation of burned area products (Oe: omission error; Ce: commission error; relB: relative bias).

Product	Oe	Ce	relB	Period	Stage	Reference
C3SBA10*	50 – 53	14–23	-38 – -42	2017–2019	3 (l)	Lizundia-Loiola et al., 2021
FireCCI51*	42 – 49	17–23	-27 – -35	2017–2019	3 (l)	Lizundia-Loiola et al., 2021
FireCCI51	67	54	-28	2003–2014	3 (s)	Padilla et al., 2018
FireCCI50	71	51	-40	2003–2014	3 (s)	Padilla et al., 2018
FireCCI41	81	64	-47	2005–2011	3 (s)	Padilla et al., 2018
MCD64C6	62	35	-42	2003–2014	3 (s)	Padilla et al., 2018
FireCCILT10	77	92	197	2003–2014	3 (s)	Padilla et al., 2018
MCD64C6	73	40	-54	fire year 2014/2015	3 (s)	Boschetti et al., 2019
GABAM	30	13	n.a.	2015	2 (s)	Long et al., 2019
MCD64C5	68	42	-44	2008	2 (s)	Padilla et al., 2015
MCD45	72	46	-48	2008	2 (s)	Padilla et al., 2015
Geoland2	91	74	-68	2008	2 (s)	Padilla et al., 2015
FireCCI31	76	64	-34	2008	2 (s)	Padilla et al., 2015
MCD64C6	37	24	18	2003–2010	2 (s)	Giglio et al., 2018a
MCD64C5	40	22	23	2003–2010	2 (s)	Giglio et al., 2018a
MCD45	45	23	28	2003–2010	2 (s)	Giglio et al., 2018a

* Range refers to the accuracy metrics computed for individual years.

Note: Period refers to time period over which reference data for product validation are sampled; stage indicates the targeted validation stage following Boschetti et al., (2009)). (s) and (l) indicate that the time between the pre- and post-fire reference perimeters used for validation is short (s) (up to around 16 days) or long (l) (several months) (Lizundia-Loiola et al., 2021). The calculation of the metrics is described in Padilla et al. (2015).

3.2. Characteristics of contemporary global burned area products

The following section provides a short description of contemporary global burned area products listed in Table 1.

3.2.1. OLCI C3S v1.0 (C3SBA10)

C3SBA10, released in April 2020, is a global burned area product generated within Copernicus' Climate Change Service (C3S) based on 300 m OLCI (Ocean and Land Colour Instrument) reflectance observations from the Sentinel (S) 3A and 3B satellites (Lizundia-Loiola et al. 2021). The C3SBA10 time series starts in January 2017 and, at the time of this document, extends until April 2020. Before 2019, it only uses S3A observations, and afterwards observations from S3A and S3B. As an operational C3S product, the C3SBA10 time will be progressively extended forward.

The C3SBA10 may be understood as a continuation of the global MODIS-based FireCCI51 burned area time series that cover the period 2001 to 2019 (Lizundia-Loiola et al., 2020a). An overall objective in the development of the C3SBA10 product was therefore to ensure consistency with FireCCI51 so that, when combined, the multi-decadal time series is suitable for long-term trend analysis and various other climate research applications.

To map C3SBA10 burned area, the FireCCI51 algorithm, developed for 250 m MODIS reflectances (see Section 3.2.2), was adapted to the S3 OLCI characteristics (Lizundia-Loiola et al. 2021). As in FireCCI51, the C3SBA10 algorithm uses MODIS MCD14ML C6 thermal anomaly detections in combination with a relative drop in NIR reflectance to identify pixels with high probability of being burned (Lizundia-Loiola et al., 2020a). Then, a contextual region-growing algorithm is applied around these candidate 'seeds' to detect the burned surfaces. The reflectance thresholds discriminating burned-unburned surfaces are determined in an adaptive manner using a novel spatio-temporal active-fire clustering approach (Lizundia-Loiola et al., 2020a) that aims at better representing the spectral signatures of fires dependent on the local fuel conditions.

C3SBA10 is provided as a pixel and grid product in NetCDF4 format. The pixel product has a resolution of approx. 300 m at the Equator and has three layers: date of detection, uncertainty expressed as probability of detecting a pixel as burned, and land cover information. The grid product has 0.25° spatial and monthly temporal resolution. It has 22 data layers: burned area, standard error quantifying the standard uncertainty of the burned area estimate, the fraction of burnable and observed area, and the burned area in 18 individual vegetation classes. The grid product is delivered as monthly global files and the pixel product as monthly continental files. Land cover information comes from the Land Cover C3S product, which is the consistent extension of the CCI Land Cover product (Version 2.7.1, ESA, 2017). The "per pixel" uncertainty information quantifies the probability that the pixel is actually burned and is modelled from the uncertainty of the different input variables used in the burned area detection algorithm whereas the 1- σ uncertainty information of the grid product is modelled from the pixel uncertainty information (Lizundia-Loiola et al., 2018).

Spatial accuracy of the C3SBA10 2017-2019 time series is assessed with independent Landsat-8 OLI burned area reference data that are compliant with a CEOS LPVS stage 3 validation (Padilla et al., 2018) (see Table 3).

3.2.2. MODIS Fire_cci v5.1 (FireCCI51)

FireCCI51, first released in November 2018, is a further development of FireCCI50, which constitutes the first global burned area product at 250 m spatial resolution. FireCCI50 adapts the FireCCI41 algorithm developed by Alonso-Canas and Chuvieco (2015) for 300 m MERIS imagery to MODIS 250 m red and near infrared (NIR) reflectance (Chuvieco et al., 2018). The algorithm combines temporal changes in daily reflectance with HS detections from the MODIS MCD14ML C6 product. FireCCI51 has an updated algorithm that only uses NIR reflectance, without the need of the red channel (Lizundia-Loiola et al., 2020a). FireCCI51 covers the period 2001 to 2019 and is provided as a pixel (in continental GeoTIFF files) and grid (in global NetCDF4 files) monthly products, with the same layers as the C3SBA10 dataset.

3.2.3. AVHRR LTDR Fire_cci v1.1 (FireCCILT11).

FireCCILT11, released on January 2021, uses surface reflectances from the Advanced Very High Resolution Radiometer (AVHRR) sensor on board the NOAA satellites NOAA-7, NOAA-9, NOAA-11, NOAA14, NOAA-16, NOAA-18, and NOAA-19 as input. Specifically, it uses AVHRR time-series that have been reprocessed by the Land Long-Term Data Record (LTDR) team and which consist of daily global images at a spatial resolution of 0.05° and which reaches back until the year 1982. The FireCCILT11

algorithm creates monthly composites using the maximum temperature criterion and then applies a synthetic index to detect burned area. The index builds on different bands (Red, NIR and Thermal), spectral indices (BAI, GEMI) and temporal differences. The probability obtained from a Random Forest model that was trained with FireCCI51 is then used to classify between burned and unburned pixels. The burned fraction in each pixel is estimated from a statistical analysis, which relates the classified burned pixels to the burned fraction in the FireCCI51 time series (Otón 2020; see also Section 3.2.2).

FireCCILT11 covers the period 1982 to 2018 (with a gap in 1994 due to the lack of sufficient input data). It is delivered as global monthly grid and pixel products, respectively, with 0.25° and 0.05° spatial resolution. The FireCCILT11 pixel product data layers are the date of detection of the fire, the confidence level, the burned area in the pixel and the number of observations, while the grid product layers correspond to the sum of BA per grid cell, the standard error, the fraction of burnable area and the fraction of observed area. FireCCILT11 is the improved successor version of the beta version FireCCILT10 (Otón et al., 2019) that was released by the Fire_cci project in March 2019 (Otón and Pettinari, 2019). In the MODIS era, FireCCILT10 was calibrated against MCD64C6 burned area. FireCCILT10, as pointed out by Heil et al. (2018) and Giglio and Roy (2020), has strong temporal inconsistencies during the pre-MODIS era (i.e. prior to 2001). In addition, it misses most burned area outside of tropical Africa. Giglio and Roy (2020) demonstrate that the temporal inconsistencies are related to orbit-drift artefacts in the underlying AVHRR input data and therefore advise against using the FireCCILT10 for time series analysis.

According to Otón (2020), FireCCILT11 was validated with a long-term Landsat dataset that was created for most affected fire regions. In addition, spatial and temporal consistency of the product was assessed by comparison against other global BA products and regional observation-based fire statistics. These validation and intercomparison results, however, are not yet publicly available.

3.2.4. MODIS MCD64A1 Collection 6 ("MCD64C6") and MCD64CMQ

MCD64A1 Collection 6 ("MCD64C6") (Giglio et al., 2018a), released in January 2017, supersedes MCD64A1 Collection 5.1 ("MCD64C5"). The time series starts in November 2000, and is produced with 4-month latency until the present.

Similar to its predecessor, it relies on the hybrid algorithm developed by (Giglio et al., 2009), which combines multi-temporal changes detected in the MODIS 500 m surface reflectance bands with MODIS HS. However, compared to its predecessor, it has some improvements in terms of (a) the algorithm, (b) the use of MODIS Collection 6 (versus Collection 5) for surface reflectances and HS input data, and (c) an expanded product spatial coverage. These improvements lead to a significantly enhanced detection of small burns and a reduction in omission errors. Also achieved is a reduction of the uncertainty in the date of detection and of the occurrence of unclassified grid cells (Giglio et al., 2018a). The MCD64C6 500 m resolution pixel product is delivered in different file formats – HDF, GeoTIFF, and shapefile. The HDF product consists of monthly, 10x10° tiles that contain five data layers: approximate burn date, burn date uncertainty, first and last date of reliable change detection, and a categorical quality assessment (QA) indicator.

A Climate Modelling Grid (CMG) version of the MCD64C6 product with 0.25° spatial and monthly temporal resolution was released 1.5 years later, namely in May 2018, and is called MCD64CMQ. It contains four layers: burned area, unburned fraction, burned area in 16 vegetation classes, and a QA indicator. The land cover information comes from the

Collection 6 MCD12Q1 land cover product. The MCD64C6 product of the years 2000 to 2011 is CEOS stage 2 validated by the product producers (Giglio et al., 2018a) and stage 3 validated by Padilla et al. (2018).

3.2.5. GABAM

The global annual burned area map (GABAM) product (Long et al., 2019), released in May 2018, is generated with an automated burned area mapping algorithm from time-series of 30 m Landsat images. When first released, GABAM only covered fires that burned in the year 2015. For this, all Landsat-8 images during 2014-2015 and various spectral indices were utilized to calculate the burned probability of each pixel using a random forest decision trees. The latter were globally trained with stratified samples, and a seed-growing approach was conducted to shape the final burned areas after applying several logical filters (NDVI, NBR, temporal). In December 2019, GABAM for the years 2000, 2005, 2010, and 2018 were released. GABAM is produced as a global 30 m pixel product and is delivered as annual, 10x10° tiled GeoTIFF files, which solely contain a binary burn-unburned classification layer. Validation of the GABAM targets CEOS stage 2.

3.2.6. Global Fire Emission Database v4 (GFED4) and v4s (GFED4s)

The GFED4 burned area product (Giglio et al., 2013), released in March 2013, is the monthly 0.25° CMG version of the MODIS MCD61A1 C5.1 product ("MCD64C5"), the predecessor of MCD64C6 (see Section 3.4). Before the MODIS era (i.e. before August 2000) and back to mid-1995, the GFED4 time series are temporally extended with burned area estimates that are derived from TRMM VIRS and ERS ATSR2 HS observations. GFED4 is made available as monthly global HDF-files, which contain seven layers: burned area, uncertainty, data source, burned area by land and peat cover and tree density, and fire persistence. The 1- σ -uncertainty layer contains error statistics derived from product validation with Landsat in three localised regions. In the MODIS era, a daily GFED4 product is also available. Instead of fire persistence, the HDF-files contain a layer specifying the uncertainty in the date of burn product. There was limited validation (CEOS stage 1) validation of the MCD64C5 product that underlies GFED4 in the MODIS era while there was no validation of the time series that were extended back to 1995 using VIRS and ATSR HS. The production of the GFED4 time series ended in December 2016.

The GFED4s inventory, released in May 2015, provides monthly, 0.25° gridded burned area, fuel consumption rate, and information on what fuel type burned, allowing users to calculate trace gas and aerosol emissions using emission factors. GFED4s burned area consists of the GFED4 burned area dataset, which is complemented by estimates for burned area by "small" fires, i.e. fires that fall below the detection limit of the underlying MCD64C5 product (Randerson et al., 2012, van der Werf et al. 2017). The small fire burned area is estimated from the ratio of MODIS HSs that fall inside and outside of 500 m MCD64C5 burn scars (Randerson et al., 2012). Small fire burned area in the pre-MODIS era is estimated from VIRS and ATSR HSs in an analogous approach. The GFED4s time series starts in January 1997 and continues until the present (availability with around 3-month latency). The GFED4s burned area time series, however, ended in December 2016, because afterwards, due to the cessation of GFED4 burned area, GFED4s fuel consumption and emissions are directly estimated from HSs. By default, GFED4s also provides scalars to downscale monthly emissions to daily and 3-hourly data. These scalars are also build upon active fire observations following the approach described in Mu et al. (2011).

Since recently, a GFED NRT fire emission product that relies on 375 m Suomi VIIRS HSs is publicly available via an ARCGIS server.¹

There was no validation of the GFED4s product. Zhang et al. (2018) demonstrate the limitations of the 'small fire boosting' approach for two Asian regions dominated by small agricultural fires. On the one hand, a substantial fraction of very small fires remains omitted because they fall below the detection limit of the MODIS HS product. On the other hand, the boosting introduces substantial commission errors along with false HSs.

Developments towards the release of GFED5 are ongoing. It will build on the improved MCD64C6 time series, and, among others, include 30 m Landsat and Sentinel burned area observations and VIIRS HSs to better quantify small fires. It is planned that GFED5 will provide daily, 0.1° gridded fire emissions in NRT.

3.2.7. Global Fire Atlas (GFA)

The Global Fire Atlas (GFA) (Andela et al., 2019), released in 2018, provides global information on individual fires identified from the MCD64C6 pixel product (see Section 3.4). The identification starts with mapping the local minima within the original field of burn dates. Assuming that fire follow a logical progression in time and space, the daily growth of the fire from these ignition points is tracked in the surrounding pixels. Biomes-specific “fire persistence” thresholds constrain how long a fire may take to spread from one pixel into the next. The thresholds consider satellite coverage and plausible fire spread rates. For each individual fire, several parameters characterising fire morphology (e.g. size, perimeter) and fire spread dynamic (e.g. duration, speed and direction of spread) are calculated. The GFA covers the period 2003 to 2016 and is delivered as global 500 m resolved annual GeoTIFF-files containing information on the day of burn, fire line, speed and direction. Corresponding annual shapefiles provide polygons with the fire perimeter and points of the ignition locations. The attribute tables of the shapefiles contain information on the fire ID, ignition and extinction date, fire morphology and dynamic, and the dominant MODIS MCD12Q1 collection 5.1 land cover. In addition, a monthly, 0.25° CMG version of the GFA is provided as annual global GeoTIFF-files for the following variables: monthly ignition count and, as average over the individual fires, the burned area, duration, fire line length, speed and daily expansion plus the dominant per-fire wind direction. The GFA has been subject to preliminary validation: Firstly, the temporal accuracy of GFA burn dates is globally evaluated against VIIRS HSs. Secondly, GFA fire perimeters are compared to independent Landsat-based fire perimeters for the continental US and to daily perimeters of selected large fires measured by US Forest Service aircrafts.

3.2.8. FRY global database of fire patch functional traits

The FRY global database of fire patch functional traits (Laurent et al. 2018, 2019), released in 2018, is a representation of the MCD64C6 and the FireCCI41 pixel product in form of individual fire patches and together with their morphology-based functional traits. Fire patches are defined as groups of adjacent burned pixels whose burn date is close enough in time to be considered as belonging to the same individual fire event. The number and characteristics of fire patches identified with this 'flood-fill' algorithm

¹ https://maps.nccs.nasa.gov/image02/rest/services/gfed/VIIRS_nrt_dailyEmissions/ImageServer (accessed on March 2021).

depends upon the maximum burn date difference used, and the outcome of 3, 5, 9 and 14 days cut-off values are provided with the FRY database.

For each patch, various morphological and functional and spatio-temporal descriptors are calculated and provided with the database. They comprise the ID and area of each patch, the coordinates of the patch centre, and the mean, minimum, and maximum pixel burn date of each patch. In addition, various metrics describe the morphological complexity of the fire patches and their elongation and the geographical orientation. Finally, for each patch, descriptive fire radiative power (FRP) and HS statistics calculated from MODIS C6 MCD14DL are provided. Fire patches with less than 5 burned pixels are removed from the FRY database. This cut-off relates to the number of burned pixels in a geographical latitude-longitude projection, implying that the minimum patch size in the database varies with latitude. The MCD64C6 FRY database therefore characterises only patches larger than around 140 ha at the Equator while towards the poles substantially smaller patches are included (e.g. at 70° N/S, the cut-off corresponds to around 50 ha).

The FRY database consists of ASCII delimited files that provide lists with the calculated fire patch properties for individual cut-off values. Associated 1° gridded global maps in NetCDF format provide layers with time-aggregated summaries of key patch properties.

There is no validation of the FRY against independent fire patch observations. There is, however, a regional evaluation of provisional FRY versions generated from FireCCI31 and MCD45 data (Chuvieco et al., 2016; Nogueira et al., 2017).

3.2.9. GlobFire database


GlobFire, described in Artés et al. (2019), is a global database of single fire events that are identified with a data mining approach from the MCD64C6 pixel product. The developed algorithm encodes in a graph structure a space-time contiguity relationship among burned pixels. A fire event is considered as a set of burnt pixels that are connected by touching or intersecting. Burned areas that touch each other are considered as different fires when the date of burn difference between them is more than 5 days. A fire with 16 days of inactivity is considered as ended. Fire event individuation in GlobFire is carried out globally, and not inside a tile as in the GFA or FRY databases, avoiding that fires crossing tile boundaries are artificially split. The database is provided as shapefile and as two PostgreSQL dumps. The shapefile provides for each fire the initial date, the final date and its geometry. The first dump constitutes of a table in which the final burned area of individual fire event is characterised with a numerical identifier, the start and end day of burning and multi-polygon geometry descriptors. The second dump contains the daily burned areas for each fire that can be linked to the final burned areas via the numerical identifier.

The GlobFire database provides fire patch information for the period 2000 to 2018. The database is available in the PANGAEA data repository. In addition, GlobFire is integrated into and accessible from the Global Wildfire Information System (GWIS).

4. Regional satellite-derived burned area products

4.1. Product evolution and key characteristics

In parallel to global burned area products, several satellite-derived regional and national burned area products have been developed. Newly developed products exploit Sentinel and Landsat information and provide burned area time series at 20 and 30 m spatial

	Fire_cci User Requirements Document	Ref. Fire_cci_D1.1_URD_v7.2	
		Issue 7.2	Date 28/04/2021
		Page 22	

resolution, respectively (Table 4). Due to the higher spatial resolution of the underlying satellite imagery, these products can better resolve smaller fires than coarse resolution products (Table 1 and Table 8), and consequently have lower omission error rates (see Table 5). On the other hand, due to the lower revisit times of the Sentinel-2 and Landsat sensors, the achievable temporal resolution of the products is substantially lower.

Several regional long-term burned area time series have been developed from the AVHRR Long Term Data Record (LTDR) of surface reflectances that reaches back until 1982. The focus here is on boreal regions (e.g. Eastern Siberia: Tomshin and Solovyev (2019) and García-Lázaro et al. (2018); Canada: Moreno Ruiz et al. (2012); Canada and Alaska: Pu et al. (2007, 2018)). Except for the latter, the burned area products are not publicly released, but may be available upon personal request.



Fire_cci User Requirements Document

Ref.	Fire_cci_D1.1_URD_v7.2		
Issue	7.2	Date	28/04/2021
Page			23

Table 4: Characteristics of regional burned area products (selection) (see Annex 1 for abbreviations).

Product	Region	Period	Release	Sensor/Method	Spatial	Temporal	File format	Data layers	Reference	Data access
		MM/YYYY			resolution					
FireCCIS1SA10	Amazon basin	01/2017 12/2017	07/2019	Sentinel-1 SRC & MODIS C6 HS & VIIRS HS	p: 40m	p: ~6d	p: GeoTIFF 5° tiles	p: DOB, CL, LC	Belenguer-Plomer and Pettinari (2019)	https://doi.org/10.21950/VTDZ1L
FireCCISFD11	Sub-Saharan Africa	01/2016 12/2016	10/2018	Sentinel-2A SRC & MODIS C6 HS	p: 20m g: 0.25°	p: ~10d g: m	p: GeoTIFF 5° tiles g: NetCDF	p: DOB, CL, LC g: BA, UNC, FBURN, FOA, NOP, LC	Roteta et al. (2019)	http://catalogue.ceda.ac.uk/uuid/bcef9e87740e4cbabc743d295afbe849
BAECV v1.1	Conterminous USA	01/1984 12/2015/ 12/2017 ^{*1}	07/2017	Landsat 4-8 SRC	30m	~10d	GeoTIFF: 2° tiles AEA-WGS84	BP, BC	Hawbaker et al. (2017)	https://doi.org/10.5066/F73B5X76
ABoVE	North America	05/1989 10/2000	~2018	AVHRR SRC & AVHRR HS	1km	y	SHP, KMZ	BA	Pu et al. (2007)	https://doi.org/10.3334/ORNLDAAAC/1545
NFIS-Change	Canada	01/1985 12/2015	~2018	Landsat SRC	30m	climatology 1985-2011 2012-2015	GeoTIFF	BC	Coops et al. (2018)	https://opendata.nfis.org/mapserver/nfis-change_eng.html
Landsat fire scars Queensland	Queensland, Australia	01/1986 12/2016	11/2013	Landsat SRC (Sentinel2 SRC) ^{*2}	30m	m	GeoTIFF	MOB	Goodwin and Collett (2014)	https://data.qld.gov.au/dataset/landsat-fire-scars-queensland-series
MTBS	USA	01/1984 12/2016	2005	Landsat SRC	pa: >200ha	~10d	SHP	ID, PER, DOB (First), BA	Eidenshink et al. (2009)	https://www.mtbs.gov/

^{*1} Files up to 12 2017 are accessible from EarthExplorer. The data are located under the Landsat category, Landsat Collection 1 Level-3 subcategory, and listed as Burned Area.

^{*2} By 2016, imagery from Sentinel-2 was included with the Landsat image sequence enabling increased cloud-free observations.

4.2. Characteristics of contemporary regional burned area products

The following section provides a short description of selected recent regional burned area products.

4.2.1. FireCCISFD11 (Sub-Saharan Africa)

FireCCISFD11, released by the Fire_cci project in 2018, is a Small Fire Database for Sub-Saharan Africa. The underlying burned area detection approach combines spectral information from 20-m Sentinel-2A MSI images with MODIS C6 HS information (Roteta et al., 2019). FireCCISFD11 covers the year 2016 and is provided as pixel and grid products that have the same product layers as the global Fire_cci products (see section 3.2.2). The pixel product has a resolution of approx. 20 m at the Equator. Temporal resolution is 10 days because of the satellite's revisit time. Land cover information is extracted from the CCI S2 prototype Land Cover map at 20 m. Validation of the FireCCISFD11 against Landsat images yields omission and commission error rates of 27% and 19%, respectively (long sampling unit, see Table 5).

4.2.2. FireCCIS1SA10 (Amazon basin)

FireCCIS1SA10 is a burned area product for the Amazon basin (South America) for the year 2017, released by the Fire_cci project in July 2019. Burned area mapping combines spectral information acquired from the SAR instruments onboard the Sentinel-1 A/B satellites with thermal anomalies detected in the MODIS MCD14ML C6 and Suomi VIIRS HS products (Tanase and Belenguer-Plomer 2018). The Sentinel-1 A/B SAR constellation offers images with 5 to 20 m spatial resolution and a 6 day exact repeat cycle at the equator. The spatial resolution of the FireCCIS1SA10 product is 40 m since burned area mapping was performed on spatially aggregated images (Belenguer-Plomer and Pettinari 2019, Belenguer-Plomer et al. 2019). The preliminary product validation yields overall omission and commission error rates of 36% and 37%, respectively (Table 5).

Table 5: Validation results of regional burned area products (Oe and Ce quantify the omission and commission error ratio).

Product	Validation period	Validation reference fire perimeters mapped from	Oe [%]	Ce [%]	Statistic refers to	Reference
FireCCISFD11	2016	45 Landsat scenes, stratified random sampled, with time differences of individual pairs of consecutive images: (a) "short": ≤ 16 days (b) "long": ≥ 100 days	(a) 67 (b) 27	(a) 64 (b) 19	Sub-Saharan Africa, annual product	Roteta et al. (2019)
FireCCIS1SA10	2017	40 stratified random samples; reference burned area dataset generated from Landsat and Sentinel-2 MS	36	37	Amazon Basin	Fernandez-Carrillo et al. (2018)
BAECV	1988, 1993, 1998, 2003, 2008	280 visually interpreted independent Landsat scenes, selected with stratified sampling	42	33	conterminous US, mean annual product	Vanderhoof et al. (2017)
Landsat fire scars Queensland	1987-2012	500k independent random points of Landsat samples	20	30	Queensland, Australia	Gill et al. (2010)

4.2.3. BAECV (Conterminous United States)

The Burned Area Essential Climate Variable (BAECV) product, released in mid-2017 by the U.S. Geological Survey (USGS), consists of 30 m Landsat-based annual burned area maps for the years 1984 to 2015 for the conterminous United States. The BAECV algorithm was designed to semi-automatically extract burned areas from Landsat scenes "using spatial contagion metrics and region-growing approaches to incorporate the spatial patterns of spectral reflectance among neighbouring pixels, in addition to the pixel-level spectral data to identify burned areas" (Hawbaker et al., 2017). The source code for producing the BAECV product is provided at <https://github.com/USGS-EROS/espaburned-area>, allowing users to generate BAECV maps for other regions of the world. The BAECV product is delivered as annual composites in GeoTIFF raster format and comprises a burn probability and a binary burn classification layer. BAECV was validated against an independent, visually interpreted Landsat burned area dataset created from 280 randomly sampled Landsat imagery (VanderHoof et al. 2017). Average omission and commission error rates of 42% and 33%, respectively, were found.

5. Product access and product format

All contemporary burned area products are publicly accessible via the Internet with commonly used download utility programs (e.g. ftp, wget); in some cases prior registration is required. In addition, many global and regional burned area products are nowadays integrated into web-based open data portals and/or are provided with specific open-source software tools that enable users to easily access, visualise, analyse, subset or resample the data.

To accommodate the satellite products generated by the individual ESA CCI projects, the ESA CCI Open Data Portal (ODP) (<https://climate.esa.int/en/odp/#/dashboard>) has been established. The portal provides data access using WMS, WCS and OPeNDAP remote data access protocols. The portal also links to the FTP access of the CCI ODP archive. The latter is held in the CEDA archive, and contains a directory with data produced by the ESA Fire_cci project (<ftp://anon-ftp.ceda.ac.uk/neodc/esacci/fire/>). In addition, the open-source Climate Analysis Toolbox for ESA (Cate) (<https://cate.climate.esa.int/>) facilitates accessing, processing and analysis of all the data products generated by ESA CCI, including the visualisation and cross-ECV intercomparison.

The products generated by CCI projects shall meet the CCI Data Standards (ESA Climate Office, 2019), which implies NetCDF-4 (classic) format and CF (Climate and Forecasting) convention compliancy.

6. Burned area applications and requirements

This section summarizes the main climate-related research areas that use burned area products and identifies their specific product requirements. Usage statistics of burned area information in scientific publications in general and of Fire_cci burned area products in particular complement this section.

6.1. Terrestrial models using prescribed burned area

Satellite-based burned area maps are used as boundary condition in different regional or global terrestrial models (van der Werf et al. 2003, Mouillot et al. 2006, van der Velde et al. 2014, Poulter et al. 2015, Ott et al. 2015, Landry and Matthews 2016). The models simulate various vegetation processes and estimate fuel loads and dryness, while

dynamically incorporating the direct and indirect feedbacks of fires. Fire emissions are calculated from combining modelled fuel loads with burned area maps and fuel-type dependent emission factors. .

A prominent example is the CASA-GFED modelling framework, which produces the Global Fire Emission Database (GFED), the fire emission inventory most widely used across disciplines. CASA-GFED simulation producing the latest GFED versions, version 4 and 4s (van der Werf et al. 2017), use monthly, 0.25° gridded burned area time series of the same name (see Section 3.2.6) as input. In addition, observation-based fire return interval estimates are required for model spin-up (van der Werf et al. 2010). CASA-GFED will develop towards using burned area and other fire observations with higher spatial and temporal resolution in order to capture more realistically small-scale heterogeneity and variability of flaming and smouldering combustion stages (van der Werf et al. 2017, van Wees and van der Werf 2019). Within the limits of computational feasibility, global fire emission models such as CASA-GFED will include sub-500 m modelling that uses native resolution burned area observations and observations of the fire's diurnal cycle.

6.2. Fire-enabled Dynamic Global Vegetation Models (DGVMs)

DGVMs simulate water, energy and carbon exchanges between the terrestrial biosphere and the atmosphere and can simulate the global distribution of vegetation dynamically (Sitch et al. 2003). Fire modules embedded in DGVMs are process-based fire models (Andela et al. 2013, Kloster et al. 2010, Lasslop et al. 2014) or empirical models with optimisation by observation (Knorr et al. 2014, LePage et al. 2014). The majority of fire models explicitly simulate ignitions from natural and human sources, fire propagation, fuel combustion and fire-related changes in plant species composition. DGVMs are widely used to examine the role of fires for global carbon cycling under past and future climate, and to compute fire emission inventories on centennial scales.

Fire-enabled DGVMs rely on satellite-derived burned products for

i. fire process parameterization

Relevant model parameterisations are adjusted so that burned area simulated for contemporary periods fits with the observed burned area.

ii. model benchmarking/evaluation

The performance of the DGVM to realistically model burned area is generally evaluated by comparing simulated burned area against global burned area observations.

An outstanding international initiative devoted to benchmark and systematically compare different global fire-enabled DGVMs is the “fire model intercomparison project” (FireMIP)(Hantson et al. 2016), in which nine state-of-the art models are participating (Rabin et al. 2017). The historic multi-model baseline experiments start in 1700 and reach until present. The FireMIP benchmarking tool ² calculates various metrics of model performance, including scores that quantify the spatial and temporal agreement of modelled burned area, fuel consumption, and fire size and dynamics (e.g. spread and duration) with observations. At present, fire-related observations in the FireMIP benchmarking system have 0.5° spatial resolution, since this is the highest spatial resolution of the fire modules embedded in the FireMIP models. There are two temporal resolutions: monthly for the period from 1700 until present and daily for the period from

² FireMIPTools; <https://github.com/MagicForrest/FireMIPTools> (last accessed December 6, 2020).

1958. Monthly is the temporal resolution for which the FireMIP models are typically calibrated while daily benchmarking data focuses on fire dynamics and fire extreme events (Hantson et al. 2016, Rabin et al. 2017, Li et al. 2019).

The FireMIP benchmarking tools allow for integrating multiple global satellite-derived burned area products since, conceptually, the inter-product differences are treated as indicator for observational uncertainty (Rabin et al. 2017, Teckentrup et al. 2019). The products most commonly used for FireMIP benchmarking are GFED4, GFED4s, MCD45, and FireCCI51 (Rabin et al. 2017, Teckentrup et al. 2019, Hantson et al. 2020). Recently, a 0.5° gridded version of the Global Fire Atlas (Andela et al. 2019, see Section 3.2.7) has been incorporated for a systematic evaluation of fire size and dynamics at a daily scale.

Overall, the observational basis is good for evaluating FireMIP models in terms of general spatial patterns of present-day global burned area. There are, however, also several shortcomings, namely the unavailability of products that provide (a) consistent long-term global or regional burned area observations (> 30 years) allowing a robust benchmarking of temporal trends, and (b) observations at daily time resolution. Moreover, there is a strong demand for observational constraints of the impact of fires on vegetation and soil carbon (Lasslop et al. 2020).

FireMIP is being incorporated into ISIMIP, the Inter-Sectoral Impact Model Intercomparison Project, which brings together models across sectors and scales to create consistent projections of the impacts of global climate change (Frieler et al., 2017). The requirements in terms of burned area observations are basically identical to those identified for FireMIP.

6.3. Atmospheric chemistry modelling

An important field of application of burned area products is the compilation of biomass burning emission inventories for atmospheric chemistry modelling studies. Atmospheric chemistry models help to inform our understanding of how emissions affect air quality and climate on a global or regional scale. In combination with satellite observations of atmospheric trace species or aerosols, they are also employed to constrain surface emission fluxes (Bauwens et al., 2016; Berchet et al., 2015). Atmospheric chemistry models are widely used in NRT air quality forecasting and for studying sources of air pollution during specific events or years (e.g. Aouizerats et al. 2015, Knorr et al. 2017). In contrast, so-called coupled atmospheric chemistry–climate models are used to investigate the complex interactions between atmospheric chemistry and the climate system on decadal to centennial scales (Isaksen et al., 2009; Lamarque et al., 2013).

Atmospheric chemistry models require spatio-temporally resolved fire emission fluxes as boundary conditions. The de-facto standard to compile these inventories is to take satellite observations of burned area, FRP, or HS counts – or combinations of them. Model systems working in NRT or simulating the recent past use FRP or HS for fire emission estimation. The prompt availability of these observations allows that fire emission inputs for NRT atmospheric chemistry forecasts can be computed with sufficient timeliness (latency 3-h optimal, 6-h adequate) (Benedetti et al., 2018). So far, fire emission inventories that rely on burned area observations are used in atmospheric chemistry models primarily when the focus is on multiyear trends, on global patterns of atmospheric trace species or on identifying regional sources of air pollutants. The most widely used fire emission inventory in this context is the Global Fire Emission Database GFED (van der Werf et al. 2003, 2004, 2006, 2010, 2017).

GFED integrates MODIS burned area observations into a terrestrial model to calculate the amount of fuel consumed per unit area and then fire emission fluxes at 0.25° spatial resolution (see section 3.2.6). Besides GFED, several regional BA-based fire emission inventories exist. The regional fire inventories aim at reducing uncertainties by using more region-specific parameterisations, such as e.g. fuel consumption and emission factors, and at providing regional emission information at high spatial and temporal resolutions. Regional emission inventories based on burned area include the 250 m MFLEI (Urbanski et al., 2018) or the 1 km WFEIS (French et al., 2014) inventories for North America; both provide daily estimates and exploit merged MODIS and Landsat burned area information together with active fire products.

Most global and regional atmospheric chemistry models can nowadays run at spatial resolutions down to 0.1° and lower³ and require daily to hourly resolved fire emission input data (Aleksankina et al., 2018; Hu et al., 2018; Kantzas et al., 2015). Several fire inventories or fire emission calculation frameworks have been developed that meet these requirements, such as e.g. GFAS (Kaiser et al., 2012), QFED (Darmenov and da Silva, 2015), FEER (Ichoku and Ellison, 2014), APIFLAME (Turquety et al., 2020), FINN (Wiedinmyer et al., 2011)).

Currently, the higher resolution global fire emission inventories have in common that they solely rely on active fire observations, and in particular on FRP. The exception is the APIFLAME framework (Turquety et al., 2020), where emissions can be calculated by combining 500 m MCD64C6 burned area data with active fires. The reasons why burned area observations are used less commonly are multifold, but mostly related to (a) the problems to extract sufficiently accurate time information (day and hour of the active fire) from burned area products maps and (b) the delayed availability of burned area information. In atmospheric chemistry modelling, FRP-based fire emission estimation approaches are frequently considered as advantageous as they bypass – or at least in parts bypass – the fuel consumption estimation step. This FRP-based approaches rely on the fact that the radiant energy released during a fire relates to the amount of biomass consumed (Wooster et al. 2005) and therefore directly estimate fuel consumption rates (FCR) from satellite FRP observations. For this, they either scale FRP to modelled FCR (e.g. GFAS), apply estimates of FRP-to-FCR conversion factors obtained from laboratory measurements, or determine the conversion factors by relating FRP to satellite observations of the atmospheric density of fire aerosols (e.g. Lu et al. 2019), resulting in so-called "fully top-down" fire emission inventories (Nguyen and Wooster 2020). In comparison, GFED uses outputs from the terrestrial carbon cycle model CASA to calculate dynamic fuel consumption estimates.

So far, no satellite-based public dataset of fuel consumption exists that could be combined with burned area observations to calculate the total biomass consumed during fires. Nguyen and Wooster (2020), however, demonstrated that FRP-based fully top-down fire emission inventories could be combined with burned area maps to obtain data-driven maps of fuel consumption. While still in its beginnings, prospectively such data-driven

³ It is noteworthy that also most anthropogenic emission inventories nowadays have 0.1° spatial resolution globally (e.g. EDGAR, EMEP) – and regionally even 0.05° resolution (e.g. Kuenen et al. (2014), Zheng et al. (2014)). In addition, various CMG products covering precipitation and land surface properties are nowadays provided at these resolutions and allow for an in-depth quantification of fire drivers when combined with similarly resolved CMG fire products.

fuel consumption estimates could strongly improve and facilitate the computation of fire emission inventories from any satellite-derived burned area products.

Generally, it becomes also increasingly essential to atmospheric chemistry applications that the fire satellite observations they use as input have fully quantified uncertainties (Davis et al., 2015), especially when models are combined with data assimilation techniques (Bocquet et al., 2015). Another increasingly important aspect is the correct parameterisation of the injection height, which reflects the vertical updraft of fire emissions. Its calculation requires information on the size and dynamics of individual fires (Paugam et al. 2016) – such as provided in recently released fire patch products (see sections 3.2.7 to 3.2.9).

In summary, four developments could enhance the usage of burned area-based fire emission inventories in atmospheric chemistry modelling:

- 1) burned area products that contain ancillary information allowing users to perform a downscaling to hourly fire emissions,
- 2) complementary products that provide observational constraints on fuel consumption,
- 3) NRT burned area products,
- 4) fully quantified uncertainties.

The focus of coupled chemistry climate models – in contrast to the above-mentioned atmospheric chemistry models – is on assessing how emissions, through various feedback processes in the Earth System, affect climate. In terms of fires, such applications require multi-decadal to centennial global emission inventories. The BB4CMIP6 fire emission reconstruction by van Marle et al. (2017), for example, used as input to the coupled model intercomparison project phase 6 (CMIP6) simulations (Eyring et al., 2016) to support the IPCC Sixth Assessment Report (AR6), covers the period 1750 to 2015 and provides fire emissions at monthly temporal and 0.25° spatial resolution. BB4CMIP6 employs a historical reconstruction of burned area by merging satellite observations of burned area, namely MCD64C5, with active fire observations, official fire statistics, observations of fire proxies such as charcoal records or visibility, and/or modelled burned area from fire-enabled DGVMs (Lamarque et al., 2010; van Marle et al., 2017; Mieville et al., 2010; Mouillot and Field, 2005; Schultz et al., 2008). Clearly, such reconstructions first require the longest possible time series of observed burned area. Optimally, such products have global spatial coverage, but continental-scale products are also beneficial. .

6.4. Greenhouse gas (GHG) inventories in support of the UNFCCC

The United Nations Framework Convention on Climate Change (UNFCCC) sets an overall framework for international efforts to contain climate change by stabilization of greenhouse gas concentrations in the atmosphere.

Developed countries shall submit standardised annual reports of national GHG emissions, including those from vegetation fires, to the UNFCCC. GHG emission reporting must follow IPCC reporting guidelines (IPCC 2006). Starting with 2014, developing countries are also required to submit GHG inventories, but only biennially (Rossi et al., 2016). Annual emissions shall be calculated from 1990 to present and be reported in a transparent and verifiable manner (United Nations, 1998). The reporting guidelines prescribe that fire emissions are estimated and reported separately for different land cover and land use classes and for the kind of fire (controlled burning or wildfires). To achieve this involves intersecting maps of burned area, land cover and use. In the optimal case, the calculations

rely on high-resolution spatial data (e.g. 30 m resolution) to minimize misclassification errors (Mascorro et al., 2015). Annual temporal resolution of the data is sufficient as calculations are done on annual time steps. Gap filling through interpolation or extrapolation ensures data completeness. The GHG guidelines allow countries to choose between three estimation approaches of varying complexity. The simplest Tier 1 approach consists of multiplying burned area totals by generalised default values for fuel consumption and emission factors. Tier 2 requires spatially-explicit maps and country-specific values while in Tier 3, the values must emanate from complex models that can dynamically predict available biomass and fuel consumption (Rossi et al., 2016).

Relatively few countries so far take advantage of burned area observations from satellites for their reporting of GHG emissions from biomass burning, despite better other information is commonly missing. An example is Ghana's national forest reference fourth National Inventory Report (NIR) submitted to the UNFCCC in 2019 (Environmental Protection Agency of Ghana, 2019). It contains the national annual GHG emission estimates for the period 1990 to 2016. 500 m MODIS burned area data of the years 2001 to 2015 (product version is unspecified), processed to annual burned area maps and extrapolated back in time, is used as basis for calculating of biomass burning emissions (National REDD+ Secretariat, 2017). In earlier inventory reports, burned area estimates were solely based on best guess judgements of national agriculture and forestry experts. The national GHG inventory report for South Africa, in turn, uses annual burned area maps generated from the 500 m MCD45 MODIS product (DEA 2015).

The REDD+ programme, codified in the 2015 UNFCCC Paris agreement, encourages developing countries to reduce GHG emissions from deforestation and forest degradation, including those related to fires. The programme entails incentive result-based payments for the implementation of REDD+ activities. For preparing and participating in REDD+, developing countries have worked towards determining Forest Reference Levels (FRLs). The reference levels quantify emissions from deforestation and forest degradation over a reference period and are estimated from historical data. Typically, the reference period expands over 10 to 15 years, dependent upon data availability. The calculated reference levels serve as benchmark against which the country's performance in implementing REDD+ activities, expressed in REDD+ emission reductions, is subsequently assessed. Countries widely use different input data and methods for REDD+ emission estimation than in their national GHG inventories since REDD+ has higher demands for high-quality, reliable observational data (FAO 2019). Monitoring and reporting REDD+ activities requires the establishment of a robust and transparent national forest monitoring system that is based on a combination of satellite and ground-based observations. Since fires are crucial to various REDD+ efforts, satellite burned area products are already or will, in near future, become an essential component in the monitoring systems (Armenteras et al., 2017). Optimally, the products shall meet the following aspects:

- High-resolution burned area maps (e.g. from 30 m Landsat) are beneficial over coarser sensor burned area products since they can better resolve small fires. Small fires such as e.g. set during shifting cultivation widely occur in developing countries and it is important that they are captured.
- For establishing reference emission levels, annual burned area time series are required that reach at least 10 years backwards. Data continuity and temporal consistency is essential to allow for continuously tracing the country's REDD+ achievements.

- Burned area products shall provide information on the vegetation type burned to facilitate the calculation of fire-related GHG emissions, either as an integrated data layer or as separate but consistent data products. Consistent here means that they have compatible spatial resolution, temporal coverage, and file formats. The land cover classification shall allow a discrimination between fires in forested and non-forested areas since this is essential for reporting GHG emissions in the REDD+ framework (Mitchell et al., 2017).
- Many developing countries are in the tropics where cloud cover is common. Burned area products relying on cloud-penetrating sensors are therefore particularly valuable as cloud-related omission errors are common in products derived from optical sensors (Müller et al., 2013).
- Since fires in tropical peatlands leads to particularly high GHG emissions per unit area burned, an accurate mapping of burned areas in these regions shall be targeted since this is crucial to correctly monitor GHG emissions.
- Finally, burned area information included into the monitoring system must have quantified uncertainties.

6.5. Statistical analysis to quantify fire controls and fire feedbacks

Satellite-based burned area products in combination with climate and other socio-economic data are widely used in statistical analysis that target at identifying and quantifying the various factors that control global or regional fire patterns. The insights gained enhance the general understanding of fire occurrence and are an important input for realistically parameterising fire risk and fire-climate models. Several continental to global-scale studies, for example, address the linkage between burned area and climate or population density, partly also considering vegetation characteristics (Andela and Van Der Werf, 2014; Bistinas et al., 2013; Forkel et al., 2019a; Knorr et al., 2014; Morton et al., 2013). They generally use and require relatively coarse CMG burned area products (0.25° to 1° gridded monthly data). The relatively short length of present-day global satellite burned area time series, however, frequently limits the statistical evidence that can be drawn (Archibald et al., 2013; Fanin and Van Der Werf, 2017; Forkel et al., 2019b). Studies that explore the factors controlling fire activity at daily temporal resolution (Barrett et al., 2016; Fanin and Van Der Werf, 2017; Pereira et al., 2015) preferentially use active fire products, since the information on the day of burn contained in burned area products is not considered sufficiently accurate.

Burned area products are also used in statistical studies that investigate the regional to global feedbacks of fire on land cover and biophysical processes (Liu et al., 2019; López-Saldaña et al., 2015). The studies benefit from high spatial detail information provided with pixel products when combining them with observations of land surface condition, such as albedo or land cover.

In the last decade, an increasing number of statistical analyses have been conducted at the fire patch level. The main objective here is to characterise fire regimes based on fire size distributions (Archibald et al., 2010, 2013; Curt et al., 2013; Hantson et al., 2015; Tarimo et al., 2015). However, the low accuracy of the date of burn in contemporary pixel products together with observational gaps strongly hampers a robust fire patch identification (Oom et al., 2016).

6.6. Fire danger and early warning systems

Fire danger systems identify the main factors controlling the probability, spread and effects of fires and produce fire danger rating maps which support preventive and responsive fire management at local to continental scales (Miller and Ager, 2013; Pettinari and Chuvieco, 2020). At the core of these systems, there are statistical models that predict fire danger indicators either solely from meteorological variables or from combining meteorological information with vegetation maps, topography and/or fire history (Pinto et al., 2018; Xi et al., 2019).

The Fire Danger Forecast Module implemented within the Global Wildfire Information System (GWIS), for example, computes 1 to 9 day global forecast maps of the Fire Weather Index (FWI) at 8 km spatial resolution.⁴ There are also longer range model forecasts that predict fire danger on sub-seasonal to seasonal scale (Di Giuseppe et al., 2020).

Complementary to fire danger forecasts, there are reanalysis products of fire danger, providing global or regional information on the climatological expectation of fire danger at certain times of the year (Vitolo et al., 2019). In many cases, these fire risk assessments rely on statistics that are calculated from historical fire observations. In GWIS, for example, historic fire frequency statistics are calculated from MCD64C6 burned area time series (2002–present). Furthermore, historical fire size information from the GlobFire database is included. An important statistical parameter in this framework is the mean fire return interval (Chuvieco et al., 2014). Burned area information from space is widely used for its determination (e.g. Berner et al., 2012; Oliveras et al., 2014; Archibald et al., 2013). The estimates, however, are of limited validity in regions where fire return intervals are substantially longer (i.e. ≥ 50 years) than the observational time series (e.g. tropical or boreal forests).

Operational early warning systems that provide short-range fire danger forecasts together with NRT fire observations support fire managers and emergency responders to react in a prompt and adequate manner when a fire occurs (Pettinari and Chuvieco, 2020). Most of these systems use HS or FRP to display the current fire situation because NRT-burned area mapping is inherently more difficult (Urbanski et al., 2018). For example, GWIS allows interactively browsing and displaying global MODIS and VIIRS hotspots within 3 hours of the acquisition of the satellite image. In addition, fire perimeters are generated automatically and with a similar latency from spatially clumping the coordinates of VIIRS 375 m active fires detections. The system also displays the area burned of individual fire events (fire patches), determined from MCD64C6 information (section 3.2.4) following the GlobFire methodology (see section 3.2.9). This product, however, is only available with several months' latency. Few systems also provide quasi-NRT maps of burned areas. An example is the Brazilian ALARMES system⁵. It uses VIIRS observations of surface reflectance and thermal anomalies in a deep learning model that produces maps showing the daily evolution of burned area over Pantanal and Cerrado with 500m spatial resolution.

⁴ https://gwis.jrc.ec.europa.eu/apps/gwis_current_situation/index.html (last accessed 4 February 2021).

⁵ Alerta de Área queimada com Monitoramento Estimado por Satélite; in English: alarm system of satellite-derived burned area estimations; <https://lasa.ufjf.br/news/burned-area-pantanal-2020/> (last accesses February 2, 2021).

There is a great demand for NRT burned area information for fire management activities, and also for air quality forecasting (see section 4.3) (Geller, 2018; Schwert et al., 2016; Urbanski et al., 2018). And there are several efforts to improve the timeliness and accuracy of NRT-burned area mapping systems (Filipponi, 2018; Jang et al., 2019; Urbanski et al., 2018) to make them more suitable for these user communities.

6.7. Usage statistics of burned area information

The use of burned area information in scientific publication over the past four decades was quantitatively analysed with a Web of Science (WoS) literature database query. The query searched for the terms "burned area" OR "burnt area" OR "area burned" OR "area burnt" OR "burn scar*" in the topic field (i.e. title, abstract, author keywords and KeyWords Plus). Publications in all fields of research are included, except those relating to medical publications⁶.

3,161 scientific publications dealing with burned area information were published between 1980 to 2020. Before 1991, at most two articles were published per year; it could be considered that the scientific publications of topics related to burned area started in the 90'. Since then, publication rate increased almost exponentially, reaching 246 articles by the year 2020, with a maximum of 276 in the year 2019; in parallel, also the number of publications citing these articles sharply increased to 4600 in 2020 (Figure 1).

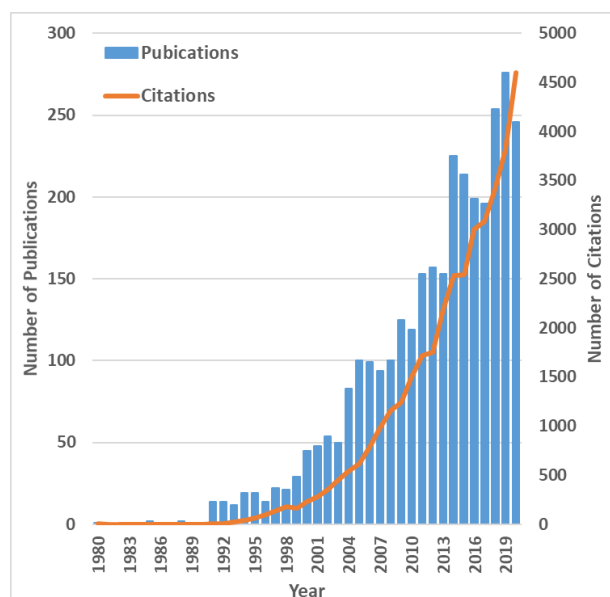


Figure 1: Web of Science (WoS) literature database query results on the temporal evolution of peer-reviewed papers dealing with burned area across 1980 to 2020: annual number of publications and sum of times cited (without self-citations)

Before 2005, most of the publications related to burned area information from satellites mention AVHRR (Figure 2a). In the following years, most publications mention MODIS, followed by Landsat. Since 2015, publications related to burned area information from Sentinel have gained an increased importance, and VIIRS publications are also increasing since 2017.

The boreal zone has been the main climatic region studied in relation with burned area, followed by the Mediterranean biome, and the fires in the tropics (Figure 2c).

⁶ Burned area can also refer to skin burns.

The WoS survey pinpoints the increasing importance of burned information for climate-related research and for various model applications over the last three decades (Figure 2d). Similarly, there is a strong increase in the number of publications addressing fire management issues and the link between burned area and emissions. The results largely agree with the detailed, full-text literature analysis conducted in 2011 by Mouillot et al. (2014) who showed that burned area products are predominantly used for atmospheric chemistry and for forest and fire management applications.

Topics such as small fires, in particular agricultural fires, are increasing, reflecting the research interest in developing methods to better detect and quantify these fires and to assess their impact on carbon budgets and fire emissions. Likewise, topics connected to health issues related to fires are also rising, showing the increased awareness of the effects of fire emissions on the population health.

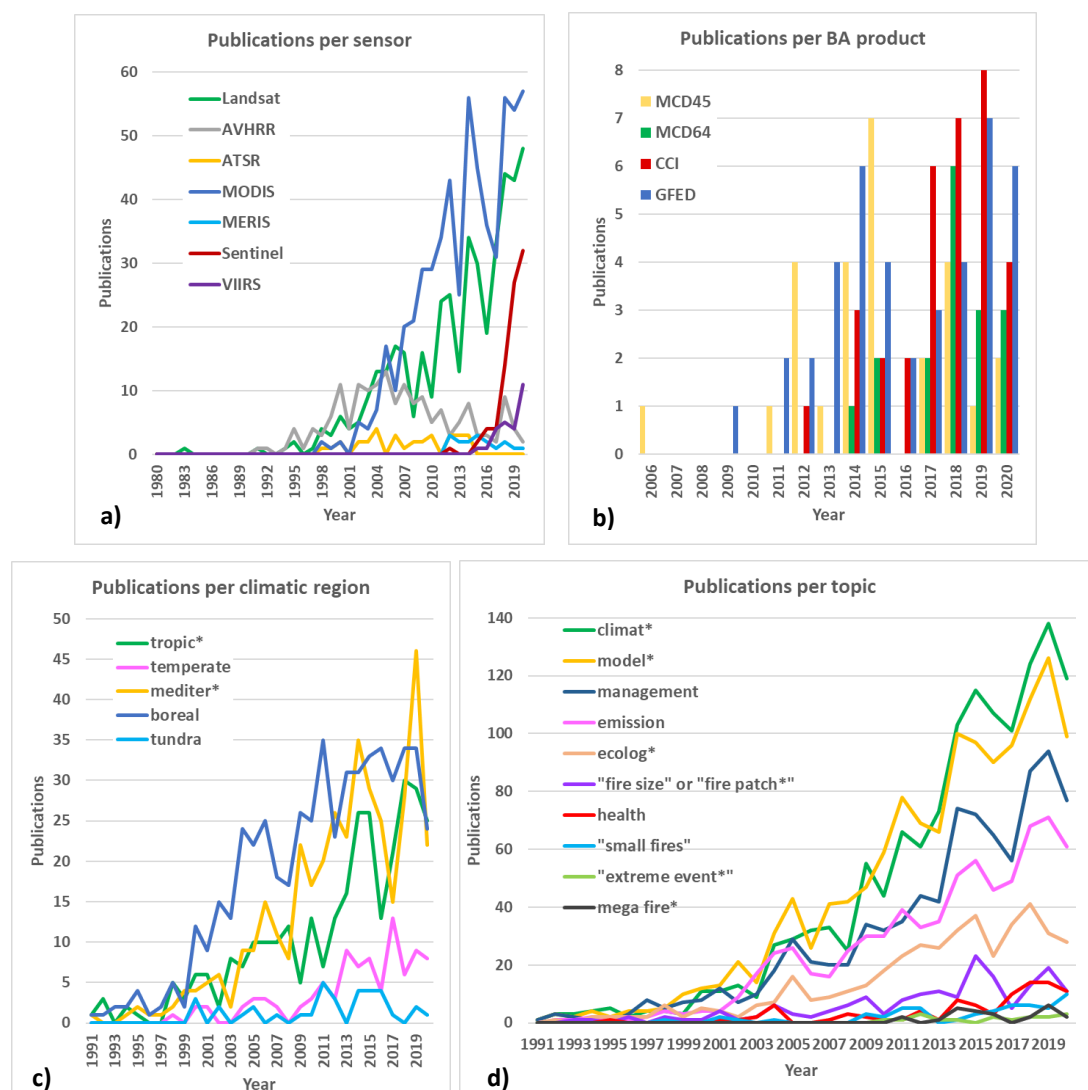


Figure 2: Web of Science (WoS) literature database query results on the temporal evolution of peer-reviewed papers dealing with burned area across 1980 to 2020: a) annual number of publications per selected sensors, b) annual number of publications per selected widely used burned area products, c) annual number of publications per climatic regions, and d) number of publications per year mentioning some selected topic keywords.

Most authors of the publications are from a U.S. institution (Figure 3). Authors from Mediterranean Europe are almost similarly active in publishing. Leading here are researchers from Spain, followed by Portugal, Italy, France and Greece (with a total of 1,005 publications between the four countries). In the U.S., most authors come from governmental agencies such as the U.S. Department of Agriculture (USDA) and its forest service, the National Aeronautics and Space Administration (NASA) and its Goddard Space Flight Center, the U.S. Department of the Interior and its Geological Survey agency (USGS), the Department of Energy (DOE) and the National Oceanic Atmospheric Administration (NOAA). Between them, they include more than 32% of all the scientific communications dealing with burned area. In Mediterranean Europe, most authors are also affiliated with governmental scientific organizations, such as the Centre National de la Recherche Scientifique (CNRS), the Consejo Superior de Investigaciones Científicas (CSIC), the Commissariat à l'énergie atomique (CEA), the Consiglio Nazionale delle Ricerche (CNR), the Institut national de la recherche agronomique (INRAE), the European Commission Joint Research Centre (JRC), and the Centro de Investigación ecológica y aplicaciones forestales (CREAF). These institutions account for 11.8% of all the publications related to burned area. Natural Resources Canada, and its Canadian Forest Service account for 5.2 % of the publications, and the Chinese Academy of Sciences for 4.6%. In all of these countries, the universities also have an important role, although lower than the public national research organizations.

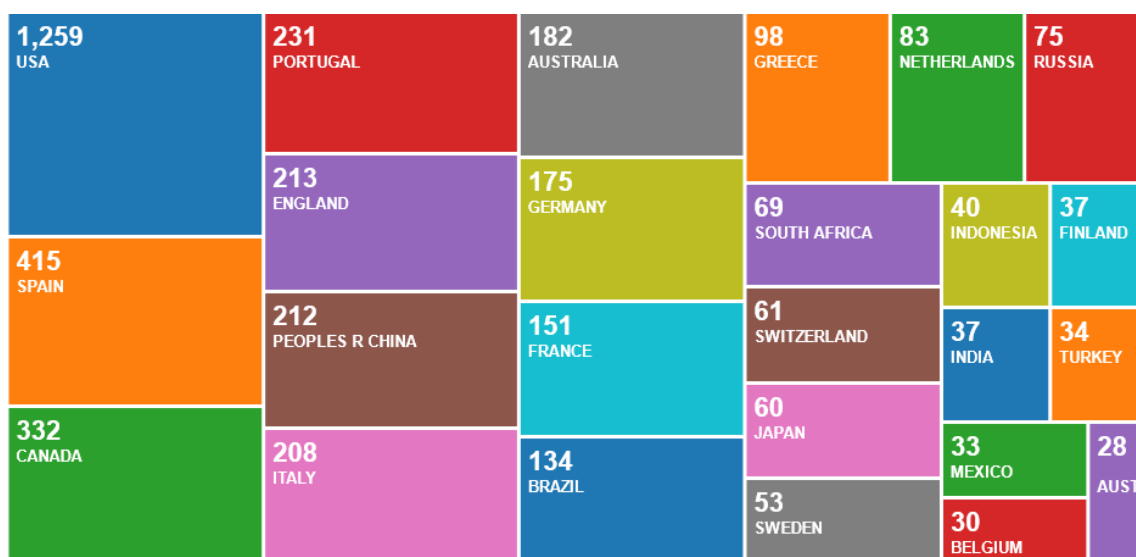


Figure 3: Tree-map showing, in terms of author affiliation, the top 25 countries in all publications dealing with burned area during 1980 to 2020 (Web of Science database query).

6.8. Usage statistics of Fire_cci products

Over the last five years, more than 40 scientific publications have been released which use Fire_cci burned area products (Table 6). The regional scope of the studies is evenly distributed between global and regional, and also grid and pixel products are evenly used. Publications focussing on the intercomparison or validation of different burned area products predominate, followed by DGVM model evaluation studies and statistical analysis on burned area trends and controls. Most of the studies only use the product's first layer (e.g. burned area or date of first detection, respectively, in the grid and pixel product). In a few cases, the layers specifying uncertainty and land cover burned are used, and in a single case the observational coverage layer was taken into account. None of the

publications uses the fire patch number layer that was provided with the Fire_cci grid products until 2020.

These usage statistics show that Fire_cci burned area products are rapidly taken up by different science communities, including climate modellers, reflecting the imminent need for new and improved satellite burned area products.

The statistics also reflect that many publications, by the time they are published in a journal, use superseded product versions. For example, several publications of the year 2020 use FireCCI50 or FireCCI41 (e.g. Lasslop et al., 2020; Pessôa et al., 2020; Hantson et al., 2020; Valencia et al., 2020) despite these products being superseded by improved versions in 2018. In analogy, the superseded MCD45 and MCD64C5 products are still widely used (Table 8). Lange et al. (2020) provides a very drastic example for the usage of outdated satellite burned area products: to evaluate burned area simulated within the Inter-Sectoral Impact Model Intercomparison Project phase 2b (ISIMIP2b (Frieler et al., 2017)) against satellite observations, they use time series from the deprecated products GLOBCARBON (Plummer et al., 2007), L3JRC (Tansey et al., 2008) and GFED3.1 (Giglio et al., 2010). The first two rely on SPOT-VGT imagery, and it is well established that related burned area products suffer from strong omission errors in the tropics while substantially overestimating burned area in boreal and temperate regions (Humber et al. 2018; see also section 3.1.1). Hao et al. (2020, in review) uses the beta FireCCILT10 product which was released in 2019 (see section 3.2.3). The usage of outdated, faulty and/or too immature burned area products is unfortunate as it diminishes the gain in knowledge and can cause misleading interpretations (Giglio and Roy, 2020)

One aspect, for example, is that it becomes more difficult – if not impossible – to compare climate studies when they use different versions of a burned area product. While this phenomenon can be partially explained by the long time needed to prepare and submit a manuscript and to get it accepted by a journal, there is also substantial misinformation among climate scientist about which burned area product version is most up-to-date for their application. It therefore deems imperative that those responsible for the public release of burned area products keep their product users informed whenever a new product supersedes another version. It is also similarly essential to carefully balance between version stability and the requirement that product improvements are made accessible in a timely manner.



Fire_cci **User Requirements Document**

Ref.	Fire_cci_D1.1_URD_v7.2		
Issue	7.2	Date	28/04/2021
Page			37

Table 6: Peer-reviewed publications using of Fire_cci products.

Reference	Product	Product type	Target resolution		Layer	Period	ROI	Other BA products	Application of Fire_cci products
Hantson et al., 2016*	FireCCI31	grid	0.5°	month	BA	2006-2008	Global	GFED4, L3JRC, MCD45	Analysis of uncertainties in BA products used in DGVM benchmarking; inter-product differences as indicator for observational uncertainty
Nogueira et al., 2017b*	FireCCI31	pixel	fire patch	year	DOB, CL	2006-2008	Brazil	MCD45	Evaluation of the ability of global BA products to accurately represent morphological features of fire patches
Fornacca et al., 2017	FireCCI41	pixel	fire patch	year	DOB, LC	2006, 2009	China	MCD45, MCD64C6	Evaluation of performance of multiple BA products
Forkel et al., 2017*	FireCCI41	grid	0.25°	month	BA	2005-2011	Global	GFED4	Evaluation of a data-driven fire model; inter-product differences as indicator for observational uncertainty
Nogueira et al., 2017a*	FireCCI40	grid	0.5°	month	BA	2002-2011	Brazil	MCD45, GFED4, GFED4s	Evaluation of biome-specific BA – fire danger relationship; inter-product differences as indicator for observational uncertainty
Arora and Melton, 2018	FireCCI41	grid	2.8°	year	BA	2005-2011	Global	GFED4s	Evaluation of BA modeled by process-based TEM
Lasko and Vadvu, 2018	FireCCI31	grid	0.5°	month	BA	2006-2008	Vietnam	MCD64C5	Fire emission calculation; inter-product differences as indicator for observational uncertainty
Laurent et al., 2018*	FireCCI41	pixel	fire patch	day	DOB	2005-2011	Global	MCD64C6	Creation of a global database of fire patch functional traits
Santana et al., 2018	FireCCI41?	pixel	pixel	day	DOB	2005-2011?	Brazil	MCD64C5/6?, MCD45	Evaluation a new BA detection approach by intercomparison with other BA product
Schaphoff et al., 2018	FireCCI41	grid	0.5°	multiyear average	BA	2005-2011	Global	GFED4	Evaluation of BA modeled by DGVMs
Zheng et al., 2018	FireCCI41	pixel	pixel*	month	DOB	2005-2011	Africa	GFED4, GFED4s, GFED3	Intercomparison of fire seasonality in different BA products
Barbero et al., 2019	FireCCI50	pixel	large fire patches		DOB	2001-2016	France	–	Development of a nationwide statistical model including wildfire-prone regions
Brennan et al., 2019*	FireCCI50	grid	0.25°	month	BA, UNC	2001-2013	Global	MCD64C6, MCD45	Estimation of theoretical uncertainties from multiple BA products and comparison with uncertainties provided with products
	FireCCI50	pixel	pixel to 1°	day	DOB, CL	2001-2013	Global		
Burton et al.,	FireCCI31	grid	1.3°x1.9°	year	BA	2006-	Global	MCD45,	Benchmarking a Bayesian interference model to construct



Fire_cci **User Requirements Document**

Ref.	Fire_cci_D1.1_URD_v7.2		
Issue	7.2	Date	28/04/2021
Page			38

Reference	Product	Product type	Target resolution		Layer	Period	ROI	Other BA products	Application of Fire_cci products
2019						2008		GFED4, GFED4s	BA; inter-product differences as indicator for observational uncertainty
Forkel et al., 2019a*	FireCCI41, FireCCI50	grid	1.9°x2.5°	month	BA,(Fire CCI41: BA, FOA)	2005-2011	Global	GFED4, GFED4s, MCD64C6	Evaluating the relationship between BA and controlling factors in DGVMs
Forkel et al., 2019b*	FireCCI50	grid	0.25°	month	BA	2001-2015	Global	GFED4	Assessment of the spatio-temporal robustness of observed BA trends and their controls
Humber et al., 2019	FireCCI41	pixel	pixel to coarse	day	DOB	2005-2011	Global	MCD45, MCD64C6, GIO-GL1	General intercomparison of BA products
Long et al., 2019	FireCCI50	pixel	pixel	year	DOB	2015	Global	GFED4	Assessment of the GABAM BA product by intercomparison
Moreno-Ruiz et al., 2019	FireCCI51	pixel	pixel	year	DOB	2001-2015	Alaska	MCD64C6, BALDR	General intercomparison of BA products
Mota et al., 2019	FireCCI41	pixel	0.05°	month	DOB	2005-2011	Global	MCD64C6, GIO-GL1	Evaluation of consistency between albedo and BA products; inter-product differences as indicator for observational uncertainty
Silva Junior et al., 2019	FireCCI51	pixel	30 m	year	DOB	2006-2016	Brazil	—	Investigation of fire responses to droughts years
Teckentrup et al., 2019*	FireCCI50	grid	2.8°	year (clim)	BA, UNC	2001-2013	Global	GFED4, GFED4s	Evaluation of BA modelled by FireMIP DGVMs
Turco et al., 2019*	FireCCI51	grid	0.25°	month	BA, LC	2001-2011	Europe	MCD64C6, GFED4s, GFED	General intercomparison of BA products
Lizundia-Loiola et al., 2020b*	FireCCI51	grid	0.25°	year	BA	2001-2019	Amazonia	—	Compare BA during the 2019 fire year with mean of previous years and assess burned area anomalies
Bowman et al., 2020*	FireCCI51	grid	0.25°	year	BA	2001-2020	Australia	—	Compare BA during the 2019–20 fire year with mean of previous years and assess which fuel type burned
Vetrina et al, 2020	FireCCI51	pixel	pixel	day	DOB	2014	Indonesia	MCD64C6, MCD45	Assess how accurately BA products detect burn scars from fires in peatlands and non-peatlands
Lasslop et al., 2020	FireCCI50	grid	2.8°	year (clim)	BA	2001-2012	Global	GFED4, GFED4s	Evaluate FireMIP model results; inter-product differences as indicator for observational BA uncertainty
Pessôa et al., 2020	FireCCI50	pixel	10 km	year	DOB	2015	Brazil	INPE-TREES, MCD64C6, GABAM	Intercomparison of BA products and implications for carbon emission estimation

Reference	Product	Product type	Target resolution		Layer	Period	ROI	Other BA products	Application of Fire_cci products
Pinto et al., 2020	FireCCI51 FireCCILT10	pixel	0.01° pixel	day	DOB	2012-2017, 2016	Global Mozambique	MCD64C6, ICNF, TERN, MTBS	Intercomparison with BA mapped with deep learning approach; product validation
Shimabukuro et al., 2020	FireCCI51	pixel	10 km	year	DOB	2015	Brazil	MCD45, MCD64C6,	Evaluate a new BA mapping approach based on PROBA-V&VNP09GA&LS8-OLI by intercomparison with other BA products
Bar et al., 2020	FireCCI5?	pixel	fire patch	year	DOB	2016-2019	Himalaya	MCD64C6	Evaluate new BA mapping approaches based in LS8 and S2 by intercomparison with other BA products
Chen et al., 2020	FireCCI51	grid	0.5°	month	BA	2001-2016	China	GFED4s	Intercomparison with GFED4s and with BA from ELM fire model
Mitsopoulos et al., 2020	FireCCI51	pixel	pixel	year	BA	2007-2018	Greece	—	BA information is used to establish a national fire hazard database with focus on wildland-urban interface areas
Bastos et al., 2020	FireCCI51	grid	1°	year	BA	2001-2017	Global	GFED4s	Comparison of DGVM-simulated BA with observed BA
Hantson et al., 2020	FireCCI41, FireCCI51	grid	0.5°	month	BA	2001-2013	Global	MCD45, GFED4, GFED4s	Benchmark FireMIP model results; inter-product differences as indicator for observational BA uncertainty
Valencia et al., 2020	FireCCI41, FireCCI50	pixel	pixel, fire patch	year	DOB	2007-2008	Africa, S-America	MCD45, MCD64C5/6	Demonstrate a new validation-comparison method for burned area products
Nguyen and Wooster, 2020	FireCCISFD11	grid	0.25°	month	BA	2016	Africa	GFED4s	Compute data-driven fuel consumption maps by dividing FRP-based top-down emission estimates with FireCCISFD11 burned area
Campagnolo et al., 2021	FireCCI51	pixel	pixel, fire patch	fire season	DOB	2015	Brazil	MCD64C6	Product validation by land cover and fire size
Chuvieco et al., 2021*	FireCCI51	grid	0.25	year	BA	2001-2018	Global	—	Evaluate burning variability according to human and climate global drivers of fire
Liu and Crowley, 2021	FireCCI51	grid	0.25	year	BA	2003-2019	Asia	MCD64C6	Comparison of tiling artifacts in burned area products.
Ramo et al., 2021*	FireCCISFD11	grid	0.25	year	BA	2016	Africa	GFED4s	Analysis of small fires for burned area and carbon emissions estimation
Hao et al., 2021*	FireCCILT10	grid	country total	year	BA, UNC	1982-2017	Eurasia	MCD64C6, FEI-NEI	Discuss long-term BA trend in relation to economic situation

Note: year (clim) means a climatological year (multiyear average)

* Includes as co-authors members of the Fire_cci consortium.

6.9. User requirement surveys

Several user requirement surveys by questionnaire or workshops were conducted in recent years within the Fire_cci project (Heil et al., 2017; Pettinari et al., 2017; Schultz et al., 2011). The 2017 FireMIP workshop and EGU 2018 Fire_cci product review meeting constitute the most recent and in-depth Fire_cci user requirement gathering workshops. Most participants were DGVM modellers, particularly those participating in the FireMIP initiative (see Section 4.2), which constitute a key climate user group of global burned area products. The requirements expressed in the Fire_cci surveys largely agree with the key requirements stated in recent scientific publications (see Section 4). The outcomes of the user requirement surveys are documented in detail in Heil et al. (2017).

Here, we only provide a summary of specific user requirement aspects not addressed before:

(a) Accuracy and stability

- Quantitative statements on accuracy and stability requirements of burned area products as expressed in surveys or by science initiatives cannot be meaningfully interpreted because it is unclear to what the statements exactly relate to. It is, e.g., not clear to what statistical measure of accuracy/stability the statements are referring to and whether they relate to global or regional products or to monthly, annual or multiannual average; see also Heil et al. (2017).
- General consensus across all user communities is that they require higher accuracies than achieved in contemporary burned area products. Of particular concern is their inability to resolve smaller fires, which is why developments of regional to optimally global burned area products that rely on sensors with higher spatial resolution are highly supported. Atmospheric chemistry modellers additionally request improvements in the date of burn information towards temporal accuracies of less than 2 days error. Inherent to burned area products from higher resolution sensors is a lower temporal resolution. Consequently, they are primarily suitable for advancing the general understanding of the relative contribution of small fires in different regions of the world.
- In view of the global relevance of emissions from fires in peatlands, there is a strong demand for an improved mapping of burned areas in these regions. An accurate characterisation of burned area in peatlands is not only essential to atmospheric chemistry applications, but also for greenhouse gas reporting. The unavailability of an adequately accurate long-term dataset of burned area in peatlands still impedes a better knowledge of the climatic drivers of peatland fires. Developments in this direction are therefore urgently requested.

(b) Fire-enabled DGVM modellers

Contemporary burned area products cannot meet all requirements for fire-enabled DGVMs, and specifically those participating in the FireMIP initiative (see Hantson et al. (2016) and Annex 4 of Heil et al. (2017)):

- Most importantly is the need for sufficiently long and temporally consistent time series with regional to optimally global coverage. Sufficiently implies that they are long enough for robustly detecting trends, adequately sampling extreme events, or encompassing the full range of inter-annual and multi-decadal variability. This is not fulfilled by the maximally around 20 years of observations

provided by present burned area products (Forkel et al., 2019b). When contemporary products are used for model calibration, the model's ability to realistically capture these features is therefore limited (Teckentrup et al., 2019). As important as the record length is the consistency of the time series. Consistency implies that the burned area time series have no unquantified artificial trends and variability due to e.g. changes in the underlying satellites or sensors. Of the different merging strategies that can be applied to create long burned area time series from multi-sensor information, FireMIP scientists considered merging at the reflectance level as most attractive.

- Missing observational constraints on several fire characteristics such as the rate of spread, fire-line intensity, and fuel consumption and on proxies of the fire's impact on vegetation and soil (e.g. fire-induced tree mortality and the post-fire recovery dynamics) currently strongly hamper efforts to improve the representation of fire-related processes in FireMIP models. The FireMIP community therefore strongly promotes product developments, which will deliver related observational information either as extra data layer within burned area products or as separate ancillary data products.
- Recent developments in FireMIP model evaluation address benchmarking the model's capacity to capture the size distribution, duration and speed of fires. This requires patch-based burned area products providing these parameters.
- The under-representation of small fires in contemporary burned area products has various implications on the parameterisation and benchmarking of spatio-temporal patterns of fire occurrence and of fire size distribution, with complex consequences on how realistic fire characteristics, dynamics and impacts are captured. Developments of regional to optimally global burned area products that rely on high spatial resolution sensors able of better resolving small fires are therefore highly requested.
- FireMIP validation will also address short-term model behaviour, which demands for high temporal resolution (hourly to daily) burned area benchmark datasets.
- The estimation of burned area in gridded burned area products shall preferentially be based on probabilistic aggregation of pixel-level burn probabilities, yielding a description of the distribution of burned area within the grid cell. Presuming a Gaussian distribution, this is the mean and the standard deviation of the distribution. The latter is a quantitative measure for the spread of possible values within the grid cell and hence of the uncertainty of the estimate.
- Prospectively, the calculation of FireMIP benchmark scores shall also explicitly account for the uncertainties in the observational data (Hantson et al., 2016). This requires gridded burned area products to provide uncertainty layers that reflect the true uncertainties involved in the burned area estimation, complemented by a user guide that provides explanations and instructions on how the product-inherent uncertainties are to be interpreted and correctly used. Grid level uncertainty shall be provided as standard deviation in a layer that is unequivocally named (c.f. section 6.3. and Annex 4 in Heil et al., 2017).
- Most participants clearly favoured grid products that compute the estimated burned area from probabilistic aggregation of burn uncertainties. As an intermediate solution, a best guess fixed-threshold-based BA estimate combined with a realistic estimate of the variance, e.g. as standard deviation, would be beneficial

(c) Users of burned area pixel products

- Users of pixel products requested product-inherent quality information layers that flag whenever the algorithm or the sensor failed, contaminations by clouds, cloud or topographic shadows or smoke, or otherwise poorly or unobservable pixels, and the sensor type in merged products.

(d) Requirements across all product users

- Product users require public web-based data access that allows for convenient systematic and fast download (Schultz et al., 2011) – a request that is met by all current burned area products (see e.g. Table 1).
- Consistent naming and versioning of products is recommended to ensure that they can be unambiguously referenced.
- Most users are content with a NetCDF file format for grid products and GeoTIFF for the pixel products - a requirement already met by Fire_cci burned area products.

7. Recommendations

Several recommendations for future Fire_cci product developments and activities can be drawn from the analysis of how and from what sensor burned area products are presently used, the specific needs expressed by key user communities, and the gap between requirements and the characteristics of present Fire_cci burned area products. Table 7 gives a synthesis overview of the key recommendations. The recommendations are elucidated in more detail below.

(a) Product resolution, format and types

- Burned area products shall be provided as a CMG version together with a consistent pixel product version, and shall be complemented by a patch product providing information on the size of individual fires. CMG products generated by the Fire_cci project shall be delivered in CF-compliant NetCDF-4 (classic) format, while GeoTIFF format for pixel products is similarly adequate.
- Fire_cci products shall prospectively respond to the needs of the climate community for grid products. The CMG spatial resolution requested by most users is 0.1° and 0.25° . Several global to regional CMG fire products have developed towards 0.1° or 0.05° spatial resolution. Particularly for regional Fire_cci CMG products from high-resolution sensors, a 0.1° or 0.05° spatial resolution grid product shall be envisaged. Optimally, grid products shall be provided at 0.25° , 0.1° and 0.05° to enhance flexibility, or, alternatively, a single product at high resolution and instructions how to upscale the product's data layers to a user-defined coarser resolution, e.g. by providing guidance and python code for doing so using the ESA's Climate Analysis Toolbox (Cate)
- While monthly temporal resolution of CMG burned area products is still adequate for many climate applications, there is a strongly increasing request for products with daily resolution. If CMG products are provided with monthly resolution, then supplementary proxy information shall be developed that help these users generating the best possible daily to hourly estimates.

Table 7: Key recommendations for future fire ECV developments.

Item	Fire ECV burned area product developments shall target with priority
Product resolution (spatial, temporal)	<ul style="list-style-type: none"> - global grid products: 0.25° and/or 0.1° daily - regional grid products: 0.05°, daily - regional pixel products: 30 m, yearly
Temporal coverage	>> 20 years
Validation	<ul style="list-style-type: none"> - at least stage 3 validation (or equivalent) along the entire BA time series - complementary qualitative product assessments
Documentation	<ul style="list-style-type: none"> - documentation on product validation released together with products - guidance on how to resample products
Ancillary data layers	<ul style="list-style-type: none"> - full uncertainty quantification: <ul style="list-style-type: none"> pixel product: burn probability and uncertainty in the day of burn grid product: overall BA uncertainty as standard deviation - indicator on observational quality (e.g. no observation due to clouds) - land cover burned, land cover classification supporting GHG emission stocktaking for UNFCCC
Ancillary products	<ul style="list-style-type: none"> - fire patch database with information on fire dynamics - observational constraints on fuel consumption - observations of the impact of fires (e.g. tree mortality) - NRT burned area mapping products
Priority BA mapping improvements	<ul style="list-style-type: none"> - frequently cloud covered areas - areas covered by organic soils - small fires, including crop residue burning
Product release management	<ul style="list-style-type: none"> - balanced release frequency of new product versions - directly inform product users when products are superseded/revoked

(b) Temporal coverage and timeliness

- Developments of global burned area time series shall target the longest possible temporal coverage. Multi-sensor products, optimally merged at the reflectance level, are highly desired for this purpose provided that temporal consistency can be assured.
- Most applications are not affected by the one to two years of latency that burned area products typically have. Measures, however, shall be taken to secure similar timeliness in case that the underlying sensor fails (e.g. Vetrita et al., 2020). A secured temporal continuity also has the advantage that burned area time series get longer as time progresses.
- For NRT atmospheric forecasting and fire emergency management systems to use burned area products would require developments towards NRT-burned area mapping.

(c) Accuracy and stability

- There is common qualitative agreement among users that future developments shall achieve higher accuracies than contemporary burned area products and that the burned area time series shall have high temporal stability. Implicitly, users request that burned area products are generated with the best algorithm possible.

This request calls for efforts directed towards the development of novel algorithms, algorithm improvements and algorithm performance comparisons (e.g. Campagnolo et al. (2019) or Ramo et al. (2018)).

- Contemporary burned area products do not provide an accurate mapping of fires in peatlands, despite their particular relevance to global GHG emissions and regional air pollution. The development of new remote sensing products that tackle this problem is a repeated request from researchers and decision makers. Vetrina et al. (2020), e.g., recommend the development of multi-sensor integration products which combine information from passive and active sensors.
- An easy-to-understand documentation demonstrating and explaining the prominent error characteristics of individual products shall be provided, detailing e.g. which fire types are commonly missed and how products inter-compare to other products.
- For atmospheric chemistry modellers, improvements in the date of burn information shall be envisaged, optimally by achieving timing errors less than 1-2 days.

(d) Uncertainty characterisation


- Product uncertainty characterisation is considered most intuitive when provided as burn probabilities in the pixel product, with the layer also named accordingly. The uncertainty characterisation for the estimation of burned area in the grid product shall be delivered as standard uncertainty (i.e. expressed as standard deviation) in a layer named accordingly. Prospectively, uncertainty information on the detected date of burn shall also be provided.
- Burned area products shall therefore be provided with user guidelines, which provide practical instructions how to correctly use and interpret uncertainty information provided with the products.

(e) Evaluation and validation

- Any product shall be subject to comprehensive product validation by independent validators. The validation approach shall target at least CEOS stage 3, i.e. it shall include a large number of stratified random samples over a multi-year time period. The validation plan shall ensure that, with a product's release, omission and commission errors are well quantified and described in the products' validation reports.
- Validation shall be performed on the temporal extensions of already validated products prior to their release.
- Evaluation activities of the performance of burned area products in specific regions, biomes and periods shall complement the conventional product validation and shall encompass product intercomparison and cross-ECV consistency. It is essential that the results of these assessments are made available along with the validation results.

(f) Data layers

- A data layer providing information on the vegetation cover that burned, both in pixel and CMG products, is a common request from climate users and also supports activities towards improving reporting fire-related GHG emissions to the

 fire cci	Fire_cci User Requirements Document	Ref.	Fire_cci_D1.1_URD_v7.2	
		Issue	7.2	Date 28/04/2021
				Page 45

UNFCCC. To ensure cross-ECV consistency, the latest ESA CCI Land Cover product shall be used for this purpose.


- Grid products shall contain a layer quantifying the observational coverage, e.g. in form of the fraction of observed area. Pixel products shall contain data quality information comprising a specific flagging for cloud contamination/shadow, aerosol contamination, saturation, algorithm or sensor failure, etc. To guarantee traceability, users also request pixel-based information on the sensors used when merged multi-sensor products are provided.
- A clear description of the errors, detailing which fire types are commonly missed by the product seems to be a common requirement among users. There is a particular increasing demand for a detailed characterisation of small fires missed by most satellite sensors. Ancillary, regional-scale products from high resolution satellite observation are expected to detect small fires which are missed by the coarser resolution satellite products and are therefore increasingly requested.

(g) Supplementary observations

- The scientific user community has an emergent request for fire patch products, which describe the characteristics of individual fires identified through spatio-temporal clustering. Fire patch products shall be computed from and provided complementary to Fire_cci pixel products. The patch products shall contain information on fire patch morphology and dynamics and shall be evaluated and documented to users.
- Fuel consumption and various other parameters reflecting the impacts of fire on vegetation, such as tree mortality or timescales of post-fire recovery, are still poorly constrained by observations, but are essential to improve the parameterisation and evaluation of DGVM models and of fire emission estimates. Related product developments are therefore highly recommended. A common suggestion in this direction is the production of combined burned area – FRP products. Also the provision of fire temperature estimates shall be envisaged.
- Algorithms and products allowing to identify and quantify of crop residue burning shall be envisaged to improve fire emission estimation and air quality forecasting.

(h) Product version planning, control, dissemination and user information

- Fire_cci burned area products shall be provided with a product user guide that describes the individual data layers and that also contains a description of the product's limitations and usage recommendations. In addition, a more detailed documentation of the product's quality assessment shall be delivered.
- The continued use of deprecated or revoked product versions is common in climate science applications and frequently caused by ignorance, except for dedicated product inter-comparisons. This shall be circumvented by stringent product version labelling, careful planning to avoid too frequent product updates, and clear user information whenever a product is superseded by a newer version, including a description of what relevant aspects changed.
- Data access to the Fire_cci products shall be possible via non-interactive download (e.g. wget, ftp) and via the CCI Open Data Portal (ODP). Fire_cci products shall meet CCI data standards, which implies NetCDF format as a

	Fire_cci User Requirements Document	Ref.	Fire_cci_D1.1_URD_v7.2	
		Issue	7.2	Date 28/04/2021
			Page	46

priority, but GeoTIFF for pixel products is considered similarly adequate by most users.

8. References

- Aleksankina, K., Heal, M. R., Dore, A. J., Van Oijen, M. and Reis, S.: Global sensitivity and uncertainty analysis of an atmospheric chemistry transport model: The FRAME model (version 9.15.0) as a case study, *Geosci. Model Dev.*, doi:10.5194/gmd-11-1653-2018, 2018.
- Alonso-Canas, I. and Chuvieco, E.: Global burned area mapping from ENVISAT-MERIS and MODIS active fire data, *Remote Sens. Environ.*, 163, 140–152, doi:10.1016/j.rse.2015.03.011, 2015.
- Andela, N. and Van Der Werf, G. R.: Recent trends in African fires driven by cropland expansion and El Niño to la Niña transition, *Nat. Clim. Chang.*, doi:10.1038/nclimate2313, 2014.
- Andela, N., Liu, Y. Y., van Dijk, A. I. J. M., de Jeu, R. A. M., McVicar, T. R.: Global changes in dryland vegetation dynamics (1988–2008) assessed by satellite remote sensing: comparing a new passive microwave vegetation density record with reflective greenness data, *Biogeosciences*, 10, 6657–6676, doi:10.5194/bg-10-6657-2013.
- Andela, N., Morton, D. C., Giglio, L., Paugam, R., Chen, Y., Hantson, S., van der Werf, G. R. and Anderson, J. T.: The Global Fire Atlas of individual fire size, duration, speed and direction, *Earth Syst. Sci. Data*, 11(2), 529–552, doi:10.5194/essd-11-529-2019, 2019.
- Aouizerats, B., van der Werf, G. R., Balasubramanian, R., Betha, R.: Importance of transboundary transport of biomass burning emissions to regional air quality in Southeast Asia during a high fire event, *Atmos. Chem. Phys.*, 15, 363–373, doi:10.5194/acp-15-363-2015, 2015.
- Archibald, S., Lehmann, C. E. R., Gomez-Dans, J. L. and Bradstock, R. A.: Defining pyromes and global syndromes of fire regimes, *Proc. Natl. Acad. Sci.*, 110(16), 6442–6447, doi:10.1073/pnas.1211466110, 2013.
- Archibald, S., Scholes, R. J., Roy, D. P., Roberts, G. and Boschetti, L.: Southern African fire regimes as revealed by remote sensing, *Int. J. Wildl. Fire*, 19(7), 861–878, doi:10.1071/WF10008, 2010.
- Armenteras, D., Gibbes, C., Anaya, J. A. and Dávalos, L. M.: Integrating remotely sensed fires for predicting deforestation for REDD+, *Ecol. Appl.*, doi:10.1002/eap.1522, 2017.
- Arora, V. K. and Melton, J. R.: Reduction in global area burned and wildfire emissions since 1930s enhances carbon uptake by land, *Nat. Commun.*, doi:10.1038/s41467-018-03838-0, 2018.
- Azhar, R., Zeeshan, M. and Fatima, K.: Crop residue open field burning in Pakistan; multi-year high spatial resolution emission inventory for 2000–2014, *Atmos. Environ.*, 20–33, doi:10.1016/j.atmosenv.2019.03.031, 2019.
- Ban, J.-W., Stevens, R. and Perera, R.: Predictors for independent external validation of cardiovascular risk clinical prediction rules: Cox proportional hazards regression analyses, *Diagnostic Progn. Res.*, doi:10.1186/s41512-018-0025-6, 2018.
- Bar, S., Parida, B. R. and Pandey, A. C.: Landsat-8 and Sentinel-2 based Forest fire burn area mapping using machine learning algorithms on GEE cloud platform over Uttarakhand, Western Himalaya, *Remote Sensing Applications: Society and Environment*, 18, 100324, <https://doi.org/10.1016/j.rsase.2020.100324>, 2020.
- Barbero, R., Curt, T., Ganteaume, A., Maillé, E., Jappiot, M. and Bellet, A.: Simulating the effects of weather and climate on large wildfires in France, *Nat. Hazards Earth Syst. Sci.*, doi:10.5194/nhess-19-441-2019, 2019.
- Barrett, K., Loboda, T., McGuire, A. D., Genet, H., Hoy, E. and Kasischke, E.: Static and dynamic

controls on fire activity at moderate spatial and temporal scales in the Alaskan boreal forest, *Ecosphere*, doi:10.1002/ecs2.1572, 2016.


- Bastos, A., O'Sullivan, M., Ciais, P., Makowski, D., Sitch, S., Friedlingstein, P., Chevallier, F., Rödenbeck, C., Pongratz, J., Lujckx, I. T., Patra, P. K., Peylin, P., Canadell, J. G., Lauerwald, R., Li, W., Smith, N. E., Peters, W., Goll, D. S., Jain, A. K., Kato, E., Lienert, S., Lombardozzi, D. L., Haverd, V., Nabel, J. E. M. S., Poulter, B., Tian, H., Walker, A. P. and Zaehle, S.: Sources of Uncertainty in Regional and Global Terrestrial CO₂ Exchange Estimates, *Global Biogeochemical Cycles*, 34(2), e2019GB006393, <https://doi.org/10.1029/2019GB006393>, 2020.
- Bauwens, M., Stavrakou, T., Müller, J. F., De Smedt, I., Van Roozendaal, M., Van Der Werf, G. R., Wiedinmyer, C., Kaiser, J. W., Sindelarova, K. and Guenther, A.: Nine years of global hydrocarbon emissions based on source inversion of OMI formaldehyde observations, *Atmos. Chem. Phys.*, doi:10.5194/acp-16-10133-2016, 2016.
- Belenguer-Plomer, M. A., Pettinari, M. L.: ESA CCI ECV Fire Disturbance: D3.3.5. Product User Guide – Sentinel-1 South America, version 1.0. Available at: <https://www.esa-fire-cci.org/documents>, 2019.
- Belenguer-Plomer, M. A., Tanase, M. A., Fernandez-Carrillo, A. and Chuvieco, E., Burned area detection and mapping using Sentinel-1 backscatter coefficient and thermal anomalies, *Remote Sens. Environ.*, 233, 111345, doi:10.1016/j.rse.2019.111345, 2019.
- Benedetti, A., Reid, J. S., Knippertz, P., Marsham, J. H., Di Giuseppe, F., Rémy, S., Basart, S., Boucher, O., Brooks, I. M., Menut, L., Mona, L., Laj, P., Pappalardo, G., Wiedensohler, A., Baklanov, A., Brooks, M., Colarco, P. R., Cuevas, E., Da Silva, A., Escribano, J., Flemming, J., Huneus, N., Jorba, O., Kazadzis, S., Kinne, S., Popp, T., Quinn, P. K., Sekiyama, T. T., Tanaka, T. and Terradellas, E.: Status and future of numerical atmospheric aerosol prediction with a focus on data requirements, *Atmos. Chem. Phys.*, doi:10.5194/acp-18-10615-2018, 2018.
- Berchet, A., Pison, I., Chevallier, F., Paris, J. D., Bousquet, P., Bonne, J. L., Arshinov, M. Y., Belan, B. D., Cressot, C., Davydov, D. K., Dlugokencky, E. J., Fofonov, A. V., Galanin, A., Lavrič, J., Machida, T., Parker, R., Sasakawa, M., Spahni, R., Stocker, B. D. and Winderlich, J.: Natural and anthropogenic methane fluxes in Eurasia: A mesoscale quantification by generalized atmospheric inversion, *Biogeosciences*, 12(18), 5393–5414, doi:10.5194/bg-12-5393-2015, 2015.
- Bistinas, I., Oom, D., Sá, A. C. L., Harrison, S. P., Prentice, I. C. and Pereira, J. M. C.: Relationships between human population density and burned area at continental and global scales, *PLoS One*, 8(12), doi:10.1371/journal.pone.0081188, 2013.
- Bocquet, M., Elbern, H., Eskes, H., Hirtl, M., Aabkar, R., Carmichael, G. R., Flemming, J., Inness, A., Pagowski, M., Pérez Camaño, J. L., Saide, P. E., San Jose, R., Sofiev, M., Vira, J., Baklanov, A., Carnevale, C., Grell, G. and Seigneur, C.: Data assimilation in atmospheric chemistry models: Current status and future prospects for coupled chemistry meteorology models, *Atmos. Chem. Phys.*, doi:10.5194/acp-15-5325-2015, 2015.
- Bojinski, S., Verstraete, M., Peterson, T. C., Richter, C., Simmons, A. and Zemp, M.: The concept of essential climate variables in support of climate research, applications, and policy, *Bull. Am. Meteorol. Soc.*, 95(9), 1431–1443, doi:10.1175/BAMS-D-13-00047.1, 2014.
- Boschetti, L., Roy, D. P. and Justice, C. O.: International Global Burned Area Satellite Product Validation Protocol, [online] Available from: <http://lpvs.gsfc.nasa.gov/PDF/BurnedAreaValidationProtocol.pdf>, last accessed 30 July 2009, 2009.
- Boschetti, L., Roy, D. P., Giglio, L., Huang, H., Zubkova, M. and Humber, M. L.: Global validation of the collection 6 MODIS burned area product, *Remote Sens. Environ.*, 235,

111490, doi:10.1016/j.rse.2019.111490, 2019.


- Bowman, D., Williamson, G., Yebra, M., Lizundia-Loiola, J., Pettinari, M. L., Shah, S., Bradstock, R. and Chuvieco, E.: Wildfires: Australia needs national monitoring agency, *Nature*, 584(7820), 188–191, <https://doi.org/10.1038/d41586-020-02306-4>, 2020.
- Brennan, J., Gómez-Dans, J. L., Disney, M. and Lewis, P.: Theoretical uncertainties for global satellite-derived burned area estimates, *Biogeosciences Discuss.*, 1–25, doi:10.5194/bg-2019-115, 2019.
- Burton, C., Betts, R., Cardoso, M., Feldpausch, R. T., Harper, A., Jones, C. D., Kelley, D. I., Robertson, E. and Wiltshire, A.: Representation of fire, land-use change and vegetation dynamics in the Joint UK Land Environment Simulator vn4.9 (JULES), *Geosci. Model Dev.*, doi:10.5194/gmd-12-179-2019, 2019.
- Campagnolo, M. L., Libonati, R., Rodrigues, J. A. and Pereira, J. M. C.: A comprehensive characterization of MODIS daily burned area mapping accuracy across fire sizes in tropical savannas, *Remote Sens. Environ.*, 252, 112115, <https://doi.org/10.1016/j.rse.2020.112115>, 2021.
- Campagnolo, M. L., Oom, D., Padilla, M. and Pereira, J. M. C.: A patch-based algorithm for global and daily burned area mapping, *Remote Sens. Environ.*, 232(June), 111288, doi:10.1016/j.rse.2019.111288, 2019.
- Carmona-Moreno, C., Belward, A., Malingreau, J. P., Hartley, A., Garcia-Alegre, M., Antonovskiy, M., Buchshtaber, V. and Pivovarov, V.: Characterizing interannual variations in global fire calendar using data from Earth observing satellites, *Glob. Chang. Biol.*, 11(9), 1537–1555, doi:10.1111/j.1365-2486.2005.01003.x, 2005.
- Chen, A., Tang, R., Mao, J., Yue, C., Li, X., Gao, M., Shi, X., Jin, M., Ricciuto, D., Rabin, S., Ciais, P. and Piao, S.: Spatiotemporal dynamics of ecosystem fires and biomass burning-induced carbon emissions in China over the past two decades, *Geography and Sustainability*, 1(1), 47–58, <https://doi.org/10.1016/j.geosus.2020.03.002>, 2020.
- Chen, B., Andersson, A., Lee, M., Kirillova, E. N., Xiao, Q., Kruså, M., Shi, M., Hu, K., Lu, Z., Streets, D. G., Du, K. and Gustafsson, Ö.: Source forensics of black carbon aerosols from China, *Environ. Sci. Technol.*, 47(16), 9102–9108, doi:10.1021/es401599r, 2013.
- Chen, J., Anderson, K., Pavlovic, R., Moran, M. D., Englefield, P., Thompson, D. K., Munoz-Alpizar, R. and Landry, H.: The FireWork v2.0 air quality forecast system with biomass burning emissions from the Canadian Forest Fire Emissions Prediction System v2.03, *Geosci. Model Dev. Discuss.*, 1–41, doi:10.5194/gmd-2019-63, 2019.
- Chevallier, F., Palmer, P. I., Feng, L., Boesch, H., O'Dell, C. W. and Bousquet, P.: Toward robust and consistent regional CO₂ flux estimates from in situ and spaceborne measurements of atmospheric CO₂, *Geophys. Res. Lett.*, 41(3), 1065–1070, doi:10.1002/2013GL058772, 2014.
- Chuvieco, E., Aguado, I., Yebra, M., Nieto, H., Salas, J., Martin, M.P., Vilar, L., Martinez, J., Martin, S., Ibarra, P., de la Riva, J., Baeza, J., Rodriguez, F., Molina, J.R., Herrera, M.A., Zamora, R.: Development of a framework for fire risk assessment using remote sensing and geographic information system technologies. *Ecological Modelling* 221 (1), 46-58, 2010.
- Chuvieco, E., Lizundia-Loiola, J., Pettinari, L. M., Ramo, R., Padilla, M., Tansey, K., Mouillot, F., Laurent, P., Storm, T., Heil, A. and Plummer, S.: Generation and analysis of a new global burned area product based on MODIS 250 m reflectance bands and thermal anomalies, *Earth Syst. Sci. Data*, 10(4), 2015–2031, doi:10.5194/essd-10-2015-2018, 2018.
- Chuvieco, E., Mouillot, F., van der Werf, G. R., San Miguel, J., Tanasse, M., Koutsias, N., García, M., Yebra, M., Padilla, M., Gitas, I., Heil, A., Hawbaker, T. J. and Giglio, L.: Historical background and current developments for mapping burned area from satellite Earth

	Fire_cci User Requirements Document	Ref.	Fire_cci_D1.1_URD_v7.2	
		Issue	7.2	Date 28/04/2021
		Page		49

- observation, Remote Sens. Environ., 225(November 2018), 45–64, doi:10.1016/j.rse.2019.02.013, 2019.
- Chuvieco, E., Pettinari, M.L., Koutsias, N., Forkel, M., Hatson, S., Turco, M. Human and climate drivers of global biomass burning variability. *Science of the Total Environment* 779, 146361, doi: 10.1016/j.scitotenv.2021.146361, 2021
- Chuvieco, E., Yue, C., Heil, A., Mouillot, F., Alonso-Canas, I., Padilla, M., Pereira, J. M., Oom, D. and Tansey, K.: A new global burned area product for climate assessment of fire impacts, *Glob. Ecol. Biogeogr.*, 25(5), 619–629, doi:10.1111/geb.12440, 2016.
- CMUG CCI+: D1.1 User Requirement Document | Meeting the needs of the Climate Community - Requirements. https://climate.esa.int/documents/452/CMUG_Baseline_Requirements_D1.1_v2.2_EUBGoPz.pdf, version 2.2, issue date, 12 January 2021, last access: 28 January 2021, 2021.
- Coops, N. C., Hermosilla, T., Wulder, M. A., White, J. C. and Bolton, D. K.: A thirty year, fine-scale, characterization of area burned in Canadian forests shows evidence of regionally increasing trends in the last decade, *PLoS One*, 13(5), doi:10.1371/journal.pone.0197218, 2018.
- Curt, T., Borgniet, L. and Bouillon, C.: Wildfire frequency varies with the size and shape of fuel types in southeastern France: Implications for environmental management, *J. Environ. Manage.*, doi:10.1016/j.jenvman.2012.12.006, 2013.
- Darmenov, A. and da Silva, A. M.: The Quick Fire Emissions Dataset (QFED) - Documentation of versions 2.1, 2.2 and 2.4. [online] Available from: <https://ntrs.nasa.gov/archive/nasa/casi.ntrs.nasa.gov/20180005253.pdf>, last accessed 30 July 2019, 2015.
- Davis, A. Y., Ottmar, R., Liu, Y., Goodrick, S., Achtemeier, G., Gullett, B., Aurell, J., Stevens, W., Greenwald, R., Hu, Y., Russell, A., Hiers, J. K. and Odman, M. T.: Fire emission uncertainties and their effect on smoke dispersion predictions: A case study at Eglin Air Force Base, Florida, USA, *Int. J. Wildl. Fire*, doi:10.1071/WF13071, 2015.
- DEA (Department Of Environmental Affairs, Republic of South Africa): GHG Inventory for South Africa, 2000-2010, submitted November 2014. [online] Available from: https://www.environment.gov.za/sites/default/files/docs/greenhousegas_inventorysouthafrica.pdf, 2015.
- Di Giuseppe, F., Vitolo, C., Krzeminski, B., Barnard, C., Maciel, P., and San-Miguel, J.: Fire Weather Index: the skill provided by the European Centre for Medium-Range Weather Forecasts ensemble prediction system, *Nat. Hazards Earth Syst. Sci.*, 20, 2365–2378, <https://doi.org/10.5194/nhess-20-2365-2020>, 2020.
- Duncanson, L., Armston, J., Disney, M., Avitabile, V., Barbier, N., Calders, K., Carter, S., Chave, J., Herold, M., Crowther, T. W., Falkowski, M., Kellner, J. R., Labrière, N., Lucas, R., MacBean, N., McRoberts, R. E., Meyer, V., Næsset, E., Nickeson, J. E., Paul, K. I., Phillips, O. L., Réjou-Méchain, M., Román, M., Roxburgh, S., Saatchi, S., Schepaschenko, D., Scipal, K., Siqueira, P. R., Whitehurst, A. and Williams, M.: The Importance of Consistent Global Forest Aboveground Biomass Product Validation, *Surv Geophys*, 40(4), 979–999, <https://doi.org/10.1007/s10712-019-09538-8>, 2019.
- Eidenshink, J., Schwind, B., Brewer, K., Zhu, Z.-L., Quayle, B. and Howard, S.: A Project for Monitoring Trends in Burn Severity, *Fire Ecol.*, 3(1), 3–21, doi:10.4996/fireecology.0301003, 2009.
- Environmental Protection Agency of Ghana: Ghana’s Fourth National Greenhouse Gas Inventory Report National Greenhouse Gas Inventory to the United Nations Framework Convention on Climate Change, https://unfccc.int/sites/default/files/resource/gh_nir4-1.pdf, 2019.

	Fire_cci User Requirements Document			Ref.	Fire_cci_D1.1_URD_v7.2	
				Issue	7.2	Date 28/04/2021
				Page		50

- ESA Climate Change Initiative Annex K: Fire Disturbance ECV (Fire_cci), Statement of Work, prepared by ESA Climate Office, Reference ESA-CCI-PRGM-EOPS-SOW-18-0118, Issue 1.0, date of issue 31 May 2018.
- ESA Climate Office: CCI Data Standards. Ref CCI-PRGM-EOPS-TN-13-0009, Issue 2.1, [online] Available from: http://cci.esa.int/sites/default/files/CCIDataStandards_v2-1_CCI-PRGM-EOPS-TN-13-0009.pdf, 2019.
- ESA. Land Cover CCI Product User Guide Version 2. Tech. Rep. [online] Available from: http://maps.elie.ucl.ac.be/CCI/viewer/download/ESACCI-LC-Ph2-PUGv2_2.0.pdf, 2017.
- Eyring, V., Bony, S., Meehl, G. A., Senior, C. A., Stevens, B., Stouffer, R. J. and Taylor, K. E.: Overview of the Coupled Model Intercomparison Project Phase 6 (CMIP6) experimental design and organization, *Geosci. Model Dev.*, doi:10.5194/gmd-9-1937-2016, 2016.
- Fanin, T. and Van Der Werf, G. R.: Precipitation-fire linkages in Indonesia (1997-2015), *Biogeosciences*, doi:10.5194/bg-14-3995-2017, 2017.
- FAO: From reference levels to results reporting: REDD+ under the United Nations Framework Convention on Climate Change. 2019 update. Rome, 2019.
- Fernandez-Carrillo, A., Tanase, M. A., Belenguer-Plomer, M. A. and Chuvieco, E.: Effects of sample size on burned areas accuracy estimates in the Amazon Basin, p. 63, *SPIE-Intl Soc Optical Eng.*, 2018.
- Filipponi, F.: BAIS2: Burned Area Index for Sentinel-2. 2nd International electronic conference on remote sensing Proceedings. 2(7):364. doi:10.3390/ecrs-2-05177, 2018.
- Forkel, M., Andela, N., P Harrison, S., Lasslop, G., Van Marle, M., Chuvieco, E., Dorigo, W., Forrest, M., Hantson, S., Heil, A., Li, F., Melton, J., Sitch, S., Yue, C. and Arneeth, A.: Emergent relationships with respect to burned area in global satellite observations and fire-enabled vegetation models, *Biogeosciences*, 16(1), 57–76, doi:10.5194/bg-16-57-2019, 2019a.
- Forkel, M., Dorigo, W., Lasslop, G., Chuvieco, E., Hantson, S., Heil, A., Teubner, I., Thonicke, K. and Harrison, S. P.: Recent global and regional trends in burned area and their compensating environmental controls, *Environ. Res. Commun.*, 1(5), 051005, doi:10.1088/2515-7620/ab25d2, 2019b.
- Forkel, M., Dorigo, W., Lasslop, G., Teubner, I., Chuvieco, E. and Thonicke, K.: A data-driven approach to identify controls on global fire activity from satellite and climate observations (SOFIA V1), *Geosci. Model Dev.*, doi:10.5194/gmd-10-4443-2017, 2017.
- Fornacca, D., Ren, G. and Xiao, W.: Performance of Three MODIS fire products (MCD45A1, MCD64A1, MCD14ML), and ESA Fire_CCI in a mountainous area of Northwest Yunnan, China, characterized by frequent small fires, *Remote Sens.*, 9(11), 1–20, doi:10.3390/rs9111131, 2017.
- Franquesa, M., Vanderhoof, M. K., Stavrakoudis, D., Gitas, I. Z., Roteta, E., Padilla, M. and Chuvieco, E.: Development of a standard database of reference sites for validating global burned area products, *Earth System Science Data*, 12(4), 3229–3246, <https://doi.org/10.5194/essd-12-3229-2020>, 2020.
- French, N. H. F., McKenzie, D., Erickson, T., Koziol, B., Billmire, M., Arthur Endsley, K., Yager Scheinerman, N. K., Jenkins, L., Miller, M. E., Ottmar, R. and Prichard, S.: Modeling regional-scale wildland fire emissions with the Wildland Fire Emissions Information System, *Earth Interact.*, 18(16), doi:10.1175/EI-D-14-0002.1, 2014.
- Frieler, K., Lange, S., Piontek, F., Reyher, C. P. O., Schewe, J., Warszawski, L., Zhao, F., Chini, L., Denvil, S., Emanuel, K., Geiger, T., Halladay, K., Hurtt, G., Mengel, M., Murakami, D., Ostberg, S., Popp, A., Riva, R., Stevanovic, M., Suzuki, T., Volkholz, J., Burke, E., Ciais, P., Ebi, K., Eddy, T. D., Elliott, J., Galbraith, E., Gosling, S. N., Hattermann, F., Hickler, T.,

	Fire_cci User Requirements Document	Ref.	Fire_cci_D1.1_URD_v7.2	
		Issue	7.2	Date 28/04/2021
				Page 51

Hinkel, J., Hof, C., Huber, V., Jägermeyr, J., Krysanova, V., Marcé, R., Müller Schmied, H., Mouratiadou, I., Pierson, D., Tittensor, D. P., Vautard, R., van Vliet, M., Biber, M. F., Betts, R. A., Bodirsky, B. L., Deryng, D., Froking, S., Jones, C. D., Lotze, H. K., Lotze-Campen, H., Sahajpal, R., Thonicke, K., Tian, H. and Yamagata, Y.: Assessing the impacts of 1.5 °C global warming – simulation protocol of the Inter-Sectoral Impact Model Intercomparison Project (ISIMIP2b), *Geosci. Model Dev.*, 10(12), 4321–4345, <https://doi.org/10.5194/gmd-10-4321-2017>, 2017.

García-Lázaro, J., Moreno-Ruiz, J., Riaño, D. and Arbelo, M.: Estimation of Burned Area in the Northeastern Siberian Boreal Forest from a Long-Term Data Record (LTDR) 1982–2015 Time Series, *Remote Sens.*, 10(6), 940, doi:10.3390/rs10060940, 2018.

GCOS: Implementation Plan for the Global Observing System for Climate in Support of the UNFCCC (2010 Update) (GCOS-138), 2010.

GCOS: Systematic Observation requirements for satellite-based products for climate: Supplemental details to the satellite-based component of the implementation plan for the global observing system for climate in support of the UNFCCC (GCOS-107), 2006.

GCOS: The Global Observing System for Climate: Implementation Needs (GCOS-200). [online] Available from: https://library.wmo.int/opac/doc_num.php?explnum_id=3417, 2016-

Geller, C.: Automated burned area identification in real-time during wildfire events using WorldView imagery for the insurance industry, p. 45., 2018.

Giglio, L. and Roy, D. P.: On the outstanding need for a long-term, multi-decadal, validated and quality assessed record of global burned area: Caution in the use of Advanced Very High Resolution Radiometer data, *Science of Remote Sensing*, 2, 100007, <https://doi.org/10.1016/j.srs.2020.100007>, 2020.

Giglio, L., Boschetti, L., Roy, D. P., Humber, M. L. and Justice, C. O.: The Collection 6 MODIS burned area mapping algorithm and product, *Remote Sens. Environ.*, 217, 72–85, doi:10.1016/j.rse.2018.08.005, 2018a.

Giglio, L., Boschetti, L., Roy, D., Humber, M., Hall, J. V.: Collection 1 VIIRS Burned Area Product User's Guide, Version 1.0. [online] Available from: https://viirsland.gsfc.nasa.gov/PDF/VIIRS_C1_BA_User_Guide_1.0.pdf, 2018b.

Giglio, L., Loboda, T., Roy, D. P., Quayle, B. and Justice, C. O.: An active fire based burned area mapping algorithm for the MODIS sensor, *Remote Sens. Environ.*, 113(2), 408–420, doi:10.1016/j.rse.2008.10.006, 2009.

Giglio, L., Randerson, J. T. and van der Werf, G. R.: Analysis of daily, monthly, and annual burned area using the fourth-generation global fire emissions database (GFED4), *J. Geophys. Res. Biogeosciences*, 118(1), 317–328, doi:10.1002/jgrg.20042, 2013.

Giglio, L., Randerson, J. T., van der Werf, G. R., Kasibhatla, P. S., Collatz, G. J., Morton, D. C. and Defries, R. S.: Assessing variability and long-term trends in burned area by merging multiple satellite fire products, *Biogeosciences*, 7(3), 1171–1186, doi:10.5194/bg-7-1171-2010, 2010.

Giglio, L., van der Werf, G. R., Randerson, J. T., Collatz, G. J. and Kasibhatla, P.: Global estimation of burned area using MODIS active fire observations, *Atmos. Chem. Phys.*, 6(4), 957–974, doi:10.5194/acp-6-957-2006, 2006.

Gill, T., Collett, L., Armston, J., Eustace, A., Danaher, T., Scarth, P., Flood, N. Phinn, S.: Geometric correction and accuracy assessment of Landsat-7 ETM+ and Landsat-5 TM imagery used for vegetation cover monitoring in Queensland, Australia, 2010.


Goodwin, N. R. and Collett, L. J.: Development of an automated method for mapping fire history captured in Landsat TM and ETM+ time series across Queensland, Australia, *Remote Sens. Environ.*, 148, 206–221, doi:10.1016/j.rse.2014.03.021, 2014.

- Hantson, S., Arneth, A., Harrison, S. P., Kelley, D. I., Colin Prentice, I., Rabin, S. S., Archibald, S., Mouillot, F., Arnold, S. R., Artaxo, P., Bachelet, D., Ciais, P., Forrest, M., Friedlingstein, P., Hickler, T., Kaplan, J. O., Kloster, S., Knorr, W., Lasslop, G., Li, F., Mangeon, S., Melton, J. R., Meyn, A., Sitch, S., Spessa, A., van der Werf, G. R., Voulgarakis, A. and Yue, C.: The status and challenge of global fire modelling, *Biogeosciences*, 13(11), 3359–3375, doi:10.5194/bg-13-3359-2016, 2016.
- Hantson, S., Kelley, D. I., Arneth, A., Harrison, S. P., Archibald, S., Bachelet, D., Forrest, M., Hickler, T., Lasslop, G., Li, F., Mangeon, S., Melton, J. R., Nieradzik, L., Rabin, S. S., Prentice, I. C., Sheehan, T., Sitch, S., Teckentrup, L., Voulgarakis, A. and Yue, C.: Quantitative assessment of fire and vegetation properties in simulations with fire-enabled vegetation models from the Fire Model Intercomparison Project, *Geoscientific Model Development*, 13(7), 3299–3318, <https://doi.org/10.5194/gmd-13-3299-2020>, 2020.
- Hantson, S., Pueyo, S. and Chuvieco, E.: Global fire size distribution is driven by human impact and climate, *Glob. Ecol. Biogeogr.*, 24(1), 77–86, doi:10.1111/geb.12246, 2015.
- Hao, W. M., Reeves, M. C., Baggett, L. S., Balkanski, Y., Ciais, P., Nordgren, B. L., Petkov, A., Corley, R. E., Mouillot, F., Urbanski, S. P. and Yue, C.: Wetter environment and increased grazing reduced the area burned in northern Eurasia: 2002 – 2016, *Biogeosciences*, 18, 2559–2572, <https://doi.org/10.5194/bg-18-2559-2021>, 2021.
- Hawbaker, T. J., Vanderhoof, M. K., Beal, Y. J., Takacs, J. D., Schmidt, G. L., Falgout, J. T., Williams, B., Fairaux, N. M., Caldwell, M. K., Picotte, J. J., Howard, S. M., Stitt, S. and Dwyer, J. L.: Mapping burned areas using dense time-series of Landsat data, *Remote Sens. Environ.*, 198, 504–522, doi:10.1016/j.rse.2017.06.027, 2017.
- Heil, A., Bouarar, I., Lamarche, C. and Flasse, C.: ESA CCI ECV Fire Disturbance: O2.D4 FireCCILT10 Product Assessment Report, version 1.0., 2018.
- Heil, A., Yue, C., Mouillot, F. and Kaiser, J. W.: ESA CCI ECV Fire Disturbance: D.1.1 User requirement document, version 5.2. Available from: <https://www.esa-fire-cci.org/documents>, last accessed 30 July 2019, 2017.
- Hu, L., Keller, C. A., Long, M. S., Sherwen, T., Auer, B., Da Silva, A., Nielsen, J. E., Pawson, S., Thompson, M. A., Trayanov, A. L., Travis, K. R., Grange, S. K., Evans, M. J. and Jacob, D. J.: Global simulation of tropospheric chemistry at 12.5 km resolution: Performance and evaluation of the GEOS-Chem chemical module (v10-1) within the NASA GEOS Earth system model (GEOS-5 ESM), *Geosci. Model Dev.*, doi:10.5194/gmd-11-4603-2018, 2018.
- Humber, M. L., Boschetti, L., Giglio, L. and Justice, C. O.: Spatial and temporal intercomparison of four global burned area products, *Int. J. Digit. Earth*, 12(4), 460–484, doi:10.1080/17538947.2018.1433727, 2019.
- Ichoku, C. and Ellison, L.: Global top-down smoke-aerosol emissions estimation using satellite fire radiative power measurements, *Atmos. Chem. Phys.*, doi:10.5194/acp-14-6643-2014, 2014.
- IPCC: 2006 IPCC guidelines for national greenhouse gas inventories, prepared by the National Greenhouse Gas Inventories Programme, H.S. Eggleston, L. Buendia, K. Miwa, T. Ngara & K. Tanabe, eds. Vol. 4, Chap. 3.2. Intergovernmental Panel on Climate Change. Kanagawa, Japan, Institute for Global Environmental Strategies, 2006.
- Isaksen, I. S. A., Granier, C., Myhre, G., Berntsen, T. K., Dalsøren, S. B., Gauss, M., Klimont, Z., Benestad, R., Bousquet, P., Collins, W., Cox, T., Eyring, V., Fowler, D., Fuzzi, S., Jöckel, P., Laj, P., Lohmann, U., Maione, M., Monks, P., Preved, A. S. H., Raes, F., Richter, A., Rognerud, B., Schulz, M., Shindell, D., Stevenson, D. S., Storelvmo, T., Wang, W.-C., van Weele, M., Wild, M. and Wuebbles, D.: Atmospheric composition change: Climate–Chemistry interactions, *Atmos. Environ.*, 43(33), 5138–5192, doi:<https://doi.org/10.1016/j.atmosenv.2009.08.003>, 2009.


- Jang, E., Kang, Y., Im, J., Lee, D. W., Yoon, J. and Kim, S. K.: Detection and monitoring of forest fires using Himawari-8 geostationary satellite data in South Korea, *Remote Sens.*, doi:10.3390/rs11030271, 2019.
- Jiang, Z., Worden, J. R., Jones, D. B. A., Lin, J. T., Verstraeten, W. W. and Henze, D. K.: Constraints on Asian ozone using aura TES, OMI and terra MOPITT, *Atmos. Chem. Phys.*, 15(1), 99–112, doi:10.5194/acp-15-99-2015, 2015.
- Kaiser, J. W., Heil, A., Andreae, M. O., Benedetti, A., Chubarova, N., Jones, L., Morcrette, J. J., Razinger, M., Schultz, M. G., Suttie, M. and van der Werf, G. R.: Biomass burning emissions estimated with a global fire assimilation system based on observed fire radiative power, *Biogeosciences*, 9(1), 527–554, doi:10.5194/bg-9-527-2012, 2012.
- Kantzas, E. P., Quegan, S. and Lomas, M.: Improving the representation of fire disturbance in dynamic vegetation models by assimilating satellite data: A case study over the Arctic, *Geosci. Model Dev.*, 8(8), 2597–2609, doi:10.5194/gmd-8-2597-2015, 2015.
- Kloster, S., Mahowald, N. M., Randerson, J. T., Thornton, P. E., Hoffman, F. M., Levis, S., Lawrence, P. J., Feddema, J. J., Oleson, K. W., Lawrence, D. M.: Fire dynamics during the 20th century simulated by the Community Land Model, *Biogeosciences*, 7, 1877–1902, doi:10.5194/bg-7-1877-2010, 2010.
- Knorr, W., Dentener, F., Lamarque, J.-F., Jiang, L., Arneth, A.: Wildfire air pollution hazard during the 21st century, *Atmos. Chem. Phys.*, 17, 9223–9236, <https://doi.org/10.5194/acp-17-9223-2017>, 2017.
- Knorr, W., Kaminski, T., Arneth, A. and Weber, U.: Impact of human population density on fire frequency at the global scale, *Biogeosciences*, doi:10.5194/bg-11-1085-2014, 2014.
- Kuenen, J. J. P., Visschedijk, A. J. H., Jozwicka, M. and Denier Van Der Gon, H. A. C.: TNO-MACC-II emission inventory; A multi-year (2003-2009) consistent high-resolution European emission inventory for air quality modelling, *Atmos. Chem. Phys.*, doi:10.5194/acp-14-10963-2014, 2014.
- Lamarque, J. F., Bond, T. C., Eyring, V., Granier, C., Heil, A., Klimont, Z., Lee, D., Liousse, C., Mieville, A., Owen, B., Schultz, M. G., Shindell, D., Smith, S. J., Stehfest, E., Van Aardenne, J., Cooper, O. R., Kainuma, M., Mahowald, N., McConnell, J. R., Naik, V., Riahi, K. and Van Vuuren, D. P.: Historical (1850-2000) gridded anthropogenic and biomass burning emissions of reactive gases and aerosols: Methodology and application, *Atmos. Chem. Phys.*, doi:10.5194/acp-10-7017-2010, 2010.
- Lamarque, J. F., Shindell, D. T., Josse, B., Young, P. J., Cionni, I., Eyring, V., Bergmann, D., Cameron-Smith, P., Collins, W. J., Doherty, R., Dalsoren, S., Faluvegi, G., Folberth, G., Ghan, S. J., Horowitz, L. W., Lee, Y. H., MacKenzie, I. A., Nagashima, T., Naik, V., Plummer, D., Righi, M., Rumbold, S. T., Schulz, M., Skeie, R. B., Stevenson, D. S., Strode, S., Sudo, K., Szopa, S., Voulgarakis, A. and Zeng, G.: The atmospheric chemistry and climate model intercomparison Project (ACCMIP): Overview and description of models, simulations and climate diagnostics, *Geosci. Model Dev.*, 6(1), 179–206, doi:10.5194/gmd-6-179-2013, 2013.
- Landry, J.-S., Matthews, H. D.: Non-deforestation fire vs. fossil fuel combustion: the source of CO₂ emissions affects the global carbon cycle and climate responses, *Biogeosciences*, 13, 2137–2149, <https://doi.org/10.5194/bg-13-2137-2016>, 2016.
- Lasko, K. and Vadrevu, K. P.: Biomass Burning Emissions Variation from Satellite-Derived Land Cover, Burned Area, and Emission Factors in Vietnam, In *Land-Atmospheric Research Applications in South and Southeast Asia*, Vadrevu, K. P.; Ohara, T.; Justice, C., Eds. Springer International Publishing: Cham; pp 171–201, 2018.
- Lasslop, G., Hantson, S., Harrison, S. P., Bachelet, D., Burton, C., Forkel, M., Forrest, M., Li, F., Melton, J. R., Yue, C., Archibald, S., Scheiter, S., Arneth, A., Hickler, T. and Sitch, S.:

- Global ecosystems and fire: Multi-model assessment of fire-induced tree-cover and carbon storage reduction, *Global Change Biology*, 26(9), 5027–5041, <https://doi.org/10.1111/gcb.15160>, 2020.
- Lasslop, G., Thonicke, K., Kloster, S.: SPITFIRE within the MPI Earth system model: Model development and evaluation, *J. Adv. Model. Earth Syst.*, 6, 740–755, doi:10.1002/2013MS000284, 2014.
- Laurent, P., Mouillot, F., Vanesa Moreno, M., Yue, C. and Ciais, P.: Varying relationships between fire radiative power and fire size at a global scale, *Biogeosciences*, 16(2), 275–288, doi:10.5194/bg-16-275-2019, 2019.
- Laurent, P., Mouillot, F., Yue, C., Ciais, P., Moreno, M. V. and Nogueira, J. M. P.: Data Descriptor: FRY, a global database of fire patch functional traits derived from space-borne burned area products, *Sci. Data*, 5, doi:10.1038/sdata.2018.132, 2018.
- LePage, Y., Morton, D., Bond-Lamberty, B., Pereira, J. M. C., Hurtt, G.: HESFIRE: an explicit fire model for projections in the coupled Human-Earth System, *Biogeosciences Discuss.*, 11, 10779–10826, doi:10.5194/bgd-11-10779-2014, 2014.
- Li, F., Val Martin, M., Andreae, M. O., Arneth, A., Hantson, S., Kaiser, J. W., Lasslop, G., Yue, C., Bachelet, D., Forrest, M., Kluzek, E., Liu, X., Mangeon, S., Melton, J. R., Ward, D. S., Darmenov, A., Hickler, T., Ichoku, C., Magi, B. I., Sitch, S., van der Werf, G. R., Wiedinmyer, C., and Rabin, S. S.: Historical (1700–2012) global multi-model estimates of the fire emissions from the Fire Modeling Intercomparison Project (FireMIP), *Atmos. Chem. Phys.*, 19, 12545–12567, <https://doi.org/10.5194/acp-19-12545-2019>, 2019.
- Liu, T., Crowley and M. A.: Detection and impacts of tiling artifacts in MODIS burned area classification. *IOP SciNotes* 2:014003 doi:10.1088/2633-1357/abd8e2, 2021.
- Liu, Z., Ballantyne, A. P. and Cooper, L. A.: Biophysical feedback of global forest fires on surface temperature, *Nat. Commun.*, doi:10.1038/s41467-018-08237-z, 2019.
- Lizundia-Loiola, J., Franquesa, M., Boettcher, M., Kirches, G., Pettinari, M. L. and Chuvieco, E.: Operational implementation of the burned area component of the Copernicus Climate Change Service: from MODIS 250m to OLCI 300m data, *Earth System Science Data Discussions*, 1–37, <https://doi.org/10.5194/essd-2020-399>, 2021.
- Lizundia-Loiola, J., Otón, G., Ramo, R. and Chuvieco, E.: A spatio-temporal active fire clustering approach for global burned area mapping at 250 m from MODIS data. *Remote Sens. Environ.*, 236. doi:10.1016/j.rse.2019.111493, 2020a.
- Lizundia-Loiola, J., Pettinari, L. M. and Chuvieco, E.: ESA CCI ECV Fire Disturbance: D3.3.3 Product User Guide - MODIS, version 1.3. [online] Available from: <https://www.esa-fire-cci.org/documents>, last accessed 30 July 2019, 2018.
- Lizundia-Loiola, J., Pettinari, M. L. and Chuvieco, E.: Temporal Anomalies in Burned Area Trends: Satellite Estimations of the Amazonian 2019 Fire Crisis, *Remote Sensing*, 12(1), 151, <https://doi.org/10.3390/rs12010151>, 2020b.
- Long, T., Zhang, Z., He, G., Jiao, W., Tang, C., Wu, B., Zhang, X., Wang, G. and Yin, R.: 30m resolution global annual burned area mapping based on landsat images and Google Earth Engine, *Remote Sens.*, 11(5), 489, doi:10.3390/rs11050489, 2019.
- López-Saldaña, G., Bistinas, I. and Pereira, J. M. C.: Global analysis of radiative forcing from fire-induced shortwave albedo change, *Biogeosciences*, doi:10.5194/bg-12-557-2015, 2015.
- Lu, X., Zhang, X., Li, F. and Cochrane, M. A.: Investigating Smoke Aerosol Emission Coefficients Using MODIS Active Fire and Aerosol Products: A Case Study in the CONUS and Indonesia, *Journal of Geophysical Research: Biogeosciences*, 124(6), 1413–1429, <https://doi.org/10.1029/2018JG004974>, 2019.

- Maier, S. W.: Changes in surface reflectance from wildfires on the Australian continent measured by MODIS, *Int. J. Remote Sens.*, 31(12), 3161–3176, doi:10.1080/01431160903154408, 2010.
- Marécal, V., Peuch, V. H., Andersson, C., Andersson, S., Arteta, J., Beekmann, M., Benedictow, A., Bergström, R., Bessagnet, B., Cansado, A., Chéroux, F., Colette, A., Coman, A., Curier, R. L., Van Der Gon, H. A. C. D., Drouin, A., Elbern, H., Emili, E., Engelen, R. J., Eskes, H. J., Foret, G., Friese, E., Gauss, M., Giannaros, C., Guth, J., Joly, M., Jaumouillé, E., Josse, B., Kadyrov, N., Kaiser, J. W., Krajsek, K., Kuenen, J., Kumar, U., Liora, N., Lopez, E., Malherbe, L., Martinez, I., Melas, D., Meleux, F., Menut, L., Moinat, P., Morales, T., Parmentier, J., Piacentini, A., Plu, M., Poupkou, A., Queguiner, S., Robertson, L., Rouil, L., Schaap, M., Segers, A., Sofiev, M., Tarasson, L., Thomas, M., Timmermans, R., Valdebenito, Van Velthoven, P., Van Versendaal, R., Vira, J. and Ung, A.: A regional air quality forecasting system over Europe: The MACC-II daily ensemble production, *Geosci. Model Dev.*, doi:10.5194/gmd-8-2777-2015, 2015.
- Mascorro, V. S., Coops, N. C., Kurz, W. A. and Olguín, M.: Choice of satellite imagery and attribution of changes to disturbance type strongly affects forest carbon balance estimates, *Carbon Balance Manag.*, doi:10.1186/s13021-015-0041-6, 2015.
- Mieville, A., Granier, C., Liousse, C., Guillaume, B., Mouillot, F., Lamarque, J. F., Grégoire, J. M. and Pétron, G.: Emissions of gases and particles from biomass burning during the 20th century using satellite data and an historical reconstruction, *Atmos. Environ.*, 44(11), 1469–1477, doi:10.1016/j.atmosenv.2010.01.011, 2010.
- Mitchell, A. L., Rosenqvist, A. and Mora, B.: Current remote sensing approaches to monitoring forest degradation in support of countries measurement, reporting and verification (MRV) systems for REDD+, *Carbon Balance and Management*, 12(1), 9, <https://doi.org/10.1186/s13021-017-0078-9>, 2017.
- Mithal, V., Nayak, G., Khandelwal, A., Kumar, V., Nemani, R. and Oza, N. C.: Mapping burned areas in tropical forests using a novel machine learning framework, *Remote Sens.*, 10(1), 69, doi:10.3390/rs10010069, 2018.
- Mitsopoulos, I., Mallinis, G., Dimitrakopoulos, A., Xanthopoulos, G., Eftychidis, G. and Goldammer, J. G.: Vulnerability of peri urban and residential areas to landscape fires in Greece: Evidence by wildland-urban interface data, *Data in Brief*, 31, 106025, <https://doi.org/10.1016/j.dib.2020.106025>, 2020.
- Moreno Ruiz, J. A., García Lázaro, J. R., Del Águila Cano, I. and Leal, P. H.: Burned area mapping in the North American boreal forest using terra-MODIS LTDR (2001-2011): A comparison with the MCD45A1, MCD64A1 and BA GEOLAND-2 products, *Remote Sens.*, 6(1), 815–840, doi:10.3390/rs6010815, 2013.
- Moreno Ruiz, J. A., Riaño, D., Arbelo, M., French, N. H. F., Ustin, S. L. and Whiting, M. L.: Burned area mapping time series in Canada (1984-1999) from NOAA-AVHRR LTDR: A comparison with other remote sensing products and fire perimeters, *Remote Sens. Environ.*, 117, 407–414, doi:10.1016/j.rse.2011.10.017, 2012.
- Moreno-Ruiz, J. A., García-Lázaro, J. R., Arbelo, M. and Riaño, D.: A comparison of burned area time series in the alaskan boreal forests from different remote sensing products, *Forests*, doi:10.3390/f10050363, 2019.
- Morton, D. C., Le Page, Y., DeFries, R., Collatz, G. J. and Hurtt, G. C.: Understorey fire frequency and the fate of burned forests in southern Amazonia, *Philos. Trans. R. Soc. B Biol. Sci.*, doi:10.1098/rstb.2012.0163, 2013.
- Mota, B., Gobron, N., Cappucci, F. and Morgan, O.: Burned area and surface albedo products: Assessment of change consistency at global scale, *Remote Sens. Environ.*, doi:10.1016/j.rse.2019.03.001, 2019.

	Fire_cci User Requirements Document			Ref.	Fire_cci_D1.1_URD_v7.2	
				Issue	7.2	Date
				Page		56

- Mouillot, F. and Field, C. B.: Fire history and the global carbon budget: A $1^\circ \times 1^\circ$ fire history reconstruction for the 20th century, *Glob. Chang. Biol.*, 11(3), 398–420, doi:10.1111/j.1365-2486.2005.00920.x, 2005.
- Mouillot, F., Narasimha, A., Balkanski Y., Lamarque J.F., Field, C.B.: Global carbon emissions from biomass burning in the 20th century. *Geophysical Research Letters* 33(1), L01801, 2006.
- Mouillot, F., Schultz, M. G., Yue, C., Cadule, P., Tansey, K., Ciais, P. and Chuvieco, E.: Ten years of global burned area products from spaceborne remote sensing-A review: Analysis of user needs and recommendations for future developments, *Int. J. Appl. Earth Obs. Geoinf.*, 26(1), 64–79, doi:10.1016/j.jag.2013.05.014, 2014.
- Mu, M., Randerson, J. T., van der Werf, G. R., Giglio, L., Kasibhatla, P., Morton, D., Collatz, G. J., Defries, R. S., Hyer, E. J., Prins, E. M., Griffith, D. W. T., Wunch, D., Toon, G. C., Sherlock, V. and Wennberg, P. O.: Daily and 3-hourly variability in global fire emissions and consequences for atmospheric model predictions of carbon monoxide, *Journal of Geophysical Research-Atmospheres*, 116(D24), –n/a, doi:10.1029/2011JD016245, 2011.
- Müller, D., Suess, S., Hoffmann, A. A. and Buchholz, G.: The Value of Satellite-Based Active Fire Data for Monitoring, Reporting and Verification of REDD+ in the Lao PDR, *Hum. Ecol.*, 41(1), 7–20, doi:10.1007/s10745-013-9565-0, 2013.
- National REDD+ Secretariat: Ghana's national forest reference level. Accra, Ghana. Available at https://redd.unfccc.int/files/ghana_national_reference_level_01.01_2017_for_unfccc-yaw_kwakye.pdf, 2017.
- Nguyen, H. M. and Wooster, M. J.: Advances in the estimation of high Spatio-temporal resolution pan-African top-down biomass burning emissions made using geostationary fire radiative power (FRP) and MAIAC aerosol optical depth (AOD) data, *Remote Sensing of Environment*, 248, 111971, <https://doi.org/10.1016/j.rse.2020.111971>, 2020.
- Nogueira, J. M. P., Ruffault, J., Chuvieco, E. and Mouillot, F.: Can we go beyond burned area in the assessment of global remote sensing products with fire patch metrics?, *Remote Sens.*, 9(1), doi:10.3390/rs9010007, 2017b.
- Nogueira, J., Rambal, S., Barbosa, J. and Mouillot, F.: Spatial Pattern of the Seasonal Drought/Burned Area Relationship across Brazilian Biomes: Sensitivity to Drought Metrics and Global Remote-Sensing Fire Products, *Climate*, 5(2), 42, doi:10.3390/cli5020042, 2017a.
- Oliveras, I., Anderson, L. O. and Malhi, Y.: Application of remote sensing to understanding fire regimes and biomass burning emissions of the tropical Andes, *Global Biogeochem. Cycles*, 28(4), 480–496, doi:10.1002/2013GB004664, 2014.
- Oom, D., Silva, P. C., Bistinas, I. and Pereira, J. M. C.: Highlighting biome-specific sensitivity of fire size distributions to time-gap parameter using a new algorithm for fire event individuation, *Remote Sens.*, doi:10.3390/rs8080663, 2016.
- Otón, G. and Pettinari M. L. ESA CCI ECV Fire Disturbance: D3.3.4 Product User Guide - LTDR, version 1.0, available at: <https://www.esa-fire-cci.org/documents>, 2019.
- Otón, G., Pettinari, M. L. and Chuvieco, E.: ESA CCI ECV Fire Disturbance: D3.3.4 Product User Guide - LTDR, version 1.1. Available at: <https://climate.esa.int/en/projects/fire/key-documents/>, 2020.
- Otón, G., Ramo, R., Lizundia-Loiola, J. and Chuvieco, E.: Global Detection of Long-Term (1982–2017) Burned Area with AVHRR-LTDR Data, *Remote Sens.*, 11(18), doi:10.3390/rs11182079, 2019.
- Otón, G.: ESA CCI ECV Fire Disturbance: D4.2.2 Product User Guide – AVHRR-LTDR, version 1.0, available at: <https://climate.esa.int/en/projects/fire/key-documents/>, 2020.

	Fire_cci User Requirements Document			Ref.	Fire_cci_D1.1_URD_v7.2	
				Issue	7.2	Date
				Page		57

- Ott, L. E., Pawson, S., Collatz, G. J., Gregg, W. W., Menemenlis, D., Brix, H., Rousseaux, C. S., Bowman, K. W., Liu, J., Eldering, A., Gunson, M. R., Kawa, S. R.: Assessing the magnitude of CO₂ flux uncertainty in atmospheric CO₂ records using products from NASA's Carbon Monitoring Flux Pilot Project, *J. Geophys. Res. Atmos.*, 120, doi:10.1002/2014JD022411, 2015.
- Padilla, M., Stehman, S. V. and Chuvieco, E.: Validation of the 2008 MODIS-MCD45 global burned area product using stratified random sampling, *Remote Sens. Environ.*, 144, 187–196, doi:10.1016/j.rse.2014.01.008, 2014.
- Padilla, M., Stehman, S. V., Ramo, R., Corti, D., Hantson, S., Oliva, P., Alonso-Canas, I., Bradley, A. V., Tansey, K., Mota, B., Pereira, J. M. and Chuvieco, E.: Comparing the accuracies of remote sensing global burned area products using stratified random sampling and estimation, *Remote Sens. Environ.*, 160, 114–121, doi:10.1016/j.rse.2015.01.005, 2015.
- Padilla, M., Wheeler, J. and Tansey, K.: ESA CCI ECV Fire Disturbance: D4.1.1. Product Validation Report, version 2.1., https://www.esa-fire-cci.org/sites/default/files/Fire_cci_D4.1.1_PVR_v2.1_0.pdf, 2018.
- Paugam, R., Wooster, M., Freitas, S. and Val Martin, M.: A review of approaches to estimate wildfire plume injection height within large-scale atmospheric chemical transport models, *Atmos. Chem. Phys.*, 16(2), 907–925, <https://doi.org/10.5194/acp-16-907-2016>, 2016.
- Pereira, J. M. C., Oom, D., Pereira, P., Turkman, A. A. and Turkman, K. F.: Religious affiliation modulates weekly cycles of cropland burning in sub-saharan Africa, *PLoS One*, 10(9), e0139189, doi:10.1371/journal.pone.0139189, 2015.
- Pessôa, A. C. M., Anderson, L. O., Carvalho, N. S., Campanharo, W. A., Junior, C. H. L. S., Rosan, T. M., Reis, J. B. C., Pereira, F. R. S., Assis, M., Jacon, A. D., Ometto, J. P., Shimabukuro, Y. E., Silva, C. V. J., Pontes-Lopes, A., Morello, T. F. and Aragão, L. E. O. C.: Intercomparison of Burned Area Products and Its Implication for Carbon Emission Estimations in the Amazon, *Remote Sensing*, 12(23), 3864, <https://doi.org/10.3390/rs12233864>, 2020.
- Pettinari, L. M., Otón, G. and Chuvieco, E.: ESA CCI ECV Fire Disturbance: O2.D1 User Requirement Document and Product Specification Document for AVHRR, version 1.1., 2017.
- Pettinari, M. L. and Chuvieco, E.: Fire Danger Observed from Space, *Surv Geophys*, 41(6), 1437–1459, <https://doi.org/10.1007/s10712-020-09610-8>, 2020.
- Pinto, M. M., DaCamara, C. C., Trigo, I. F., Trigo, R. M. and Turkman, K. F.: Fire danger rating over Mediterranean Europe based on fire radiative power derived from Meteosat, *Natural Hazards and Earth System Sciences*, 18(2), 515–529, <https://doi.org/10.5194/nhess-18-515-2018>, 2018.
- Pinto, M. M., Libonati, R., Trigo, R. M., Trigo, I. F. and DaCamara, C. C.: A deep learning approach for mapping and dating burned areas using temporal sequences of satellite images, *ISPRS Journal of Photogrammetry and Remote Sensing*, 160, 260–274, <https://doi.org/10.1016/j.isprsjprs.2019.12.014>, 2020.
- Plummer, S., Arino, O., Simon, M. and Steffen, W.: Establishing a earth observation product service for the terrestrial carbon community: The globcarbon initiative, *Mitig. Adapt. Strateg. Glob. Chang.*, 11(1), 97–111, doi:10.1007/s11027-006-1012-8, 2006.
- Pu, R., Li, Z., Gong, P., Csiszar, I., Fraser, R., Hao, W. M., Kondragunta, S. and Weng, F.: Development and analysis of a 12-year daily 1-km forest fire dataset across North America from NOAA/AVHRR data, *Remote Sens. Environ.*, 108(2), 198–208, doi:10.1016/j.rse.2006.02.027, 2007.
- Pu, R., Li, Z., Gong, P., Csiszar, I., Fraser, R., Hao, W. M., Kondragunta, S., Loboda, T.V., Hall,

- J.V. and Shevade, V.S.: ABoVE: AVHRR-Derived Forest Fire Burned Area-Hot Spots, Alaska and Canada, 1989-2000. ORNL DAAC, Oak Ridge, Tennessee, USA. <https://doi.org/10.3334/ORNLDAAAC/1545>, 2018.
- Rabin, S. S., Melton, J. R., Lasslop, G., Bachelet, D., Forrest, M., Hantson, S., Kaplan, J. O., Li, F., Mangeon, S., Ward, D. S., Yue, C., Arora, V. K., Hickler, T., Kloster, S., Knorr, W., Nieradzick, L., Spessa, A., Folberth, G. A., Sheehan, T., Voulgarakis, A., Kelley, D. I., Prentice, I. C., Sitch, S., Harrison, S., Arneth, A.: The Fire Modeling Intercomparison Project (FireMIP), phase 1: experimental and analytical protocols with detailed model descriptions, *Geosci. Model Dev.*, 10, 1175-1197, <https://doi.org/10.5194/gmd-10-1175-2017>, 2017.
- Ramo, R., García, M., Rodríguez, D. and Chuvieco, E.: A data mining approach for global burned area mapping, *Int. J. Appl. Earth Obs. Geoinf.*, 73, 39–51, doi:10.1016/j.jag.2018.05.027, 2018.
- Ramo, R., Roteta, E., Bistinas, I., Wees, D., Bastarrika, A., Chuvieco, E. & van de Werf, G. African burned area and fire carbon emissions are strongly impacted by small fires undetected by coarse resolution satellite data. *PNAS* 118 (9) e2011160118, doi:10.1073/pnas.2011160118, 2021
- Randerson, J. T., Chen, Y., van der Werf, G. R., Rogers, B. M., Morton, D. C., Global burned area and biomass burning emissions from small fires, *J. Geophys. Res.*, 117, G04012, doi:10.1029/2012JG002128, 2012.
- Rossi, S., Tubiello, F. N., Prosperi, P., Salvatore, M., Jacobs, H., Biancalani, R., House, J. I. and Boschetti, L.: FAOSTAT estimates of greenhouse gas emissions from biomass and peat fires, *Clim. Change*, 135(3–4), 699–711, doi:10.1007/s10584-015-1584-y, 2016.
- Roteta, E., Bastarrika, A., Padilla, M., Storm, T. and Chuvieco, E.: Development of a Sentinel-2 burned area algorithm: Generation of a small fire database for sub-Saharan Africa, *Remote Sens. Environ.*, 222, 1–17, doi:10.1016/j.rse.2018.12.011, 2019.
- Roy, D. P., Boschetti, L., Justice, C. O. and Ju, J.: The collection 5 MODIS burned area product - Global evaluation by comparison with the MODIS active fire product, *Remote Sens. Environ.*, 112(9), 3690–3707, doi:10.1016/j.rse.2008.05.013, 2008.
- Santana, N. C., Júnior, O. A. de C., Gomes, R. A. T. and Guimarães, R. F.: Burned-area detection in Amazonian environments using standardized time series per pixel in MODIS data, *Remote Sens.*, doi:10.3390/rs10121904, 2018.
- Schaphoff, S., Forkel, M., Müller, C., Knauer, J., von Bloh, W., Gerten, D., Jägermeyr, J., Lucht, W., Rammig, A., Thonicke, K. and Waha, K.: LPJmL4 - a dynamic global vegetation model with managed land - Part 2: Model evaluation, *Geosci. Model Dev.*, doi:10.5194/gmd-2017-146, 2018.
- Schultz, M. G., Heil, A., Hoelzemann, J. J., Spessa, A., Thonicke, K., Goldammer, J. G., Held, A. C., Pereira, J. M. C. and van Het Bolscher, M.: Global wildland fire emissions from 1960 to 2000, *Global Biogeochem. Cycles*, doi:10.1029/2007GB003031, 2008.
- Schultz, M., Mouillot, F., Yue, C., Cadule, P. and Ciais, P.: ESA CCI EVC Fire Disturbance: User Requirements Document: Fire_cci_Ph1_JUELICH_D1_1_URD_v3_5.pdf. [online] Available from: <http://www.esa-fire-cci.org/>, last accessed 10 October 2015, 2011.
- Schwert, B., Albury, C., Clark, J., Schaaf, A., Urbanski, S. and Nordgren, B. L.: Implementation of a near real-time burned area detection algorithm calibrated for VIIRS imagery. RSAC-10092-TIP1, Salt Lake City, UT., 2016.
- Sedano, F., Kempeneers, P., Miguel, J. S., Strobl, P. and Vogt, P.: Towards a pan-European burnt scar mapping methodology based on single date: Medium resolution optical remote sensing data, *Int. J. Appl. Earth Obs. Geoinf.*, 20(1), 52–59, doi:10.1016/j.jag.2011.08.003, 2012.
- Shimabukuro, Y. E., Dutra, A. C., Arai, E., Duarte, V., Cassol, H. L. G., Pereira, G. and Cardozo,

- F. da S.: Mapping Burned Areas of Mato Grosso State Brazilian Amazon Using Multisensor Datasets, *Remote Sensing*, 12(22), 3827, <https://doi.org/10.3390/rs12223827>, 2020.
- Silva Junior, C. H. L., Anderson, L. O., Silva, A. L., Almeida, C. T., Dalagnol, R., Pletsch, M. A. J. S., Penha, T. V., Paloschi, R. A. and Aragão, L. E. O. C.: Fire Responses to the 2010 and 2015/2016 Amazonian Droughts, *Front. Earth Sci.*, 7(May), 1–16, doi:10.3389/feart.2019.00160, 2019.
- Simon, M., Plummer, S., Fierens, F., Hoelzemann, J. J. and Arino, O.: Burnt area detection at global scale using ATSR-2: The GLOBSCAR products and their qualification, *J. Geophys. Res. D Atmos.*, 109(14), doi:10.1029/2003JD003622, 2004.
- Sitch, S., Smith, B., Prentice, I. C., Arneth, A., Bondeau, A., Cramer, W., Kaplan, J. O., Levis, S., Lucht, W., Sykes, M. T., Thonicke, K., Venevsky S.: Evaluation of ecosystem dynamics, plant geography and terrestrial carbon cycling in the LPJ dynamic global vegetation model. *Global Change Biology* 9, 161–185, 2003.
- Sofiev, M., Vankevich, R., Lotjonen, M., Prank, M., Petukhov, V., Ermakova, T., Koskinen, J. and Kukkonen, J.: An operational system for the assimilation of the satellite information on wild-land fires for the needs of air quality modelling and forecasting, *Atmos. Chem. Phys.*, doi:10.5194/acp-9-6833-2009, 2009.
- Soja, A. J., Shugart, H. H., Sukhinin, A., Conard, S. and Stackhouse, P. W.: Satellite-derived mean fire return intervals as indicators of change in Siberia (1995-2002), *Mitig. Adapt. Strateg. Glob. Chang.*, doi:10.1007/s11027-006-1009-3, 2006.
- Tanase, M. A. and Belenguer-Plomer, M. A.: ESA CCI ECV Fire Disturbance: O3.D1 Algorithm Theoretical Basis Document – S1 South America, v2.0. Available at: <https://www.esa-fire-cci.org/documents>, 2018.
- Tansey, K., Grégoire, J. M., Defourny, P., Leigh, R., Pekel, J. F., van Bogaert, E. and Bartholomé, E.: A new, global, multi-annual (2000-2007) burnt area product at 1 km resolution, *Geophys. Res. Lett.*, 35(1), doi:10.1029/2007GL031567, 2008.
- Tansey, K., Grégoire, J. M., Stroppiana, D., Sousa, A., Silva, J., Pereira, J. M. C., Boschetti, L., Maggi, M., Brivio, P. A., Fraser, R., Flasse, S., Ershov, D., Binaghi, E., Graetz, D. and Peduzzi, P.: Vegetation burning in the year 2000: Global burned area estimates from SPOT VEGETATION data, *J. Geophys. Res. D Atmos.*, 109(14), doi:10.1029/2003JD003598, 2004.
- Tarimo, B., Dick, Ø. B., Gobakken, T. and Totland, Ø.: Spatial distribution of temporal dynamics in anthropogenic fires in miombo savanna woodlands of Tanzania, *Carbon Balance Manag.*, doi:10.1186/s13021-015-0029-2, 2015.
- Teckentrup, L., Harrison, S. P., Hantson, S., Heil, A., Melton, J. R., Forrest, M., Li, F., Yue, C., Arneth, A., Hickler, T., Sitch, S. and Lasslop, G.: Sensitivity of simulated historical burned area to environmental and anthropogenic controls: A comparison of seven fire models, *Biogeosciences Discuss.*, 1–39, doi:10.5194/bg-2019-42, 2019.
- Tomshin, O. and Solovveyev, V.: Generating a long-term data series of burned area in Eastern Siberia using LTDR data (1984–2016), *Remote Sens. Lett.*, 10(10), 1008–1017, doi:10.1080/2150704x.2019.1637958, 2019.
- Turco, M., Herrera, S., Tourigny, E., Chuvieco, E. and Provenzale, A.: A comparison of remotely-sensed and inventory datasets for burned area in Mediterranean Europe, *Int. J. Appl. Earth Obs. Geoinf.*, doi:10.1016/j.jag.2019.05.020, 2019.
- Turquety, S., Menut, L., Siour, G., Mailler, S., Hadji-Lazaro, J., George, M., Clerbaux, C., Hurtmans, D. and Coheur, P.-F.: APIFLAME v2.0 biomass burning emissions model: impact of refined input parameters on atmospheric concentration in Portugal in summer 2016, *Geoscientific Model Development*, 13(7), 2981–3009, <https://doi.org/10.5194/gmd-13->

2981-2020, 2020.

United Nations: Kyoto Protocol to the United Framework Convention on Climate Change, Dec. 10, 1997, U.N. Doc FCCC/CP/1997/7/Add.1, Int. Leg. Mater., 1998.

United Nations: Report of the technical assessment of the proposed forest reference level of Ghana submitted in 2017. FCCC/TAR/2017/GHA., 2018.

Urbanski, S. P., Reeves, M. C., Corley, R. E., Silverstein, R. P. and Hao, W. M.: Contiguous United States wildland fire emission estimates during 2003-2015, *Earth Syst. Sci. Data*, 10(4), 2241–2274, doi:10.5194/essd-10-2241-2018, 2018.

Valencia, G. M., Anaya, J. A., Velásquez, É. A., Ramo, R. and Caro-Lopera, F. J.: About Validation-Comparison of Burned Area Products, *Remote Sensing*, 12(23), 3972, <https://doi.org/10.3390/rs12233972>, 2020.

van der Velde, I. R., Miller, J. B., Schaefer, K., van der Werf, G. R., Krol, M. C., and Peters, W.: Terrestrial cycling of 13CO₂ by photosynthesis, respiration, and biomass burning in SiBCASA, *Biogeosciences*, 11, 6553–6571, <https://doi.org/10.5194/bg-11-6553-2014>, 2014.

van der Werf, G. R., Randerson, J. T., Collatz, G. J., Giglio, L., Kasibhatla, P. S., Arellano, A. F., Olsen, S. C., Kasischke, E. S.: Continental-scale partitioning of fire emissions during the 1997 to 2001 El Nino/La Nina period, *Science*, 303, 73–76, 2004.

van der Werf, G. R., Randerson, J. T., Giglio, L., Collatz, G. J., Mu, M., Kasibhatla, P. S., Morton, D. C., Defries, R. S., Jin, Y. and Van Leeuwen, T. T.: Global fire emissions and the contribution of deforestation, savanna, forest, agricultural, and peat fires (1997-2009), *Atmos. Chem. Phys.*, doi:10.5194/acp-10-11707-2010, 2010.

van der Werf, G. R., Randerson, J. T., Giglio, L., Van Leeuwen, T. T., Chen, Y., Rogers, B. M., Mu, M., Van Marle, M. J. E., Morton, D. C., Collatz, G. J., Yokelson, R. J. and Kasibhatla, P. S.: Global fire emissions estimates during 1997-2016, *Earth Syst. Sci. Data*, 9(2), 697–720, doi:10.5194/essd-9-697-2017, 2017.

van der Werf, G.R., Randerson, J.T., Collatz, G.J., Giglio, L.: Carbon emissions from fires in tropical and subtropical ecosystems, *Global Change Biol.*, 9, 547 – 562, 2003.

van der Werf, G.R., Randerson, J.T., Giglio, L., Collatz, G. J., Kasibhatla, P. S., Arellano Jr., A. F.: Interannual variability in global biomass burning emissions from 1997 to 2004, *Atmos. Chem. Phys.*, 6, 3423–3441, doi:10.5194/acp-6-3423-2006, 2006.

Van Marle, M. J. E., Kloster, S., Magi, B. I., Marlon, J. R., Daniau, A. L., Field, R. D., Arneth, A., Forrest, M., Hantson, S., Kehrwald, N. M., Knorr, W., Lasslop, G., Li, F., Mangeon, S., Yue, C., Kaiser, J. W. and van der Werf, G. R.: Historic global biomass burning emissions for CMIP6 (BB4CMIP) based on merging satellite observations with proxies and fire models (1750-2015), *Geosci. Model Dev.*, 10(9), 3329–3357, doi:10.5194/gmd-10-3329-2017, 2017.

van Wees, D. and van der Werf, G. R.: Modelling biomass burning emissions and the effect of spatial resolution: a case study for Africa based on the Global Fire Emissions Database (GFED), *Geosci. Model Dev.*, 12, 4681–4703, <https://doi.org/10.5194/gmd-12-4681-2019>, 2019.

Vanderhoof, M. K., Fairaux, N., Beal, Y-J. G., Hawbaker T.J.: Validation of the USGS Landsat Burned Area Essential Climate Variable (BAECV) across the conterminous United States, *Remote Sens. Environ.*, 198, 292–406, doi: 10.1016/j.rse.2017.06.025, 2017.

Vetrita, Y., Cochrane, M. A., Suwarsono, Priyatna, M., Sukowati, K. A. D. and Khomarudin, M. R.: Evaluating accuracy of four MODIS-derived burned area products for tropical peatland and non-peatland fires, *Environ. Res. Lett.*, <https://doi.org/10.1088/1748-9326/abd3d1>, 2020.

- Vitolo, C., Di Giuseppe, F., Krzeminski, B. and San-Miguel-Ayanz, J.: A 1980–2018 global fire danger re-analysis dataset for the Canadian Fire Weather Indices, *Scientific Data*, 6(1), 190032, <https://doi.org/10.1038/sdata.2019.32>, 2019.
- Wiedinmyer, C., Akagi, S. K., Yokelson, R. J., Emmons, L. K., Al-Saadi, J. A., Orlando, J. J. and Soja, A. J.: The Fire INventory from NCAR (FINN): A high resolution global model to estimate the emissions from open burning, *Geosci. Model Dev.*, 4(3), 625–641, doi:10.5194/gmd-4-625-2011, 2011.
- Wooster, M. J., Roberts, G., Perry, G. L. W. and Kaufman, Y. J.: Retrieval of biomass combustion rates and totals from fire radiative power observations: FRP derivation and calibration relationships between biomass consumption and fire radiative energy release, *J. Geophys. Res.*, 110(D24), D24311, <https://doi.org/10.1029/2005JD006318>, 2005.
- World Meteorological Organization: Implementation plan for the global observing system for climate in support of the UNFCCC, GCOS-138-(1523), 180, 2010.
- World Meteorological Organization: Systematic Observation Requirements for Satellite-based Products for Climate - GCOS-107 (WMO/TD No. 1338). Available from: https://library.wmo.int/doc_num.php?explnum_id=3813, last accessed 30 July 2019, 2006.
- World Meteorological Organization: The Global Observing System for Climate: Implementation Needs. Available from: https://library.wmo.int/doc_num.php?explnum_id=3417, 2016.
- Xi, D. D. Z., Taylor, S. W., Woolford, D. G. and Dean, C. B.: Statistical Models of Key Components of Wildfire Risk, *Annual Review of Statistics and Its Application*, 6(1), 197–222, <https://doi.org/10.1146/annurev-statistics-031017-100450>, 2019.
- Yin, L., Du, P., Zhang, M., Liu, M., Xu, T. and Song, Y.: Estimation of emissions from biomass burning in China (2003-2017) based on MODIS fire radiative energy data, *Biogeosciences*, 16(7), 1629–1640, doi:10.5194/bg-16-1629-2019, 2019.
- Zhang, T., Wooster, M. J., De Jong, M. C. and Xu, W.: How well does the ‘small fire boost’ methodology used within the GFED4.1s fire emissions database allow it to represent the timing, location and magnitude of agricultural burning? *Remote Sens.*, 10(6), <https://doi.org/10.3390/rs10060823>, 2018.
- Zheng, B., Chevallier, F., Ciais, P., Yin, Y. and Wang, Y.: On the Role of the Flaming to Smoldering Transition in the Seasonal Cycle of African Fire Emissions, *Geophys. Res. Lett.*, doi:10.1029/2018GL079092, 2018.
- Zheng, B., Huo, H., Zhang, Q., Yao, Z. L., Wang, X. T., Yang, X. F., Liu, H. and He, K. B.: High-resolution mapping of vehicle emissions in China in 2008, *Atmos. Chem. Phys.*, doi:10.5194/acp-14-9787-2014, 2014.
- Zhu, C., Kobayashi, H., Kanaya, Y. and Saito, M.: Size-dependent validation of MODIS MCD64A1 burned area over six vegetation types in boreal Eurasia: Large underestimation in croplands, *Sci. Rep.*, 7(1), doi:10.1038/s41598-017-03739-0, 2017.

Annex 1: Acronyms and abbreviations

ADP	Algorithm Development Plan	CNR	Consiglio Nazionale delle Ricerche
AR	IPCC Assessment Report	CNRS	Centre Nationale de la Recherche Scientifique
ASCII	American Standard Code for Information Interchange	CSIC	Consejo Superior de Investigaciones Científicas
AATSR	Advanced Along-Track Scanning Radiometer	CSV	Comma separated values
APIFLAME	Analysis and Prediction of the Impact of Fires on Air Quality Modeling	cut	Temporal cutting threshold for patches
AVHRR	Advanced Very High Resolution Radiometer	deg	degrees
AATSR	Advanced Along-Track Scanning Radiometer	DAAC	Distributed Active Archive Center
ATSR	Along-Track Scanning Radiometer	DGVMs	Dynamic Global Vegetation Models
BA	Burned Area	DISP	Spatial dispersion of burned pixels within grid
BAI	Burn Area Index	DMSP/OLS	Defense Meteorological Program Operational Linescan System
BAECV	Burned Area Essential Climate Variable	DOB	Day of Burn
BAS	Burned Area Source	DOBUNC	Day of Burn Uncertainty
BAT	Burned Aea by tree cover	DYN	Fire Dynamics
BB4CMIP6	Biomass Burning emissions for CMIP6	ECV	Essential Climate Variables
BC	Binary Burn Classification	EDGAR	Emission Database for Global Atmospheric Research
BP	Burn Probability	EMEP	European Monitoring and Evaluation Programme'
BSQ	Band SeQuential image encoding	EMIS	Emissions
C3S	Copernicus Climate Change Service	EFFIS	European Forest Fire Information System
CAMS	Copernicus Atmosphere Monitoring Service	ENVI	Environment for Visualizing Images
CASA	Carnegie-Ames-Stanford-Approach	ERR	Crude error estimate derived from product validation
CCI	Climate Change Initiative	ERS	European Remote Sensing satellite
CDR	Climate Data Record	ESA	European Space Agency
Ce	Commission Error	EU	European Union
CEDA	Centre for Environmental Data Analysis	F&L	First and last day of reliable mapping
CEOS	Committee on Earth Observation Satellites	FBURN	Fraction of burnable area
CL	Confidence Level	FCR	Fuel Consumption Rates
CMG	Climate Modelling Grid	FEER	Fire Energetics and Emissions Research
CMIP6	Coupled Model Intercomparison Project Phase 6	FINN	Fire INventory from NCAR
CMUG	Climate Modelling User Group	FireMIP	Fire Model Intercomparison Project

FIRMS	Fire Information for Resource Management System
FOA	Fraction of observed area
FREL/FRL	Forest Reference (Emission) Levels
FRP	Fire Radiative Power
FTP	File Transfer Protocol
FWI	Fire Weather Index
g	Grid product
GABAM	Global annual burned area map
GBS	Global Burned Surfaces
GCOS	Global Climate Observing System
GEMI	Global Environmental Monitoring Index
GFA	Global Fire Atlas
GFAS	Global Fire Assimilation System
GFED	Global Fire Emissions Database
GHG	Greenhouse Gas
GIO-GL	Copernicus Global Land Service burned area product
GOES	Geostationary Operational Environmental Satellites
ha	Hectares
HDF	Hierarchical Data Format
HMS	Hazard Mapping System
HS	Hotspot
ia	Inaccessible
IBBI	Interdisciplinary Biomass Burning Initiative
ID	Individual identity number per fire
IGNS	Ignition point
IPCC	Intergovernmental Panel on Climate Change
IS4FIRES	Integrated Monitoring and Modelling System for Fires
JRC	Joint Research Centre
KMZ	Keyhole Markup Language
LC	Land Cover
LTDR	Land Long Term Data Record
m	Metres
MERIS	Medium Resolution Imaging Spectrometer

MFLEI	Missoula Fire Lab Emission Inventory
MIPs	Model Intercomparison Projects
MOB	Month of burn
MODIS	Moderate Resolution Imaging Spectroradiometer
MORPH	Fire Morphology and size
MRV	Measurement, Reporting and Verification
MTBS	Monitoring Trends in Burn Severity
NASA	National Aeronautics and Space Administration
NBR	Normalized Burned Ratio
NDVI	Normalized Difference Vegetation Index
NetCDF	NETwork Common Data Format
NFMS	National Forest Monitoring Systems
NIR	Near InfraRed
NOAA	National Oceanic and Atmospheric Administration
NOO	Number of observations
NPIX	Number of burned pixels
NRT	Near Real Time
OB	Number of observations
ODP	ESA CCI Open Data Portal
Oe	Omission Error
OPeNDAP	Open-source Project for a Network Data Access Protocol
p	Pixel product
pa	Fire patch product
PKU-PAH	Peking University Global Emission Inventory of Polycyclic Aromatic Hydrocarbons
PER	Perimeter
PERSIS	Fire Persistency
QA	Quality Assurance
QFED	Quick Fire Emission Dataset
RDA	Rapid Damage Assessment
REDD+	Reducing emissions from deforestation and forest degradation and the role of conservation, sustainable

	management of forests and enhancement of forest carbon stocks in developing countries
rev	Revoqued
ROI	Region of interest
SEAS	Seasonality
SHP	Shapefile
SIZ	Fire Size
SPOT	Satellite pour l'Observation de la Terre
SRC	Surface Reflectance Change
ss	Superseded
TEM	Terrestrial Ecosystem Model
TIFF	Tag Image File Format
TRMM	Tropical Rainfall Measuring Mission
UNC	Uncertainty

UNFCCC	United Nations Framework Convention on Climate Change
URD	User Requirements Document
USDA	U.S. Department of Agriculture
USGS	United States Geological Survey
VGT	Vegetation
VIIRS	Visible Infrared Imaging Radiometer Suite
VIRS	Visible and Infrared Scanner
WCS	Web Coverage Service
WFEIS	Wildland Fire Emissions Information System
WMS	Web Map Service
WoS	Web of Science



fire
cci

Fire_cci User Requirements Document

Ref.	Fire_cci_D1.1_URD_v7.2		
Issue	7.2	Date	28/04/2021
	Page		65

Annex 2: Supplementary information

Table 8: Characteristics of global burned area products that are superseded or with abandoned product development (see Annex 1 for abbreviations and Table 1 caption notes).

Product	Period MM/YYYY	Release	Sensor/Method	Spatial	Temporal	File format	Data layers	Reference	Data access
				resolution					
FireCCILT10 (beta)	01/1982 12/2017	03/2019	AVHRR2-3; BA scaled with MCD64C6	g: 0.25°	g: m	g: NetCDF	g: BA, UNC, FBURN, FOA, LC	Otón (2020)	https://catalogue.ceda.ac.uk/uuid/4f377defc2454db9b2a6d032abfd0cbd
FireCCI50	01/2001 12/2016	12/2017	MODIS C6 SRC & MODIS C6 HS	p: 250m g: 0.25°	p: d g: 2w	p: GeoTIFF, 6 continental tiles g: NetCDF	p: DOB, CL, LC g: BA, UNC, FBURN, FOA, NOP, LC	Chuvieco et al., (2018)	http://catalogue.ceda.ac.uk/uuid/bcef9e87740e4cbabc743d295afbe849
FireCCI41	01/2005 12/2011	07/2016	MERIS SRC & MODIS C5 HS	p: 300m g: 0.25°	p: d g: 2w	p: GeoTIFF, 6 continental tiles g: NetCDF	p: DOB, CL, LC g: BA, ERR, FOA, NOP, LC	Alonso-Canas and Chuvieco (2015)	
FireCCI31	01/2006 12/2008	10/2014	MERIS SRC & MODIS C5 HS	p: 300m g: 0.5°	p: d g: 2w	p: GeoTIFF, 6 continental tiles g: NetCDF	p: DOB, CL, LC g: BA, ERR, FOA, NOP, LC	Alonso-Canas and Chuvieco (2015)	
GFED4	06/1995 12/2016	03/2013	MODIS C5 SRC & MODIS C5 HS; <08 2000:ATSR/VIRS HS	g: 0.25°	m & also d since 08/2000	HDF4	BA, ERR, BAS, BAT, LC, PERSIS	Giglio et al., (2013)	ftp://fire:burnt@fuoco.geog.umd.edu/gfed4/
GIO-GL1 v1.3	04/1999 03/2014	02/2015	VGT	p: 1km	d	HDF5-10° tiles	DOB, NOO, SEAS	Tansey et al., (2008)	<i>retracted in 2018 due to performance degradation</i>
GIO-GL v1 1km	04/2014 08/2018	07/2015	PROBA-V SRC	p: 1km	10d	HDF5-10° tiles & continental tiles	BC, NOO, DOB (F&L)	Tansey et al., (2008)	<i>see GIO-GL 300m</i>
Geoland2	2001 2012	2012	VGT SRC	p: 1km	10d			Tansey et al., (2008)	inaccessible
L3JRC	04/2000 03/2007	2008	VGT SRC	p: 1km	d	GeoTIFF	DOB	Tansey et al., (2008)	inaccessible
MCD64C5	08/2000 12/2016	2009 to 2012*2	MODIS C5 SRC & MODIS C5 HS	p: 500m	d	HDF4-10° tiles GeoTIFF & SHP-24 tiles	DOB, DOBUNC, QA, DOB (F&L)	Giglio et al., (2009)	ftp://fire:burnt@fuoco.geog.umd.edu/MCD64A1/C5.1
MCD45	04/2000 01/2017	11/2009	MODIS C5 SRC	p: 500m	d	GeoTIFF & SHP-24tiles	DOB, NOO, QA	Roy et al., (2008)	ftp://user:burnt_data@ba1.geog.umd.edu/Collection51/



fire
cci

Fire_cci
User Requirements Document

Ref.	Fire_cci_D1.1_URD_v7.2		
Issue	7.2	Date	28/04/2021
	Page		66

Product	Period	Release	Sensor/Method	Spatial	Temporal	File format	Data layers	Reference	Data access
	MM/YYYY			resolution					
						HDF-10°tiles			
GLOBCARBON	01/1998 12/2007	2005	VGT & ATSR2 & AATSR SRC	p: 1km g: 0.1, 0.25, 0.5°	p: d g: m	ASCII	p: DOB, Sensor, Algorithm g: BA, DISP	Plummer et al., (2006)	inaccessible
GBS	01/1982 12/1999	2006	AVHRR SRC	p: 8km (1km)	climatology	GeoTIFF ASCII	BP, SEAS	Carmona-Moreno et al., (2005)	
GFED3	07/1996 02/2012	06/2010	<i>see GFED4</i>	g: 0.5°	m	HDF ASCII	BA, ERR, BAS, BAT, LC, PERSIS, EMIS, FCR	Giglio et al., (2010)	ftp://fire:burnt@fuoco.geog. umd.edu/gfed3/
GFED2	01/1997 12/2006	12/2005	MODIS C5 HS	g: 1°	m	ASCII	BA, EMIS, FCR	Giglio et al., (2006)	inaccessible
GLOBSCAR	01/2000 12/2000	2002	ATSR2 SRC	p: 1km	d	GeoTIFF, SHP, ASCII	DOB	Simon et al., (2004)	
GBA2000	01/2000 12/2000	12/2002	VGT SRC	p: 1km g: 0.25, 0.5, 1°	m	p: ASCII, BSQ g: NetCDF	p: BC g: BA	Tansey et al., (2004)	

*¹ In 2012, a reprocessed and slightly improved version of MCD64A1 v5, was released (Giglio et al., 2013).